

NO-A102 601

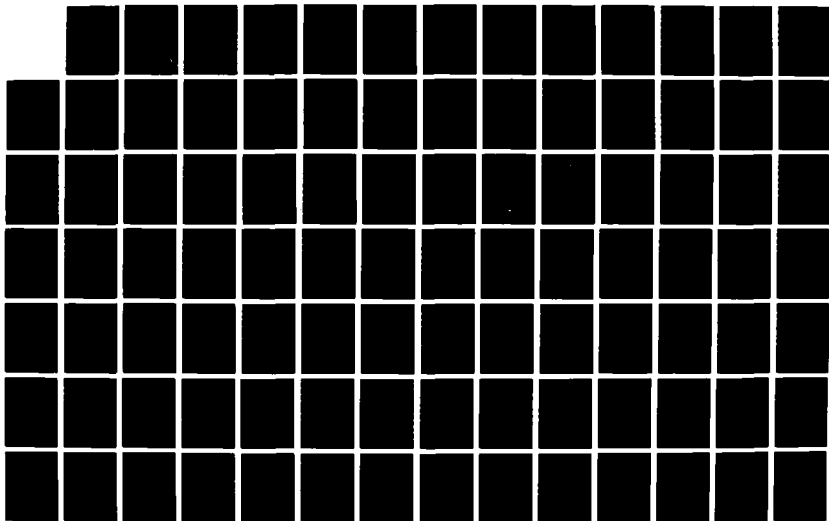
NEUTRAL BEAM PROPAGATION EFFECTS IN THE UPPER
ATMOSPHERE 2(U) BOSTON COLL CHESTNUT HILL MA DEPT OF
PHYSICS T LI ET AL. 01 MAR 86 SCIENTIFIC-2
AFGL-TR-86-0192 F19628-04-K-0039

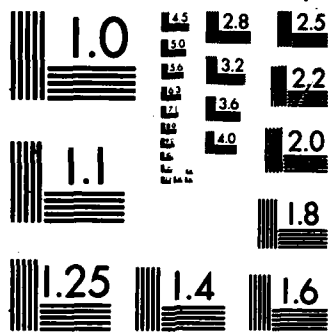
1/2

UNCLASSIFIED

F/G 20/7

NL





MICROCOPY RESOLUTION TEST CHART
NATIONAL BUREAU OF STANDARDS-1963-A

12

AFGL-TR-86-0192

DTIC FILE COPY

NEUTRAL BEAM PROPAGATION EFFECTS
IN THE UPPER ATMOSPHERE II

T. Li
G. Kalman
P. Pulsifer

Boston College
Department of Physics
Chestnut Hill, MA 02167

1 March 1986

Scientific Report No. 2

APPROVED FOR PUBLIC RELEASE; DISTRIBUTION UNLIMITED

DTIC
ELECTE
JUL 21 1987
S D
E

AIR FORCE GEOPHYSICS LABORATORY
AIR FORCE SYSTEMS COMMAND
UNITED STATES AIR FORCE
HANSCOM AIR FORCE BASE, MASSACHUSETTS 01731

AD-A182 601

87 7 00 008

A182601

REPORT DOCUMENTATION PAGE

1a. REPORT SECURITY CLASSIFICATION Unclassified			1b. RESTRICTIVE MARKINGS			
2a. SECURITY CLASSIFICATION AUTHORITY			3. DISTRIBUTION / AVAILABILITY OF REPORT Approved for public release; Distribution unlimited.			
2b. DECLASSIFICATION / DOWNGRADING SCHEDULE			4. PERFORMING ORGANIZATION REPORT NUMBER(S)			
4. PERFORMING ORGANIZATION REPORT NUMBER(S)			5. MONITORING ORGANIZATION REPORT NUMBER(S) AFGL-TR-86-0192			
6a. NAME OF PERFORMING ORGANIZATION Boston College Department of Physics		6b. OFFICE SYMBOL (if applicable)		7a. NAME OF MONITORING ORGANIZATION Air Force Geophysics Laboratory		
6c. ADDRESS (City, State, and ZIP Code) Chestnut Hill, MA 02167			7b. ADDRESS (City, State, and ZIP Code) Hanscom AFB Massachusetts 01731			
8a. NAME OF FUNDING / SPONSORING ORGANIZATION		8b. OFFICE SYMBOL (if applicable)		9. PROCUREMENT INSTRUMENT IDENTIFICATION NUMBER F19628-84-K-0039		
8c. ADDRESS (City, State, and ZIP Code)			10. SOURCE OF FUNDING NUMBERS			
PROGRAM ELEMENT NO. 62101F		PROJECT NO. 7661		TASK NO. 14		WORK UNIT ACCESSION NO. AF
11. TITLE (Include Security Classification) Neutral Beam ² , Propagation Effects in the Upper Atmosphere. 1						
12. PERSONAL AUTHOR(S) T. Li, G. Kalman, P. Pulsifer						
13a. TYPE OF REPORT Scientific No. 2		13b. TIME COVERED FROM _____ TO _____		14. DATE OF REPORT (Year, Month, Day) 1986 March 1		15. PAGE COUNT 100
16. SUPPLEMENTARY NOTATION						
17. COSATI CODES			18. SUBJECT TERMS (Continue on reverse if necessary and identify by block number)			
FIELD	GROUP	SUB-GROUP	Neutral beam, Beam induced stripping			
			Stripping, Polarization drift			
			Ionization, Cross section			
19. ABSTRACT (Continue on reverse if necessary and identify by block number)						
<p>Electron (proton) trajectory equations are obtained for various electric field and magnetic field configurations. These trajectory equations provide the basis for calculating "self-stripping", which was proposed in Scientific Report 1 as an important beam attenuation process. The average relative electron-beam energy is calculated to determine the beam energy and configuration-dependence of the stripping process.</p> <p>Results for beam attenuation due to electron-beam stripping are obtained for the zero-field model and space-charge field model. Proton-beam stripping was shown to be negligible. Attenuation-versus-distance graphs are presented for various magnetic field angles and relevant beam parameters such as beam energy, beam intensity and beam radius.</p>						
20. DISTRIBUTION / AVAILABILITY OF ABSTRACT <input type="checkbox"/> UNCLASSIFIED/UNLIMITED <input type="checkbox"/> SAME AS RPT. <input type="checkbox"/> DTIC USERS				21. ABSTRACT SECURITY CLASSIFICATION Unclassified		
22a. NAME OF RESPONSIBLE INDIVIDUAL Shu T. Lai			22b. TELEPHONE (Include Area Code)		22c. OFFICE SYMBOL AFGL/PHK	

TABLE OF CONTENTS

Introduction	1
Trajectory Equations	4
Beam-Induced Stripping	12
Estimate of the Geometric Factor	23
Conclusions	25
References	27

Accession For	
NTIS GRA&I	<input checked="" type="checkbox"/>
DTIC TAB	<input type="checkbox"/>
Unannounced	<input type="checkbox"/>
Justification	
By _____	
Distribution/	
Availability Codes	
Dist	Avail and/or Special
A-1	



LEGEND FOR FIGURES OUTSIDE THE TEXT

Fig. 3

$F(\theta)$ versus θ . (There is a symmetry with respect to $\theta = 45^\circ$.) Same maximum value = 1.59 at $\theta = 57'$ for 1 MeV, $\theta = 19'$ for 9 MeV and $\theta = 11'$ for 25 MeV.

Same angle $\theta = 45^\circ$ for minimum value = 4.52×10^{-3} for 1 MeV, minimum value = 2.46×10^{-3} for 9 MeV and minimum value = 7.51×10^{-3} for 25 MeV.

Fig. 4

(a) $F(\theta)$ versus θ . Same maximum value = 1.59 at $\theta = 57'$ for 1 MeV, $\theta = 19'$ for 9 MeV and $\theta = 11'$ for 25 MeV. Same converging value = 1 at $\theta = 0^\circ$.

(b) $F(\theta)$ versus θ . Similar to (a) at complementary angles ($\theta \rightarrow 90^\circ - \theta$).

Fig. 6

E_I (impact energy) versus E_b (beam energy); E_I in eV, E_b in MeV; with space charge.

- (a) $\theta = 2^\circ$
- (b) $\theta = 5^\circ$
- (c) $\theta = 10^\circ$
- (d) $\theta = 45^\circ$

$R_0 = 50\text{cm}, 55\text{cm}, 60\text{cm}, 70\text{cm}, 80\text{cm}, 90\text{cm}, 100\text{cm}$
(from the bottom upwards)

E_I in eV, E_b in MeV

Fig. 7

E_{I0} (impact energy) versus E_b (beam energy); E_I in eV, E_b in MeV; no space charge.

- (a) E_{I0} versus E_b , $\theta = 15^\circ$
- (b) E_{I0} versus E_b , $\theta = 20^\circ$
- (c) E_{I0} versus E_b , $\theta = 25^\circ$
- (d) E_{I0} versus E_b , $\theta = 30^\circ$
- (e) E_{I0} versus E_b , $\theta = 35^\circ$
- (f) E_{I0} versus E_b , $\theta = 40^\circ$
- (g) E_{I0} versus E_b , $\theta = 45^\circ$
- (h) E_{I0} versus E_b , $\theta = 50^\circ$
- (i) E_{I0} versus E_b , $\theta = 55^\circ$
- (j) E_{I0} versus E_b , $\theta = 60^\circ$
- (k) E_{I0} versus E_b , $\theta = 65^\circ$
- (l) E_{I0} versus E_b , $\theta = 70^\circ$
- (m) E_{I0} versus E_b , $\theta = 75^\circ$
- (n) E_{I0} versus E_b , $\theta = 80^\circ$
- (o) E_{I0} versus E_b , $\theta = 85^\circ$

$R_0 = 10\text{cm}, 20\text{cm}, 30\text{cm}, 40\text{cm}, 50\text{cm}, 55\text{cm}, 60\text{cm},$
 $70\text{cm}, 80\text{cm}, 90\text{cm}, 100\text{cm}.$
(from the bottom upwards)
 E_I in eV, E_b in MeV

Fig. 8

Cross-section for ionization of atomic hydrogen taken from Kieffer and Dunn,
Rev. Mod. Phys. 38, 1 (1966)

Fig. 9

No space charge; beam radius (in cm) vs. distance (in km) for
0.5 attenuation for various propagation angles.

- (a) 1MeV; 1,000 mA/cm²
- (b) 1MeV; 10,000 mA/cm²
- (c) 10MeV; 1,000 mA/cm²
- (d) 10MeV; 10,000 mA/cm²
- (e) 100MeV; 1,000 mA/cm²
- (f) 100MeV; 10,000 mA/cm²

Fig. 10

No space charge; beam radius (in cm) vs. distance (in km) for
0.1 attenuation for various propagation angles.

- (a) 1MeV; 1,000 mA/cm²
- (b) 1MeV; 10,000 mA/cm²
- (c) 10MeV; 1,000 mA/cm²
- (d) 10MeV; 10,000 mA/cm²
- (e) 100MeV; 1,000 mA/cm²
- (f) 100MeV; 10,000 mA/cm²

Fig. 11

No space charge; beam energy (in MeV) vs. distance (in km) for
0.5 attenuation for various propagation angles.

- (a) 10 cm; 1,000 mA/cm²
- (b) 10 cm; 10,000 mA/cm²
- (c) 55 cm; 1,000 mA/cm²
- (d) 55 cm; 10,000 mA/cm²
- (e) 100 cm; 1,000 mA/cm²
- (f) 100 cm; 10,000 mA/cm²

Fig. 12

No space charge; beam energy (in MeV) vs. distance (in km) for 0.1 attenuation for various propagation angles.

- (a) 10 cm; 1,000 mA/cm²
- (b) 10 cm; 10,000 mA/cm²
- (c) 55 cm; 1,000 mA/cm²
- (d) 55 cm; 10,000 mA/cm²
- (e) 100 cm; 1,000 mA/cm²
- (f) 100 cm; 10,000 mA/cm²

Fig. 13

Including space charge: beam radius (in cm) vs. distance (in km) for 0.5 attenuation for various propagation angles.

- (a) 1MeV; 1,000 mA/cm²
- (b) 1MeV; 10,000 mA/cm²
- (c) 10MeV; 1,000 mA/cm²
- (d) 10MeV; 10,000 mA/cm²
- (e) 100MeV; 1,000 mA/cm²
- (f) 100MeV; 10,000 mA/cm²

From top to bottom: 5°(85°), 10°(80°), 45°

Fig. 14

Including space charge: beam radius (in cm) vs. distance (in km) for 0.1 attenuation for various propagation angles.

- (a) 1MeV; 1,000 mA/cm²
- (b) 1MeV; 10,000 mA/cm²
- (c) 10MeV; 1,000 mA/cm²
- (d) 10MeV; 10,000 mA/cm²
- (e) 100MeV; 1,000 mA/cm²
- (f) 100MeV; 10,000 mA/cm²

From top to bottom: 5°(85°), 10°(80°), 45°

Fig. 15

Including space charge: beam energy (in MeV) vs. distance (in km) for 0.5 attenuation for various propagation angles.

- (a) 55 cm; 1,000 mA/cm²
- (b) 55 cm; 10,000 mA/cm²
- (c) 100 cm; 1,000 mA/cm²
- (d) 100 cm; 10,000 mA/cm²

From top to bottom: 5°(85°), 10°(80°), 45°

(NOTE: No effect is discernable for beam radius of 10 cm)

Fig. 16

Including space charge: beam energy (in MeV) vs. distance (in km) for 0.1 attenuation for various propagation angles.

- (a) 55 cm; 1,000 mA/cm²
- (b) 55 cm; 10,000 mA/cm²
- (c) 100 cm; 1,000 mA/cm²
- (d) 100 cm; 10,000 mA/cm²

From top to bottom: 5°(85°), 10°(80°), 45°

I. INTRODUCTION

When a neutral particle beam passes through the upper atmosphere, it undergoes a number of physical processes which lead to the degradation of the beam intensity and of the beam energy. Probably the most important amongst these processes is stripping which leads to the loss of (one or more) electrons of the beam particle. Stripping can be induced by collisions with neutral particle ions or electrons, without substantial differences in the stripping cross section per electron. While it is usually assumed that the stripping particles originate from the atmospheric gas or plasma through which the beam passes, this is, as we pointed out and discussed in an earlier Scientific Report, [1] (to be referred to as I) not necessarily so. The electrons, stripped off the beam particles, themselves can become agents of subsequent stripping processes. Instrumental in this scenario is the presence of the earth's geomagnetic field which helps to accumulate the beam generated electrons in the beam's path. It was actually Alfvén [2] who realized that the passage of a neutral beam through magnetic field brings about an anomalous source of ionization.

In I, certain basic aspects of this beam induced stripping (BIS) were analyzed. We demonstrated through a rather simplified, but qualitatively faithful model, that at high enough beam current BIS may become the dominant mechanism of beam degradation.

Two major conditions have to be satisfied in order for the BIS process to become effective: (i) the stripped electrons must remain within the beam for a long enough time so that they can undergo further ionizing collisions, and (ii) the stripped electrons must acquire a high enough (but not too high) relative velocity with respect to the beam particles, so that they can cause stripping collisions.

The presence of the geomagnetic field is critical in meeting both of these conditions. In addition to the direct effect of the magnetic field, the separation of the positive ions and negative electrons causes a polarization electric field which, in combination with the magnetic field generates complicated drift trajectories.

The effect of the magnetic field can be especially clearly seen in the case of the beam propagating along the magnetic field. In a stripping collision, the electrons are ejected at a large angle with respect to the beam velocity and thus, without the magnetic field, would promptly leave the beam. The magnetic field, however, forces the electrons back into the beam. For a general beam orientation the situation is more complicated; nevertheless, the general tendency of the electron becoming trapped by the magnetic (or by the combined magnetic and electric) fields, still prevails. In the other extreme situation, when the beam propagates perpendicular to the magnetic field, it is the polarization field that forces the electrons to travel, for a substantial period of time, with the beam. This scenario, although somewhat similar to the well-known problem of a plasmoid or plasma beam travelling across the magnetic field [3] is different in that the electrons are continuously created along the beam, and thus the critical transient phase of the plasma beam problem, where, upon penetration, the beam has to create the field that propels it further, plays a much less important role.

Having demonstrated in I that the BIS process, under certain conditions, can be an important factor in beam degradation, we may now list the principal problems that one has to address in order to obtain a detailed description and assessment of the BIS process.

- (a) Calculation of the "geometric factor", i.e. the fraction of time spent by the electron within the beam.
- (b) Calculation of the relative velocity of the electrons and determination of the relative energy-dependent stripping cross-section.
- (c) Calculation of the polarization electric field.

This Report addresses itself to item (b) and to one aspect of item (c).

In section II electron trajectories in a crossed electric and magnetic field configuration are calculated without the usual assumption of the electric field being uniform - a model valid only in the case of small gyro-radii. It is shown that with strong enough spatial variation of the electric field the concept of $\underline{E} \times \underline{B}$ drift doesn't apply at all. In Sections III and IV we examine in some detail the generation of the relative velocity by the magnetic field and find that it depends significantly on the beam energy, on the beam diameter and on the propagation angle of the beam. Then we calculate the beam decay distance for 10% and 50% beam degradations, as a function of beam energy and propagation angle. In all these calculations we use two scenarios: (i) no polarization electric field and (ii) a model electric field representing, in the absence of more elaborate self-consistent calculations, the polarization electric field; for the geometric factor, again in the absence of a detailed calculation, we assume the median value $\gamma = 0.5$. In Section V, we give some qualitative discussion of the mechanism determining the actual value of γ .

II. TRAJECTORY EQUATIONS

The mathematical problem of Lorentz force equation coupled with Poisson equation cannot be solved analytically. A self-consistent field approach involve making appropriate physical approximations and numerical calculations. However, under certain non-trivial conditions, the Lorentz force equation with uniform magnetic field and external electric field can be solved exactly. The resulting electron and proton trajectory equations are useful in providing estimates for the beam-induced stripping (or self-stripping.)

We will study in detail two cases: (1) beam propagation, uniform magnetic field and linear electric field are mutually orthogonal; (2) beam propagation, uniform magnetic field and constant electric field are arbitrarily oriented. These two cases are exactly solvable and their solutions provide useful insights for future work.

(1) Mutually Othogonal \vec{v}_b , \vec{B} and $\vec{E}(y)$

We designate \vec{v}_b , \vec{B} and $\vec{E}(y)$ respectively as the beam propagation velocity, geomagnetic field and linearly varying electric field. Specifically, we have $\vec{v}_b = v_b \hat{i}$, $\vec{B} = B \hat{k}$ and $\vec{E}(y) = (E - \epsilon y) \hat{j}$, where E and ϵ are constants to be specified later.

The Lorentz force equation for electron becomes

$$\begin{aligned} \ddot{x} &= -\omega \dot{y} \\ \ddot{y} &= \omega \dot{x} - \frac{eE}{m} + \frac{e\epsilon}{m} y \end{aligned} \quad (1)$$

where $\omega = \frac{eB}{m}$, and m is electron mass.

This is an exactly solvable problem and the resulting electron trajectory equations are:

$$x(t) = \left[1 - \frac{\epsilon}{\omega B} \right]^{1/2} \sin \Omega t + (v_b - \omega R_{E\epsilon}) t \quad (2)$$

$$y(t) = R_{E\epsilon} (1 - \cos\Omega t) + y_0 \quad (3)$$

where the modified frequency Ω is:

$$\Omega = \omega \left(1 - \frac{\epsilon}{\omega B}\right)^{1/2}, \quad (4)$$

and the modified radius $R_{E\epsilon}$ is

$$R_{E\epsilon} = \frac{\frac{1}{\omega} \left[v_b - \frac{1}{B} (E - \epsilon y_0) \right]}{1 - \frac{\epsilon}{\omega B}} \quad (5)$$

We have assumed the boundary conditions: $x(0) = 0$

and $y(0) = y_0$, $|y_0| < R_0$, where R_0 is the beam radius.

Eqs. (4) and (5) indicate the effect of linearly varying electric field with a non-zero ϵ . Reduction to the simple case of uniform field can be seen by setting $\epsilon = 0$, and we have $\Omega = \omega$ and $R_{E\epsilon} = \frac{1}{\omega} \left[v_b - \frac{E}{B} \right]$.

The Lorentz force for proton with an external linear field $\vec{E}(y) = (E + \alpha y)\hat{j}$ becomes

$$\begin{aligned} \ddot{x} &= \omega_p \dot{y} \\ \ddot{y} &= \omega_p \dot{x} + \frac{eE}{M} + \frac{e\alpha}{M} y \end{aligned} \quad (6)$$

where $\omega_p = \frac{eB}{M}$, M = proton mass, and the constants E and α are to be specified later. The resulting proton trajectory equations are:

$$x_p(t) = \frac{RE\alpha}{\left[1 - \frac{\alpha}{\omega_p B}\right]^{1/2}} \cdot \sin\Omega_p t + (v_b - \omega_p R_{E\alpha})t \quad (7)$$

$$y_p(t) = R_{E\alpha} (\cos\Omega_p t - 1) + y_0 \quad (8)$$

where the modified frequency and radius are respectively

$$\Omega_p = \omega_p \left(1 - \frac{\alpha}{\omega_p B}\right)^{1/2}, \quad (9)$$

$$R_{E\alpha} = \frac{\frac{1}{\omega_p} \left[v_b - \frac{1}{B} (E + \alpha y_0) \right]}{1 - \frac{\alpha}{\omega B}} \quad (10)$$

A simple model of uniformly distributed space charges (electrons and protons) resulting from beam-atmosphere ionizations yield the following expressions for $E(y)$,

$$E(y) = E - \epsilon y = \frac{en}{\epsilon_0 4LR_0} \left[\frac{2R_e + R_0}{R_e + R_0} - \frac{1}{R_e + R_0} y \right], \quad (11)$$

$$R_0 < y < 2R_e + R_0$$

$$E(y) = E - \epsilon y \quad (12)$$

$$= \frac{en}{\epsilon_0 4LR_0} \left[\frac{2R_e}{R_e + R_0} + \frac{(R_p - R_e)R_0}{(R_p + R_e)(R_e + R_0)} - \frac{(R_p - R_e)}{(R_p + R_0)(R_e + R_0)} y \right],$$

$$- R_0 < y < R_0$$

$$E(y) = E + \alpha y = \frac{en}{\epsilon_0 4LR_0} \left[\frac{2R_p + R_0}{R_p + R_0} + \frac{1}{R_p + R_0} y \right], \quad (13)$$

$$- (2R_p - R_0) < y < R_0$$

where R_p and R_e are respectively proton and electron gyroradius, L is about $6R_p$, and n is the total number of ionizations for beam traversal distance L .

The results obtained so far are based on simple assumptions, and are not adequate for physical applications. However, they constitute a basis for further considerations.

(2) Arbitrarily Oriented \vec{v}_b , \vec{B} and Constant \vec{E}

As shown in Fig. 1, we have: $\vec{v}_b = v_b \hat{i}$,

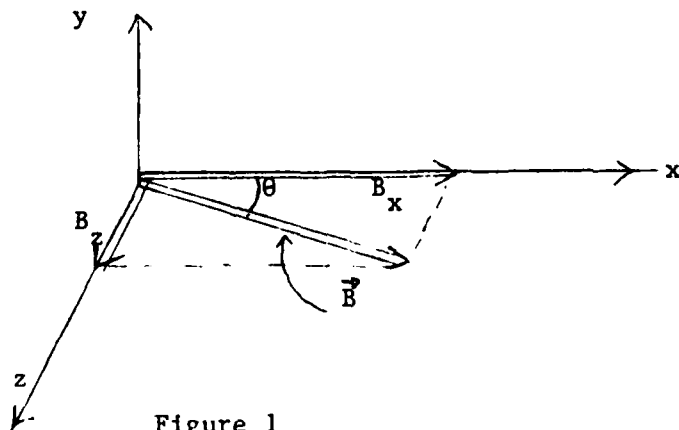


Figure 1

$$\vec{B} = B_x \hat{i} + B_z \hat{k}$$

$$\vec{E} = E_x \hat{i} + E_y \hat{j} + E_z \hat{k}$$

$$\text{and } \tan \theta = \frac{B_z}{B_x}$$

The Lorentz force equation
equation for electron can be

written as:

$$\begin{aligned} \ddot{x} &= -\gamma_x - \omega_z \dot{y} \\ \ddot{y} &= -\gamma_y - \omega_x \dot{z} + \omega_z \dot{x} \\ \ddot{z} &= -\gamma_z + \omega_x \dot{y} \end{aligned} \quad (14)$$

where $\gamma_x = \frac{eE_x}{m}$, $\gamma_y = \frac{eE_y}{m}$, $\gamma_z = \frac{eE_z}{m}$,

$$\omega_x = \frac{eB_x}{m}, \text{ and } \omega_z = \frac{eB_z}{m}.$$

This system of coupled equation can be solved exactly and the resulting electron velocity equations are:

$$\begin{aligned} \dot{x}(t) &= -\omega_z A \sin(\omega t + \phi) - \frac{\omega_x}{\omega^2} (\omega_x \gamma_x + \omega_z \gamma_z) t \\ &\quad + \frac{\omega_z \gamma_y}{\omega^2} + \left(1 - \frac{\omega_z^2}{\omega^2}\right) v_b \end{aligned} \quad (15)$$

$$\begin{aligned} \dot{z}(t) &= \omega_x A \sin(\omega t + \phi) - \frac{\omega_z}{\omega^2} (\omega_x \gamma_x + \omega_z \gamma_z) t \\ &\quad - \frac{\omega_x \gamma_y}{\omega^2} + \frac{\omega_z \omega_x}{\omega^2} v_b \end{aligned} \quad (16)$$

$$\dot{y}(t) = \omega A \cos(\omega t + \phi) + \frac{1}{\omega^2} (\omega_x \gamma_z - \omega_z \gamma_x), \quad (17)$$

where $A = \frac{1}{\omega^2} [(\gamma_y - \omega_z v_b)^2 + \frac{D^2}{\omega^2}]^{1/2}$,

$$\tan\phi = \frac{\omega}{D} (\omega_z v_b - \gamma_y),$$

$$\omega^2 = \omega_x^2 + \omega_y^2 \text{ and } D = \omega_x \gamma_z - \omega_z \gamma_x.$$

The electron trajectory equations can be obtained by integrating the above equations with the boundary conditions: $x(0) = 0$, $y(0) = y_0$, $z(0) = z_0$, with $y_0 < R_0$ and $z_0 < R_0$.

The Lorentz force equation for proton can be expressed as:

$$\begin{aligned} \ddot{x} &= -\gamma_x - \omega_z \dot{y} \\ \ddot{y} &= -\gamma_y - \omega_x \dot{z} + \omega_x \dot{x} \\ \ddot{z} &= -\gamma_z + \omega_x \dot{y} \end{aligned} \quad (18)$$

where $\gamma_x = \frac{eE_x}{M}$, $\gamma_y = \frac{eE_y}{M}$, $\gamma_z = \frac{eE_z}{M}$,
 $\omega_x = \frac{eB_x}{M}$, and $\omega_z = \frac{eB_z}{M}$.

The proton velocity equations are given by:

$$\dot{x}(t) = +\omega_z A \sin(\omega t + \phi) + \frac{\omega_x}{\omega^2} (\omega_x \gamma_x + \omega_z \gamma_z) t + \frac{\omega_z \gamma_y}{\omega^2} + \left(1 - \frac{\omega_z^2}{\omega^2}\right) v_b \quad (19)$$

$$\dot{z}(t) = -\omega_x A \sin(\omega t + \phi) + \frac{\omega_z}{\omega^2} (\omega_x \gamma_x + \omega_z \gamma_z) t + \frac{\omega_x \gamma_y}{\omega^2} + \frac{\omega_x \omega_z}{\omega^2} v_b \quad (20)$$

$$\dot{y}(t) = \omega A \cos(\omega t + \phi) + \frac{1}{\omega^2} (\omega_x \gamma_z - \omega_z \gamma_x), \quad (21)$$

where $A = \frac{1}{\omega^2} [(\gamma_y - \omega_z v_b)^2 + \frac{D^2}{\omega^2}]^{1/2}$,

$$\tan\phi = \frac{\omega}{D} (\omega_z v_b - \gamma_y),$$

$$\omega^2 = \omega_x^2 + \omega_y^2 \text{ and } D = \omega_x \gamma_z - \omega_z \gamma_x.$$

Again the proton trajectory equations can be easily obtained by integrating the above equations with the same boundary conditions as those for the electron.

It is worth noting that the accelerating terms in $\dot{x}(t)$ and $\dot{z}(t)$ for both electron and proton contain the factor $(\omega_x \gamma_x + \omega_z \gamma_z)$, which can be considered to have resulted from the presence of E_x and E_z . The sinusoidal and constant terms represent steady state motion with bounded energy. Therefore, we require that $(\omega_x \gamma_x + \omega_z \gamma_z)$ vanishes with non-vanishing E_x and E_z . This can be accomplished by making the physically reasonable assumption that for self-consistent and self-sustaining motion there exists only transverse "polarizing" electric field, i.e.,

$$\vec{E} \cdot \vec{B} = E_x B_x + E_y B_y + E_z B_z = 0$$

Since $B_y = 0$, we have $E_x B_x + E_z B_z = 0$

and therefore $\omega_x \gamma_x + \omega_z \gamma_z = 0$. Using the expressions $B^2 = B_x^2 + B_z^2$ and $\tan\theta =$

$\frac{B_z}{B_x}$, we can rewrite the velocity equations for the electron as:

$$\begin{aligned} \dot{x}_e(t) = & \tan\theta \left(\frac{E_z}{B}\right) \sin(\omega_e t) & (22) \\ & - \sin\theta \left(\frac{E_y}{B} - \sin\theta \cdot v_b\right) \cos(\omega_e t) \\ & + \sin\theta \left(\frac{E_y}{B}\right) + \cos^2\theta \cdot (v_b) \end{aligned}$$

$$\begin{aligned} \dot{z}_e(t) = & - \left(\frac{E_z}{B}\right) \sin(\omega_e t) & (23) \\ & + \cos\theta \left(\frac{E_y}{B} - \sin\theta \cdot v_b\right) \cos(\omega_e t) \\ & - \cos\theta \cdot \left(\frac{E_y}{B}\right) + \cos\theta \cdot \sin\theta (v_b) \end{aligned}$$

$$\begin{aligned} \dot{y}_e(t) = & \frac{E_z}{B \cos\theta} [1 - \cos(\omega_e t)] & (24) \\ & - \left(\frac{E_y}{B} - \sin\theta \cdot v_b\right) \sin(\omega_e t) \end{aligned}$$

$$\text{where } \omega_e = \left(\omega_x^2 + \omega_z^2\right)^{1/2} = \frac{e}{m} \left(B_x^2 + B_z^2\right)^{1/2} = \frac{eB}{m}$$

The proton velocity equations are rewritten as:

$$\begin{aligned} \dot{x}_p(t) = & -\tan\theta \left(\frac{E_z}{B} \right) \sin(\omega_p t) & (25) \\ & - \sin\theta \left(\frac{E_y}{B} - \sin\theta \cdot v_b \right) \cos(\omega_p t) \\ & + \sin\theta \cdot \left(\frac{E_y}{B} \right) + \cos^2\theta \cdot (v_b) \end{aligned}$$

$$\begin{aligned} \dot{z}_p(t) = & \frac{E_z}{B} \sin(\omega_p t) & (26) \\ & + \cos\theta \left(\frac{E_y}{B} - \sin\theta \cdot v_b \right) \cos(\omega_p t) \\ & - \cos\theta \left(\frac{E_y}{B} \right) + \cos\theta \cdot \sin\theta (v_b) \end{aligned}$$

$$\begin{aligned} \dot{y}_p(t) = & \frac{E_z}{B \cos\theta} [1 - \cos(\omega_p t)] & (27) \\ & + \left(\frac{E_y}{B} - \sin\theta \cdot v_b \right) \sin(\omega_p t) \end{aligned}$$

where $\omega_p = (\omega_x^2 + \omega_z^2)^{1/2} = \frac{e}{M} (B_x^2 + B_z^2)^{1/2} = \frac{eB}{M}$.

It is worth noting that both the electron and proton velocities along \vec{B} direction are equal to $\cos\theta \cdot v_b$. More specifically we have

$$(\dot{x}_e)_\parallel + (\dot{z}_e)_\parallel = \cos\theta \cdot v_b = v_\parallel$$

and

$$(\dot{x}_p)_\parallel + (\dot{z}_p)_\parallel = \cos\theta \cdot v_b = v_\parallel$$

where v_\parallel is component of beam velocity \vec{v}_b along the \vec{B} direction.

The velocity equations Eqs. (22) to (27) express the electron and proton velocities as functions of known quantities θ , v_b , B and assumed quantities E_y and E_z . In a self-consistent field calculation, E_y and E_z would be determined from θ , v_b and B .

III. BEAM-INDUCED STRIPPING

We designated the relative electron-beam velocity as $\vec{v}_{eb} = \vec{v}_e - \vec{v}_b$, whose components v_{ex} , v_{ey} and v_{ez} are given by Eqs. (22) to (24) as

$$v_{ex} = \dot{x}_e - v_b = \tan\theta \frac{E_z}{B} \sin(\omega_e t) - \sin\theta \cdot \left[v_b \sin\theta - \frac{E_y}{B} \right] \left[1 - \cos(\omega_p t) \right] \quad (28)$$

$$v_{ey} = \frac{E_z}{B \cos\theta} \cdot \left[1 - \cos(\omega_e t) \right] + \left[v_b \sin\theta - \frac{E_y}{B} \right] \sin(\omega_e t) \quad (29)$$

$$v_{ez} = -\frac{E_z}{B} \sin(\omega_e t) + \cos\theta \left[v_b \sin\theta - \frac{E_y}{B} \right] \left[1 - \cos(\omega_e t) \right] \quad (30)$$

For the relative proton-beam velocity $\vec{v}_{pb} = \vec{v}_p - \vec{v}_b$, the components are given by Eqs. (25) to (27) as

$$v_{px} = v_p - v_b = -\tan\theta \cdot \frac{E_z}{B} \sin(\omega_p t) - \sin\theta \cdot \left[v_b \sin\theta - \frac{E_y}{B} \right] \left[1 - \cos(\omega_p t) \right] \quad (31)$$

$$v_{py} = \frac{E_z}{B \cos\theta} \cdot \left[1 - \cos(\omega_p t) \right]$$

$$-\left(v_b \sin\theta - \frac{E_y}{B}\right) \sin(\omega_p t) \quad (32)$$

$$v_{pz} = \left(\frac{E_z}{B}\right) \sin(\omega_p t) + \cos\theta \cdot \left(v_b \sin\theta - \frac{E_y}{B}\right) [1 - \cos(\omega_p t)] \quad (33)$$

The beam (neutral) particles all travel with velocity \vec{v}_b within the beam confine which is of cylindrical form with cross-sectional area πR_0^2 . The charged particles (electrons and protons) move with velocities whose components are given by Eqs. (22) to (27). However, the charged particles spend only a short time within the beam confine. We designate the time interval as T_{\parallel} and consider the kinematics of the charged particles within the beam confine. As shown in Fig. 2(a),

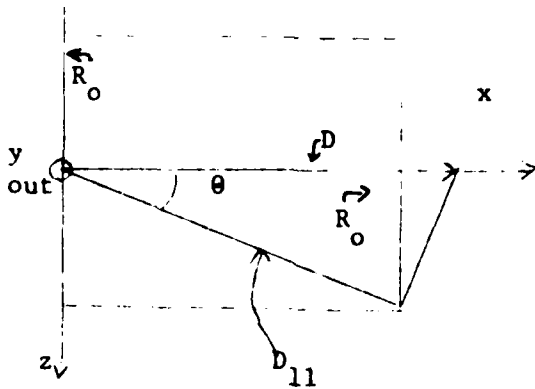


Figure 2(a)

a charged particle starting from the beam center (i.e., origin of x-y-z system) can be regarded as staying within the beam confine if its moving center's path is $< D_{\parallel} = \frac{R_0}{\sin\theta}$.

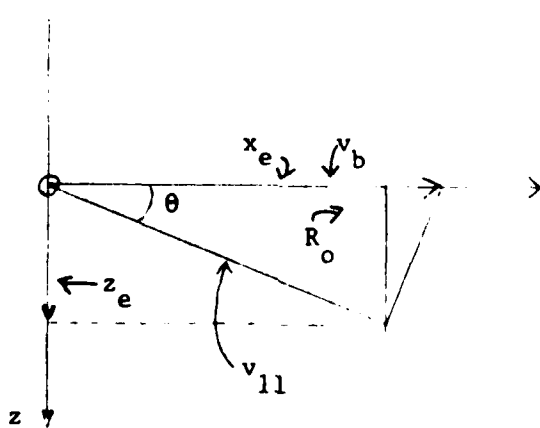


Figure 2(b)

As shown in Fig. 2(b), v_{\parallel} is the component of beam velocity \vec{v}_b in the \vec{B} direction, i.e., $v_{\parallel} = v_b \cos\theta$. We regard T_{\parallel} as the time interval during which the charged particle is within the beam confine. Thus we have

$$T_1 = \frac{D_1}{v_1} = \frac{R_0}{v_b \sin \theta \cdot \cos \theta} = \frac{2R_0}{v_b \sin 2\theta}$$

We now assume that all the charged particles starting from the cross-sectional area πR_0^2 (at $x = 0$) spend approximately the same time interval T_1 within the beam confine. For this time interval T_1 , the time-averaged relative electron-beam and proton-beam velocity components as given by Eq. (34) to (39) become

$$\begin{aligned} \langle v_{ex} \rangle &= \tan \theta \cdot \frac{E_z}{B} \frac{1}{\psi_e} \left[1 - \cos(\psi_e) \right] \\ &\quad - \sin \theta \cdot \left[v_b \sin \theta - \frac{E_y}{B} \right] \left[1 - \frac{1}{\psi_e} \sin(\psi_e) \right] \end{aligned} \quad (34)$$

$$\begin{aligned} \langle v_{ey} \rangle &= \frac{E_z}{B \cos \theta} \cdot \left[1 - \frac{1}{\psi_e} \sin(\psi_e) \right] \\ &\quad + \left[v_b \sin \theta - \frac{E_y}{B} \right] \frac{1}{\psi_e} \left[1 - \cos(\psi_e) \right] \end{aligned} \quad (35)$$

$$\begin{aligned} \langle v_{ez} \rangle &= - \frac{E_z}{B} \frac{1}{\psi_e} \left[1 - \cos(\psi_e) \right] \\ &\quad + \cos \theta \cdot \left[v_b \sin \theta - \frac{E_y}{B} \right] \left[1 - \frac{1}{\psi_e} \sin(\psi_e) \right] \end{aligned} \quad (36)$$

$$\begin{aligned} \langle v_{px} \rangle &= - \tan \theta \cdot \frac{E_z}{B} \frac{1}{\psi_p} \left[1 - \cos(\psi_p) \right] \\ &\quad - \sin \theta \cdot \left[v_b \sin \theta - \frac{E_y}{B} \right] \left[1 - \frac{1}{\psi_p} \sin(\psi_p) \right] \end{aligned} \quad (37)$$

$$\langle v_{py} \rangle = \frac{E_z}{B \cos \theta} \left[1 - \frac{1}{\psi_p} \sin(\psi_p) \right] - \left(v_b \sin \theta - \frac{E_y}{B} \right) \left(\frac{1}{\psi_p} \right) [1 - \cos(\psi_p)] \quad (38)$$

$$\langle v_{pz} \rangle = \frac{E_z}{B} \left(\frac{1}{\psi_p} \right) [1 - \cos(\psi_p)] + \cos \theta \cdot \left(v_b \sin \theta - \frac{E_y}{B} \right) \left[1 - \frac{1}{\psi_p} \sin(\psi_p) \right] \quad (39)$$

where $\psi_e = \omega_e T_{\parallel} = \frac{2eBR_0}{mv_b \sin 2\theta}$ and

$$\psi_p = \omega_p T_{\parallel} = \frac{2eBR_0}{Mv_b \sin 2\theta}$$

We expect electron-beam collision to occur for $\langle |\vec{v}_{eb}| \rangle \neq 0$, i.e., non-zero time-averaged magnitude of the relative electron-beam velocity vector

$\vec{v}_{eb} = \vec{v}_e - \vec{v}_b$. From Eqs. (36) to (40), we have

$$\langle |\vec{v}_{eb}| \rangle = \left[\langle v_{ex} \rangle^2 + \langle v_{ey} \rangle^2 + \langle v_{ez} \rangle^2 \right]^{1/2} = \langle v_{eb} \rangle$$

where the right-hand side can be simplified in the following manner to give an upper limiting value for $\langle |\vec{v}_{eb}| \rangle$.

Firstly, we let $E_y = v_b B \sin \theta = v_b B_x$, i.e., the electric field E_y is such that the charged particles move with the beam with velocity v_b . In a self-consistent space-charged polarization field, this would represent the upper limiting value for E_y . Secondly, we let $E_z = v_b B \cos \theta$, which represents the optimum E_z for charged particles having drift velocity v_b in y -direction, which, however, is balanced by $E_x = -v_b B \sin \theta$, on account of transverse field condition $E_x B_x + E_z B_z = 0$.

Similarly, proton-beam collision occurs for

$\langle |\vec{v}_{pb}| \rangle \neq 0$. From Eqs. (34) to (39), we can obtain

$$\langle v_{eb} \rangle^2 = \langle |\vec{v}_{eb}| \rangle^2 = \langle v_{ex} \rangle^2 + \langle v_{ey} \rangle^2 + \langle v_{ez} \rangle^2$$

and $\langle v_{pb} \rangle^2 = \langle |\vec{v}_{pb}| \rangle^2 = \langle v_{px} \rangle^2 + \langle v_{py} \rangle^2 + \langle v_{pz} \rangle^2$

We will now consider two limiting cases: namely, "transient" case with zero electric field, and "steady state" case with optimum electric field.

We let $E_x = E_y = E_z = 0$, and Eqs. (34) to (36) become,

$$\langle v_{ex} \rangle_0 = v_b \sin^2 \theta \left[\left(\frac{1}{\psi_e} \right) \sin(\psi_e) - 1 \right]$$

$$\langle v_{ey} \rangle_0 = v_b \sin \theta \left(\frac{1}{\psi_e} \right) [1 - \cos(\psi_e)]$$

$$\langle v_{ez} \rangle_0 = v_b \sin \theta \cdot \cos \theta \left[\left(\frac{1}{\psi_e} \right) \sin(\psi_e) - 1 \right]$$

and from which we finally get

$$\frac{\langle v_{eb} \rangle_0^2}{v_b^2} = \sin^2 \theta \left\{ 2 \left(\frac{1}{\psi_e} \right)^2 [1 - \cos(\psi_e)] + 1 - 2 \left(\frac{1}{\psi_e} \right) \sin(\psi_e) \right\} \quad (40)$$

where the subscript "o" denotes quantities with zero electric field.

Examination of Eq. (40) shows that the factor

$$\left\{ 2 \left(\frac{1}{\psi_e} \right)^2 [1 - \cos(\psi_e)] + 1 - 2 \left(\frac{1}{\psi_e} \right) \sin(\psi_e) \right\} = F(\theta)$$

is symmetric with respect to $\theta = 45^\circ$ (also the angle for minima), increases from $\theta < 45^\circ$ (and $\theta > 45^\circ$) with maxima at $\theta < 1^\circ$ (and $\theta > 89^\circ$) and then oscillates with decreasing amplitudes and increasing frequency and finally converges to unite at $\theta = 0^\circ$ (and 90°). These features are graphically given by Figure 3, Figure 4(a) and Figure 4(b).

The $\sin^2 \theta$ term in Eq. (40) destroys the symmetry of $F(\theta)$ with respect to $F(\theta)$ with respect to $\theta = 45^\circ$. The quantity $\langle v_{eb} \rangle_0^2 / v_b^2$ approaches zero as

$\theta \rightarrow 0^\circ$ and is unity at $\theta = 90^\circ$. At $\theta = 0^\circ$, we have agreement with the expected physical situation, i.e., all charged particles travel with velocity \vec{v}_b within the beam confine. At $\theta = 90^\circ$, we have upper limiting value of unity, which is larger than the actual value depending on the ratio R_0/R_e (or R_0/R_p for proton).

We now consider the situation at $\theta = 90^\circ$ with the aid of Figure 5. From the expression for the time interval $T_{\parallel} = \frac{2R_0}{v_b \sin 2\theta}$, as $\theta \rightarrow 90^\circ$, we have

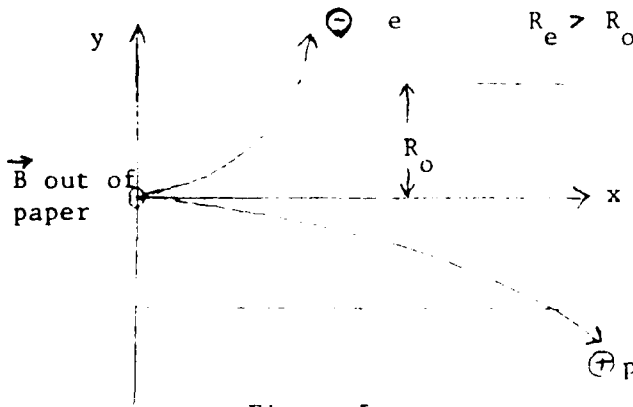


Figure 5

$\dot{z}_e = 0$, $\dot{x}_e = v_b \cos \omega_e t$ and $\dot{y}_e = v \sin \omega_e t$. Since $T_{\parallel} \rightarrow \infty$, the time-averaged quantities $\langle \dot{x}_e \rangle$ and $\langle \dot{y}_e \rangle$ are both zero. Referring to Figure 5, we can see that $\langle \dot{y}_e \rangle$ is indeed zero within the beam confine regardless of the R_0/R_e . However,

$\langle \dot{x}_e \rangle$ is not zero for $R_0/R_e < 2$ ($\langle \dot{x}_e \rangle$ is zero for $R_0/R_e > 2$). To obtain the correct value for $\langle \dot{x}_e \rangle$ within the beam confine, we proceed as follows.

First, we designate τ as the time required for the electron to reach R_0 from the origin, and we have

$$\int_0^{\tau} \dot{y}_e dt = y_e(\tau) - y_e(0) = R_e = v_b \left(\frac{1}{\omega_e} \right) [1 - \cos(\omega_e \tau)],$$

from which we get

$$\cos(\omega_e \tau) = 1 - \frac{R_0}{R_e}$$

From $\theta < 90^\circ$, the situation described above still holds, and we can write

$$\cos(\omega_e \tau) = \cos(\sigma_e) = 1 - \frac{R_o}{R_e \sin \theta}$$

Incorporation of the above results leads to two different expressions for $\langle v_{eb} \rangle_0^2 / v_b^2$ as follows:

$$\frac{\langle v_{eb} \rangle_0^2}{v_b^2} = \sin^2 \theta \left\{ 2 \left(\frac{1}{\psi_e} \right)^2 [1 - \cos(\psi_e)] + 1 - 2 \left(\frac{1}{\psi_e} \right) \sin(\psi_e) \right\} \quad (40)$$

$$\text{where } \psi_e = \frac{2R_o}{R_e \sin 2\theta}, \text{ with } \theta < 90^\circ$$

and

$$\frac{\langle v_{eb} \rangle_0^2}{v_b^2} = \sin^2 \theta \cdot \left(\frac{1}{\sigma_e} \right)^2 [1 - \cos(\sigma_e)]^2 \quad (41)$$

$$\text{where } \sigma_e = \cos^{-1} \left[1 - \frac{R_o}{R_e \sin \theta} \right], \text{ with } \theta \approx 90^\circ.$$

Similarly, for the proton case, we have

$$\frac{\langle v_{pb} \rangle_0^2}{v_b^2} = \sin^2 \theta \left\{ 2 \left(\frac{1}{\psi_p} \right)^2 [1 - \cos(\psi_p)] + 1 - 2 \left(\frac{1}{\psi_p} \right) \sin(\psi_p) \right\} \quad (42)$$

$$\text{where } \psi_p = \frac{2R_o}{R_p \sin 2\theta} = \frac{\psi_e}{1883}, \text{ with } \theta < 90^\circ$$

and

$$\frac{\langle v_{pb} \rangle_0^2}{v_b^2} = \sin^2 \theta \cdot \left(\frac{1}{\sigma_p} \right)^2 [1 - \cos(\sigma_p)]^2 \quad (43)$$

where $\sigma_p = \cos^{-1} \left[1 - \frac{R_o}{R_p \sin\theta} \right]$, with $\theta = 90^\circ$.

These two pair of equations, Eqs. (40), (41) and Eqs. (42), (43), represent the results for the "transient" case where the electric field is zero, i.e., beam propagation time duration is too short for the formation of space-charge field.

We now consider the "steady state" case where the space-charge (polarization) field has been fully established. To approximate the proper space-charge field which is to be obtained from a self-consistency calculation, we propose the following field specifications:

$$E_y = v_b B \sin\theta$$

$$E_z = v_b B \cos^2\theta \cdot \sin\theta$$

$$E_x = -v_b B \cos\theta \cdot \sin^2\theta$$

These field components agree with the reasonable physical requirements as described in the following:

- (1) $E_y = E_z = E_x = 0$ for $\theta = 0^\circ$
- (2) $E_y = v_b B$, $E_z = E_x = 0$ for $\theta = 90^\circ$
- (3) $\left| \vec{E} \right| = v_b B \sin\theta \sqrt{1 + \cos^2\theta}$, with maximum $\left| \vec{E} \right| = v_b B$ at $\theta = 90^\circ$.

In conditions (2) and (3), we have assumed optimum polarization field strength so that E_y (and \vec{E}) = $v_b B$, i.e., the charged particle velocity is equal to beam velocity v_b . Substituting these field components in Eqs. (34)

to (39), we obtain the corresponding "steady state" results as follows:

$$\frac{\langle v_{eb} \rangle^2}{v_b^2} = \frac{1}{4} (\sin 2\theta)^2 \left\{ 2 \left(\frac{1}{\psi_e} \right)^2 [1 - \cos(\psi_e)] + 1 - 2 \left(\frac{1}{\psi_e} \right) \sin(\psi_e) \right\} \quad (44)$$

$$\text{where } \psi_e = \frac{2R_o}{R_e \sin 2\theta}, \text{ with } \theta < 90^\circ,$$

$$\frac{\langle v_{eb} \rangle^2}{v_b^2} = \frac{1}{4} (\sin 2\theta)^2 \left(\frac{1}{\sigma_e} \right)^2 [1 - \cos(\sigma_e)]^2 \quad (45)$$

$$\text{where } \sigma_e = \cos^{-1} \left[1 - \frac{R_o}{R_e \sin \theta} \right], \text{ with } \theta \approx 90^\circ,$$

$$\frac{\langle v_{pb} \rangle^2}{v_b^2} = \frac{1}{4} (\sin 2\theta)^2 \left\{ 2 \left(\frac{1}{\psi_p} \right)^2 [1 - \cos(\psi_p)] + 1 - 2 \left(\frac{1}{\psi_p} \right) \sin(\psi_p) \right\} \quad (46)$$

$$\text{where } \psi_p = \frac{2R_o}{R_p \sin 2\theta}, \text{ with } \theta < 90^\circ$$

and

$$\frac{\langle v_{pb} \rangle^2}{v_b^2} = \frac{1}{4} (\sin 2\theta)^2 \left(\frac{1}{\sigma_p} \right)^2 [1 - \cos(\sigma_p)]^2 \quad (47)$$

$$\text{where } \sigma_p = \cos^{-1} \left[1 - \frac{R_o}{R_p \sin \theta} \right], \text{ with } \theta \approx 90^\circ.$$

To obtain the electron-beam "impact" energy E_{I0} for the transient field-free case, we first let $H(\alpha, \theta, f) = \langle v_{eb} \rangle_0^2 / v_b^2$ as given by Eq. (40) and write

$$E_{I0} = \frac{1}{2} m \langle v_{eb} \rangle_0^2 = \frac{1}{2} m v_b^2 H(\alpha, \theta, f) \quad (48)$$

$$\text{where } \alpha = \sqrt{\frac{10^6 \text{ eV}}{E_b}} \text{ and } f = \frac{R_o}{10 \text{ cm}}$$

we thus have $\psi_e = \frac{2R_0}{R_e \sin 2\theta} = \frac{(0.12690113)\alpha f}{\sin 2\theta}$

Noting that the beam radius $R_0 = f \times 10 \text{ cm}$ and the beam energy

$E_b = \frac{1}{2} M v_b^2 = 10^6 \text{ eV} / \alpha^2$, we can express E_{I0} as a function of E_b , R_0 and θ .

Similarly, the electron-beam impact energy E_I for the steady-state space-charge field case can be written as

$$E_I = \frac{1}{2} m \langle v_{eb} \rangle^2 = \frac{1}{2} m v_b^2 G(\alpha, \theta, f) \quad (49)$$

where $G(\alpha, \theta, f)$ is given by Eq. (44) with the same ψ_e as given in Eq. (48). E_I can again be expressed as a function of E_b , R_0 and θ . It should be mentioned that E_I is symmetric with respect to $\theta = 45^\circ$.

Figures 6(a) to 6(d) show E_I versus E_b (with seven values of R_0) for $\theta = 2^\circ, 5^\circ, 10^\circ$ and 45° respectively. Figures 7(a) to 7(q) show E_{I0} versus E_b (with eleven values of R_0) for $\theta = 5^\circ, 10^\circ, 15^\circ, \dots, 85^\circ$ respectively. The important results from Figs. 6(c) and 6(d) can be stated as follows:

- (1) The critical beam radius R_0 is 55cm, with an impact energy of 16e and an ionization cross-section σ_I equal to $0.1 (\pi a_0^2)$. [Note that $\pi a_0^2 = 1.13673 (10^{-16} \text{ cm}^2)$]. These values are constant for E_b ranging from 1Mev to 100 Mev.
- (2) For θ ranging from 10° to 80° and E_b from 5 Mev to 100 Mev, R_0 and the corresponding ionization cross section σ_I are tabulated in the following

R_0 in cm	60	70	80	90	100
σ_I in πa_0^2	0.2	0.5	0.6	0.7	0.8

- (3) For $\theta < 5^\circ$ (and $\theta > 85^\circ$), E_I decreases for $E_b < 40$ Mev. The decreases are more pronounced for larger R_0 , smaller θ and E_b .

The important features shown by Figs. 7(a) to 7(r) are as follows:

- (1) For the same values of beam radius R_0 , the impact energy E_{I0} increases with the angle θ .
- (2) For the R_0 and θ , E_{I0} is almost constant for beam energy E_b ranging from 10 MeV to 100 MeV.
- (3) For E_b ranging from 1 MeV to 10 MeV, E_{I0} decreases with E_b , and the decreases are pronounced from larger R_0 .
- (4) For $\theta = 5^\circ$, the critical R_0 is again 55cm for $E_b > 10$ MeV, and for $\theta = 80^\circ$, E_{I0} is 18 eV for $R_0 = 10$ cm.

Because of large proton to electron mass ratio $M/m = 1843$, we have null result for the case of ionization by protons. In other words, $\langle v_{pb} \rangle_0^2 / v_b^2$ and $\langle v_{pb} \rangle^2 / v_b^2$ as given by Eq. (42) and Eq. (46) respectively are less than 8×10^{-8} (even for the largest $R_0 = 100$ cm), with resulting impact energies less than the threshold ionization energies.

IV. ESTIMATE OF THE GEOMETRIC FACTOR

In this Report our principal aim has been to elucidate the dependence of the degradation of the electron impact energy on the different beam parameters. However, as discussed in the Introduction, the BIS process requires that two conditions be met: the electrons have to acquire sufficient energy for ionization and they have to be retained for a sufficiently long time within the beam to be able to interact with the beam particles. To be more precise, the electrons, in general, leave and re-enter the beam region many times. Thus, in I we have defined a "geometric factor" γ , $\gamma < 1$ which describes phenomenologically the reduction of the collision probability due to the reduced time the electrons spend within the beam. The calculation of the geometric factor for a general situation will be the subject of another Report. Some comments, however, are in order.

The mean free path of an electron with respect to ionizing collisions with the beam particles is obviously quite long, comparable to the beam degradation length. For beam propagation at very small angle the magnetic field can force the electrons to re-enter the beam many times (even though they acquire a perpendicular velocity component in the stripping process) and to effectively travel with the beam. Details of this process were discussed in I. For an arbitrary propagation angle, it is the combined effect of polarization electric field and of magnetic field that is expected to cause the electron to re-enter and travel with the beam. The details of this scenario are to be discussed in a separate Report. However, for the purpose of the calculations in the present Report we have ignored the re-entry of the electrons and calculated averages over the short time while the electron is in the beam after its emergence. We believe that because of the quasiperiodicity of the motion, this doesn't seriously affect the results concerning the velocity averaging.

It should be noted that the conditions relating to the relative velocity, on the one hand, and to the geometric factor, on the other, are in general, contradictory. Extended stay within the beam requires traveling with the beam particles and thus low average relative velocity. The difficulty is partly due, however, to the model used for our calculation, where the relative velocity is identified with the relative average velocity. Thus, in extreme situations, the latter may become zero, while the former does not. Obviously, a more rigorous calculation is called for in such cases.

The most difficult problem in a rigorous handling of the particle trajectories would be the self-consistent determination of the polarization electric field. Since such calculation is much beyond the scope of the present Report, in Section III we have used a simple physical model for the representation of the electric field. This model includes a component parallel to the beam velocity (always perpendicular, however, to the magnetic field). The justification for the existence of such a parallel component, which is not contemplated in the usual theories of cross-field propagation [3], can be found through a simple glance at the geometry generated by a neutral particle beam moving at an angle to the magnetic field and undergoing stripping. Over a distance small compared to the ion gyro-radius, the beam carries a net positive charge (since the ions deviate little from their original path), while the electrons create a triangular wedge, fanning out along the beam. It is expected that such a geometry will indeed give rise to a parallel component of the electric field.

V. CONCLUSIONS

The following conclusions emerge from this study:

1. As already discussed in I, the BIS process can become, at high altitudes, a non-negligible contribution to beam degradations. While in I we discussed the case of propagation parallel to the magnetic field, in the present Report we considered a general propagation direction at an arbitrary angle to the magnetic field.
2. The propagation of the beam at an angle to the magnetic field causes the electrons generated by the BIS process to acquire sufficient relative velocity to induce further stripping. The stripping cross section by electrons being, however, a sensitive function of the impact energy (see Fig. 8), which in turn, is a function of the beam energy, angle of propagation and beam diameter, the beam attenuation coefficient becomes a function of all these parameters, in addition to the beam current density which determines the density of the beam particles. These dependences are shown in Figs. 9 through 16. There are two major kinematic approximations used in these calculations: (a) representing the relative velocity by the average relative velocity and (b) calculating averages over the first portion of the particle's trajectory within the beam. Apart from extreme situations, both of these approximations are reasonable and also can be easily removed in future work.
3. The polarization electric field plays an important role in guiding the electrons along the beam. The determination of this field for an arbitrary propagation angle is an extremely complicated task: no attempt has been made in this direction in the present Report. We have used, however, a reasonable model for representing the polarization field and we have calculated effects both without (corresponding to a "transient"

situation) and with polarization fields. The differences can be assessed by comparing Figs. 3 and 4, Figs. 6 and 7 and Figs 9-12 and 13-16, respectively. In Section II.1 we have also examined the effect of the inhomogeneity of the electric field and have found that if the scale length of the inhomogeneity, say γ satisfies $\gamma < \frac{E}{B} \frac{1}{\omega_c}$ the usual drift, trajectories change into open trajectories and lead to an unbounded motion which cannot be described in terms of the customary drift trajectories.

REFERENCES

1. Carini, P., G. Kalman and P. Pulsifer: "Neutral Beam Propagation Through the Upper Atmosphere", AFGL-TR-85-0038, 1984.
2. Alfven, H., Rev. Mod. Phys. 32, 4 (1960) 710.
3. Schmidt, G., Phys. Fluids 3, 6 (1960) 961, and the following works:
Lindberg, L., Astrophys. and Space Science 55 (1978) 203; Peter, W., A. Ron and N. Rostoker, Phys. Fluids 22 (8) (1979) 1471; Peter W. and N. Rostoker, Phys. Fluids 25, 4 (1982) 730; Marhovic, P.D. and F.R. Scott, Phys. Fluids 14 8 (1971) 1742; Kamada R.C. Onada et al, J. Phys. Soc. Japan Letters 46 6 (1979) 1963; Robertson, S., H. Ishizuka, W. Peter and N. Rostoker, Phys. Rev. Lett. 47, 7 (1981) 508; Wessel F. and S. Robertson, Phys. Fluids 24, 4 (1981) 739.
4. Kieffer, L.J., and G.H. Dunn: Rev. Mod. Phys. 38 (1966) 1.

$F(\theta)$ versus θ . (There is a symmetry with respect to $\theta = 45^\circ$.) Same maximum value = 1.59 at $\theta = 57'$ for 1 MeV, $\theta = 19'$ for 9 MeV and $\theta = 11'$ for 25 MeV.

Fig. 3

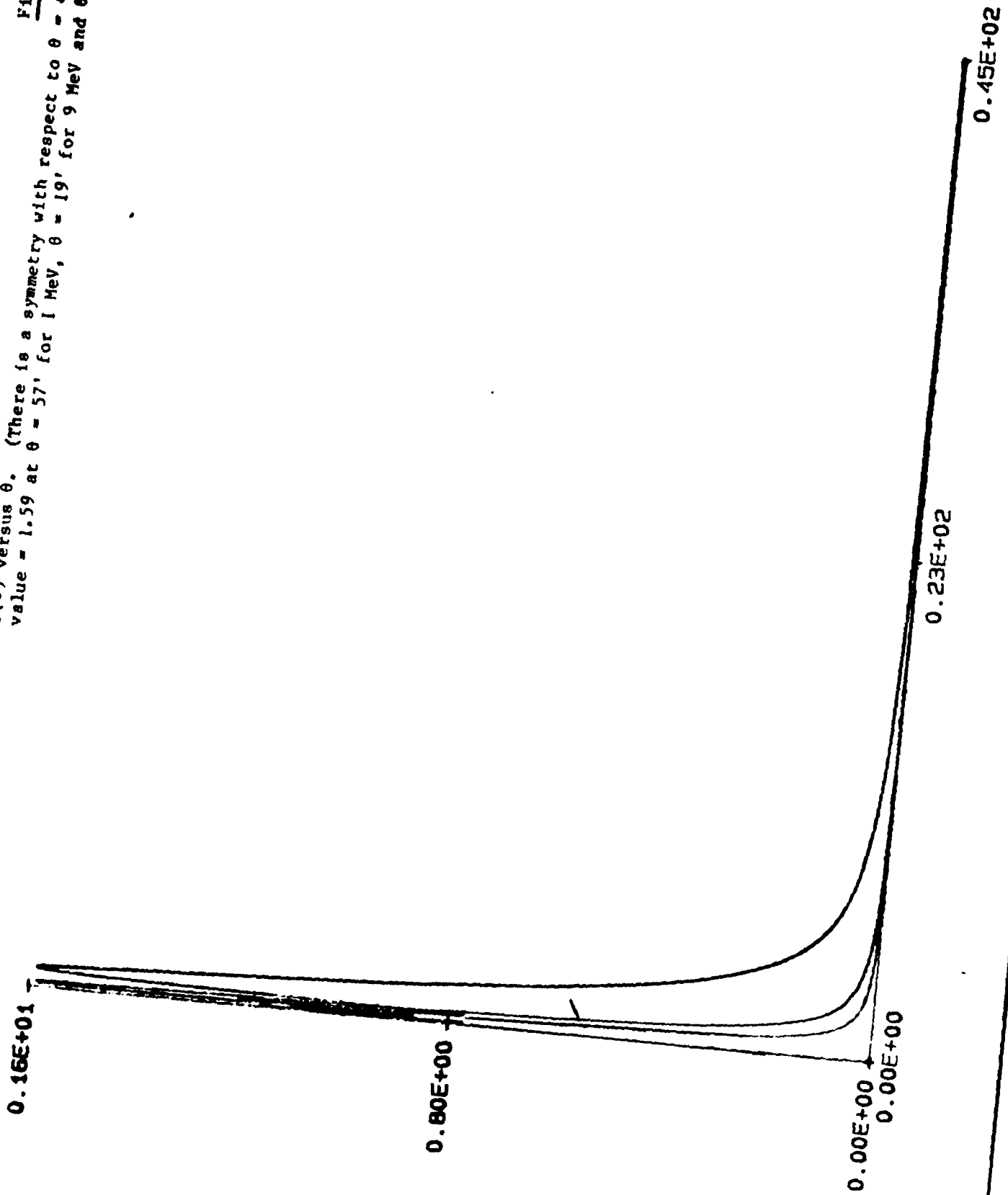


Fig. 4(a)

$F(\theta)$ versus θ . Same maximum value = 1.59 at $\theta = 57'$ for 1 MeV,
 $\theta = 19'$ for 9 MeV and $\theta = 11'$ for 25 MeV. Same converging value =
1 at $\theta = 0^\circ$.

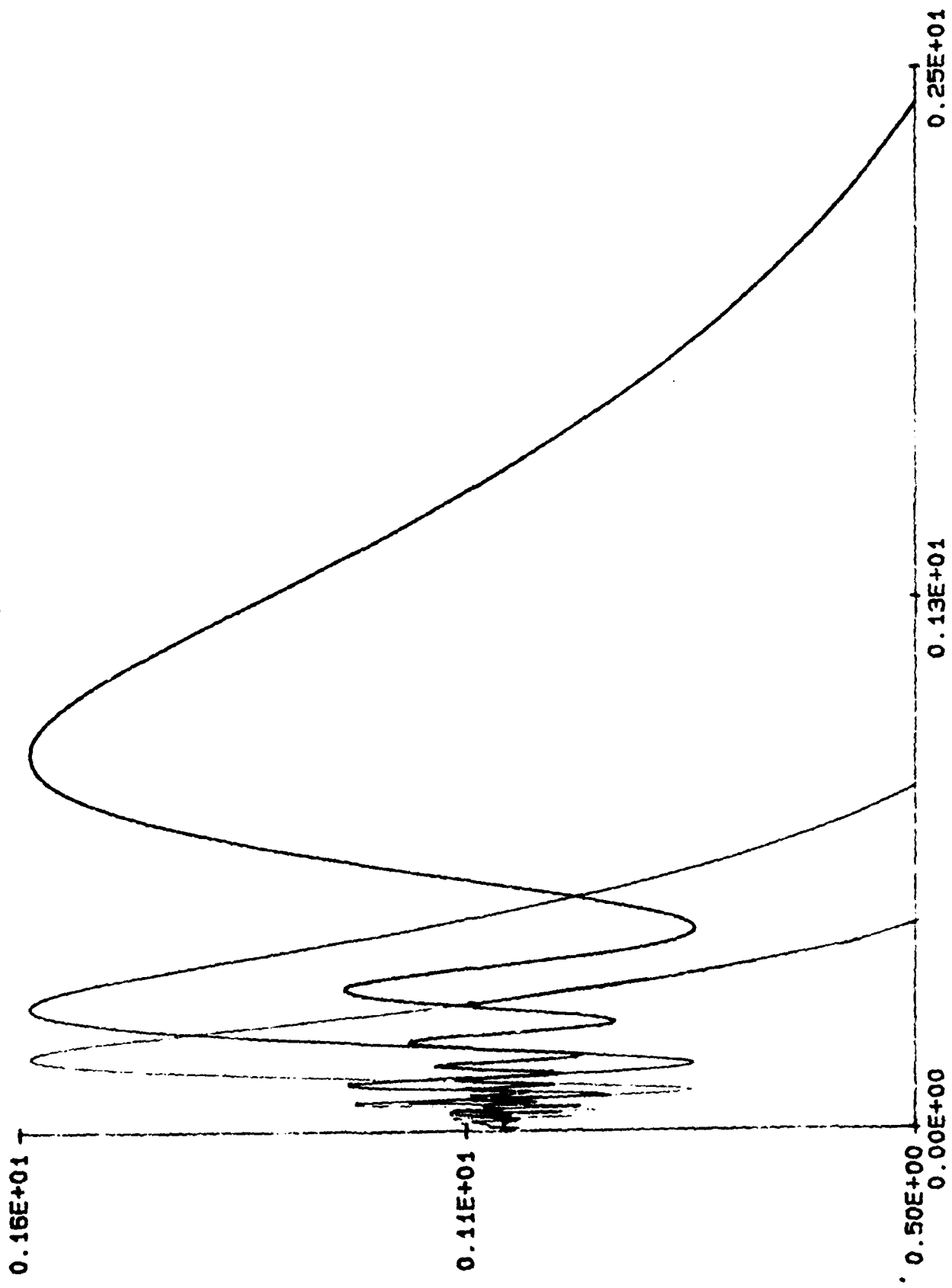


Fig. 4(b)
F(θ) versus θ . Similar to (a) at complementary angles ($\theta \rightarrow 90^\circ - \theta$)

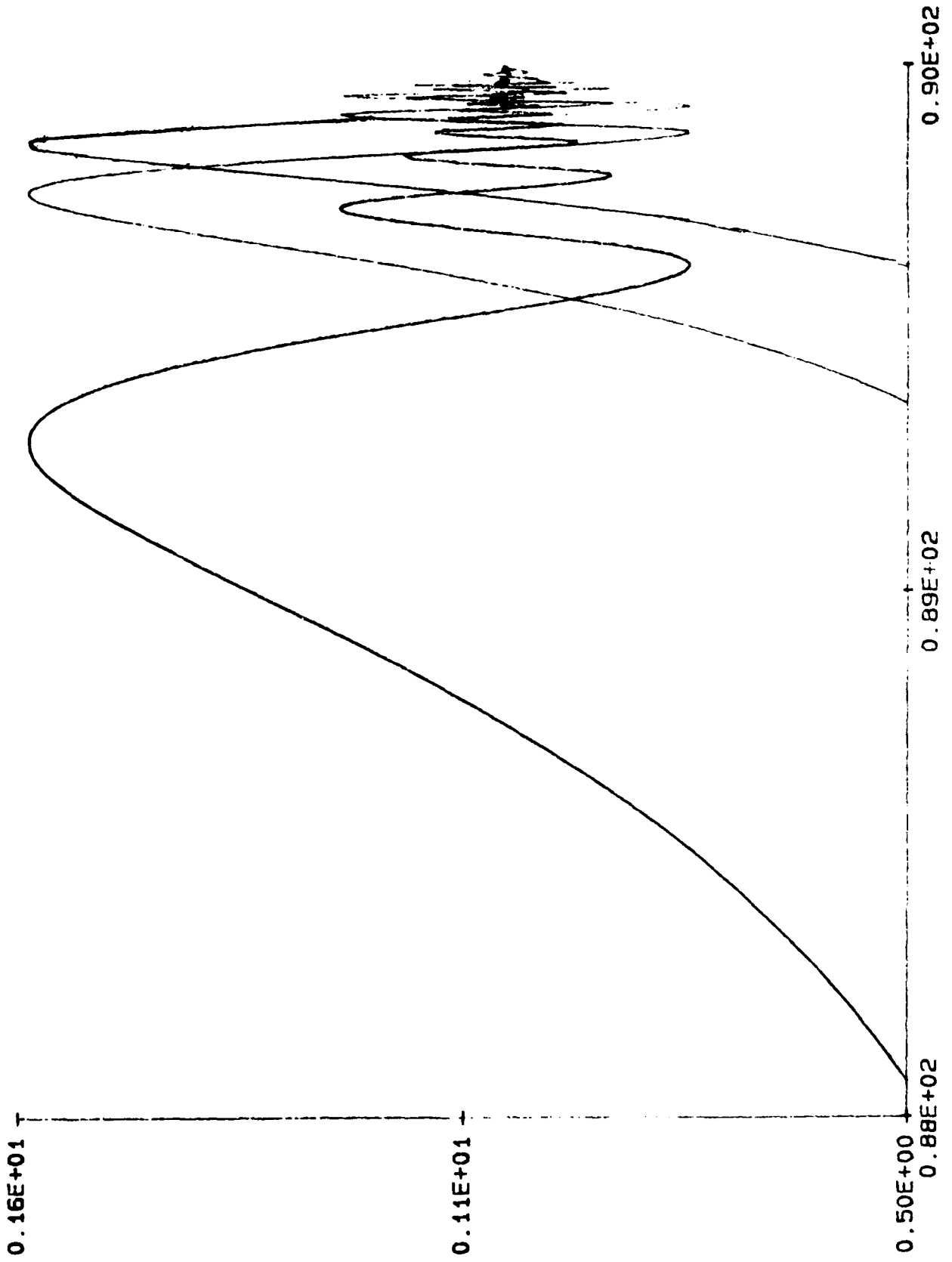


Fig. 6(a)

$\theta = 2^\circ$

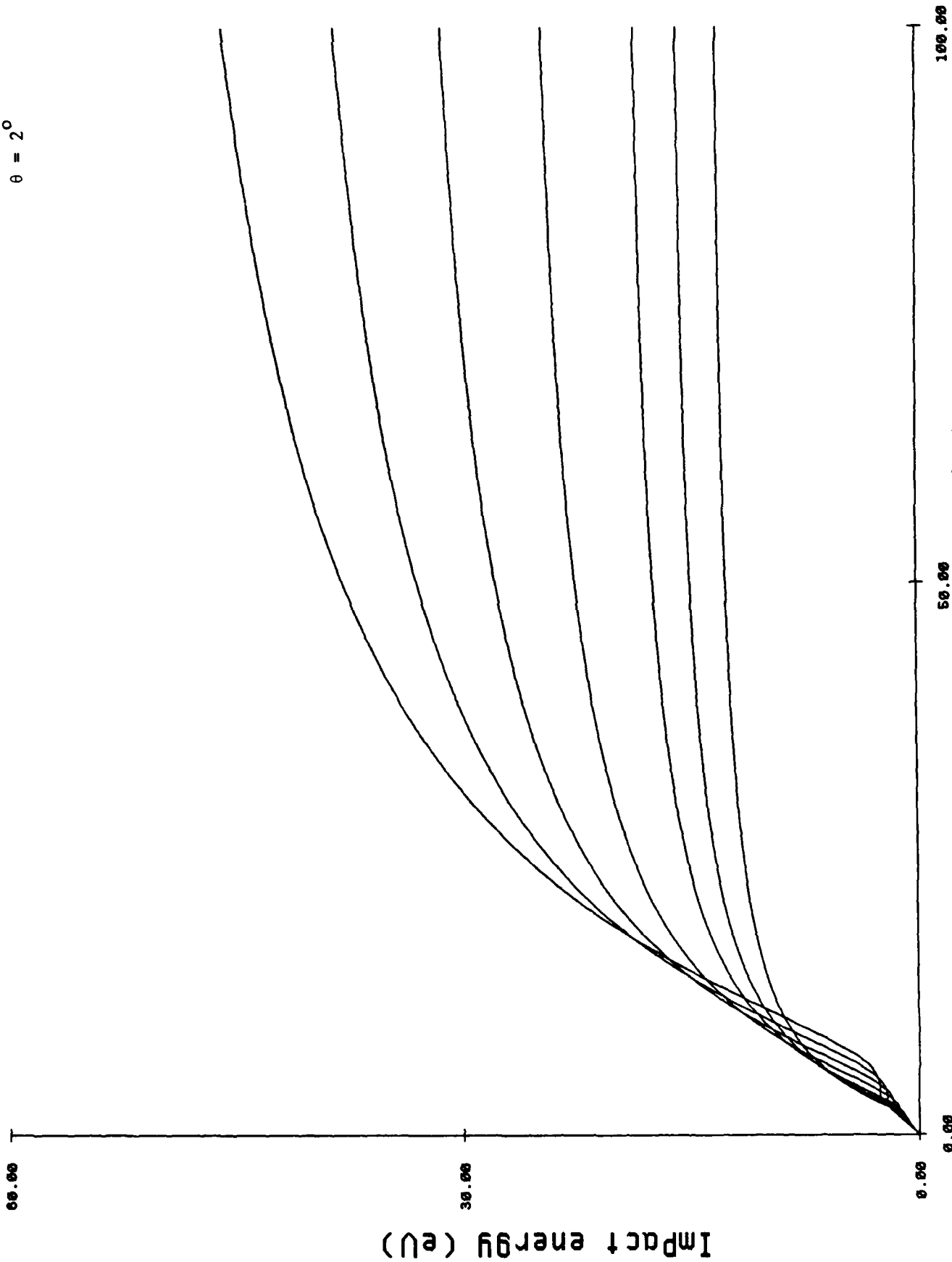


Fig. 6(a): Beam energy (MeV), $\theta = 2^\circ$

FIG. 6(b)

$\theta = 5^\circ$

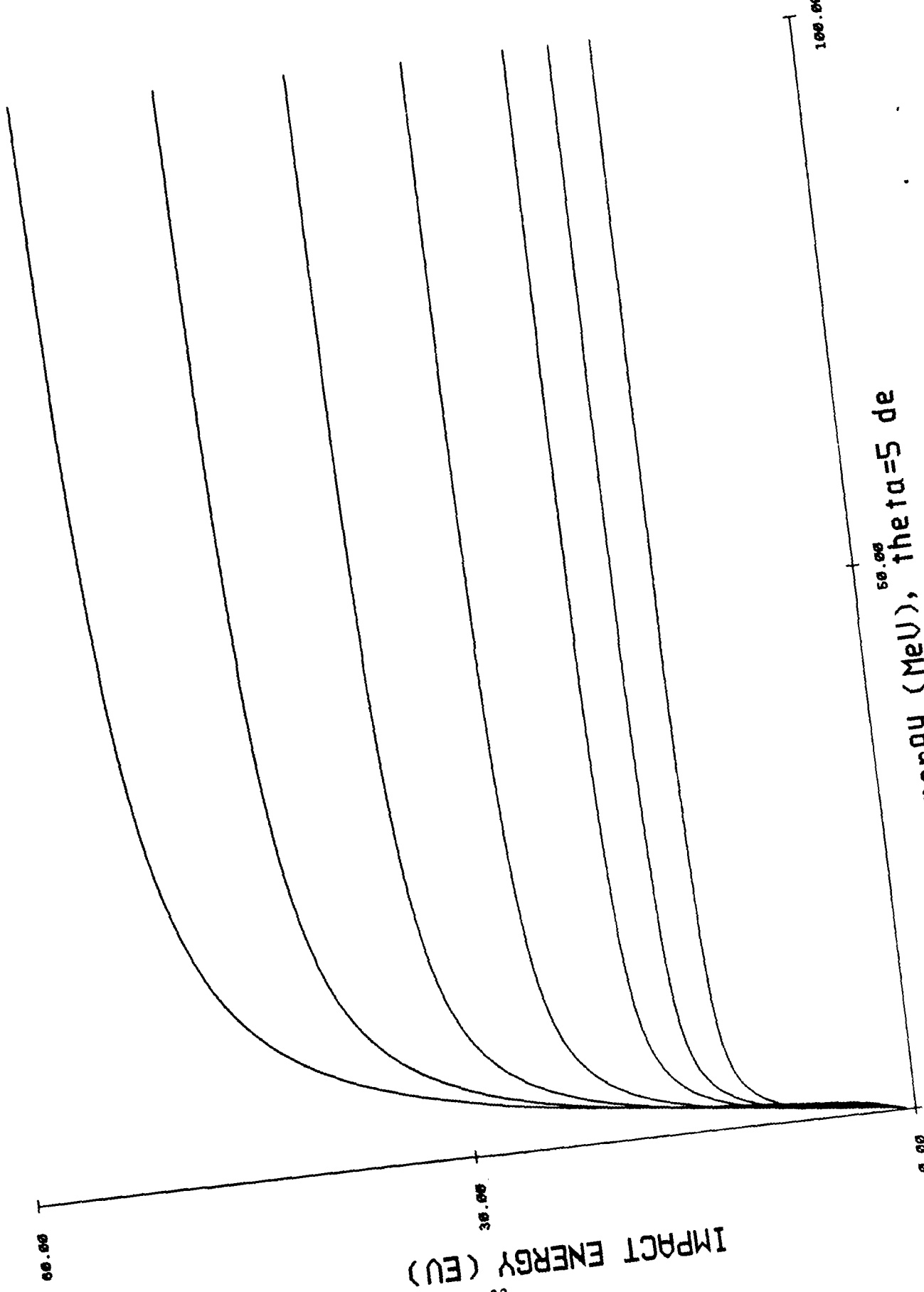


Fig. 6(b): Beam energy (MeV), $\theta = 5^\circ$

IMPACT ENERGY (eV)

Fig. 6(c)

$\theta = 10^\circ$

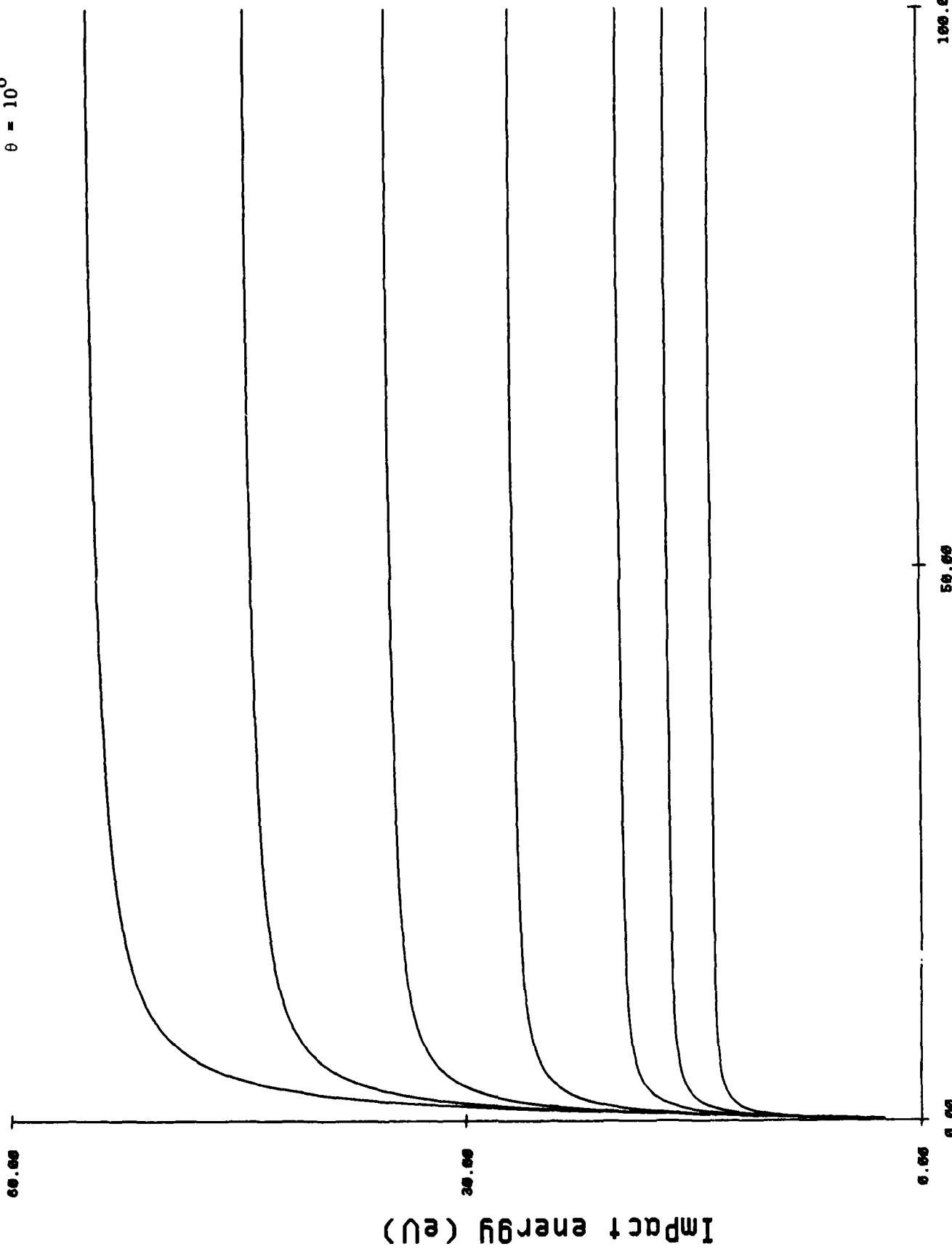


Fig. 6(c): Beam energy (MeV), 10° .

Fig. 6(d)

$\theta = 45^\circ$

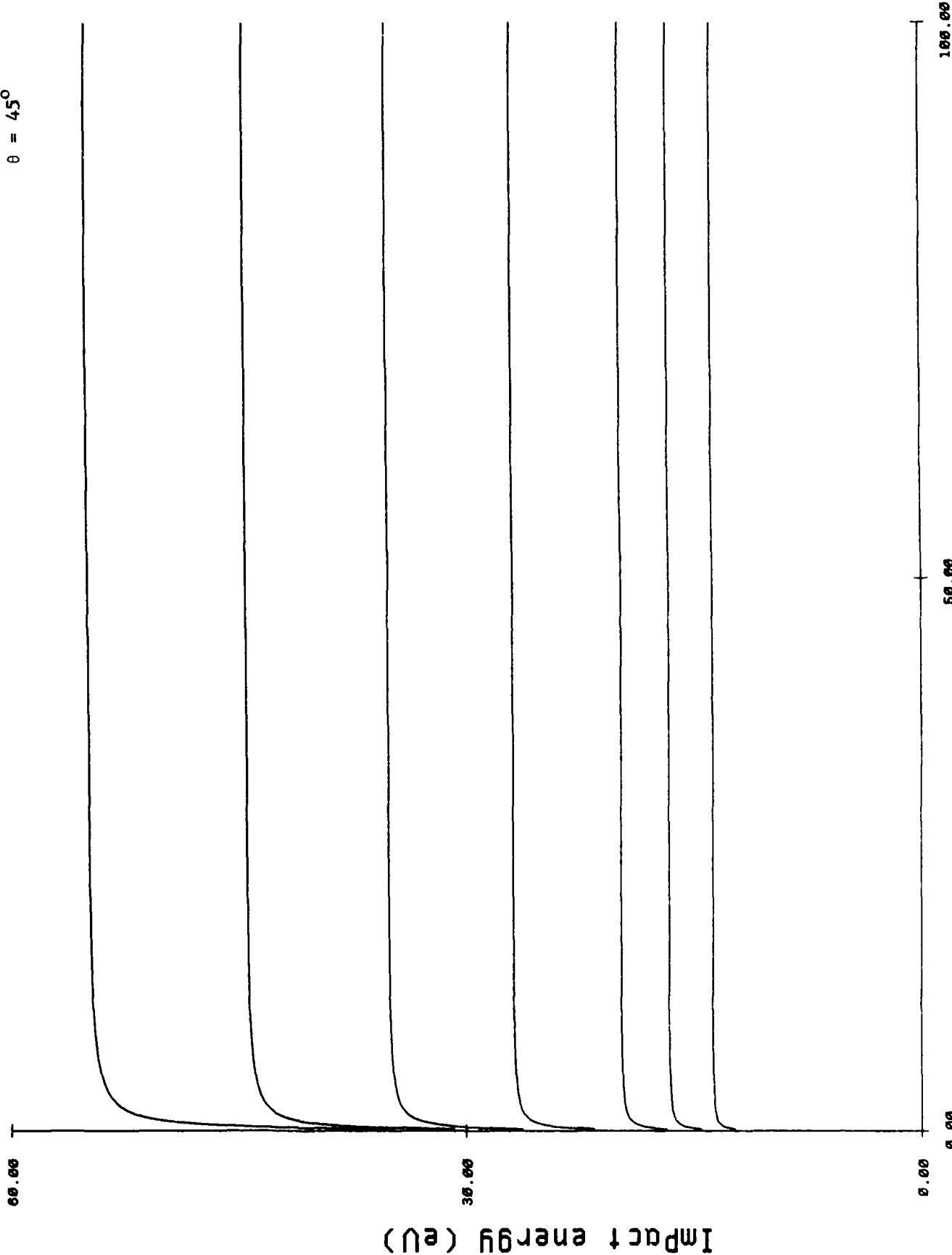


Fig 6(d): Beam energy (MeV), 45 de9.

Impact energy (eV)

Fig. 7(a)

E_{I_0} versus E_b , $\theta = 15^\circ$

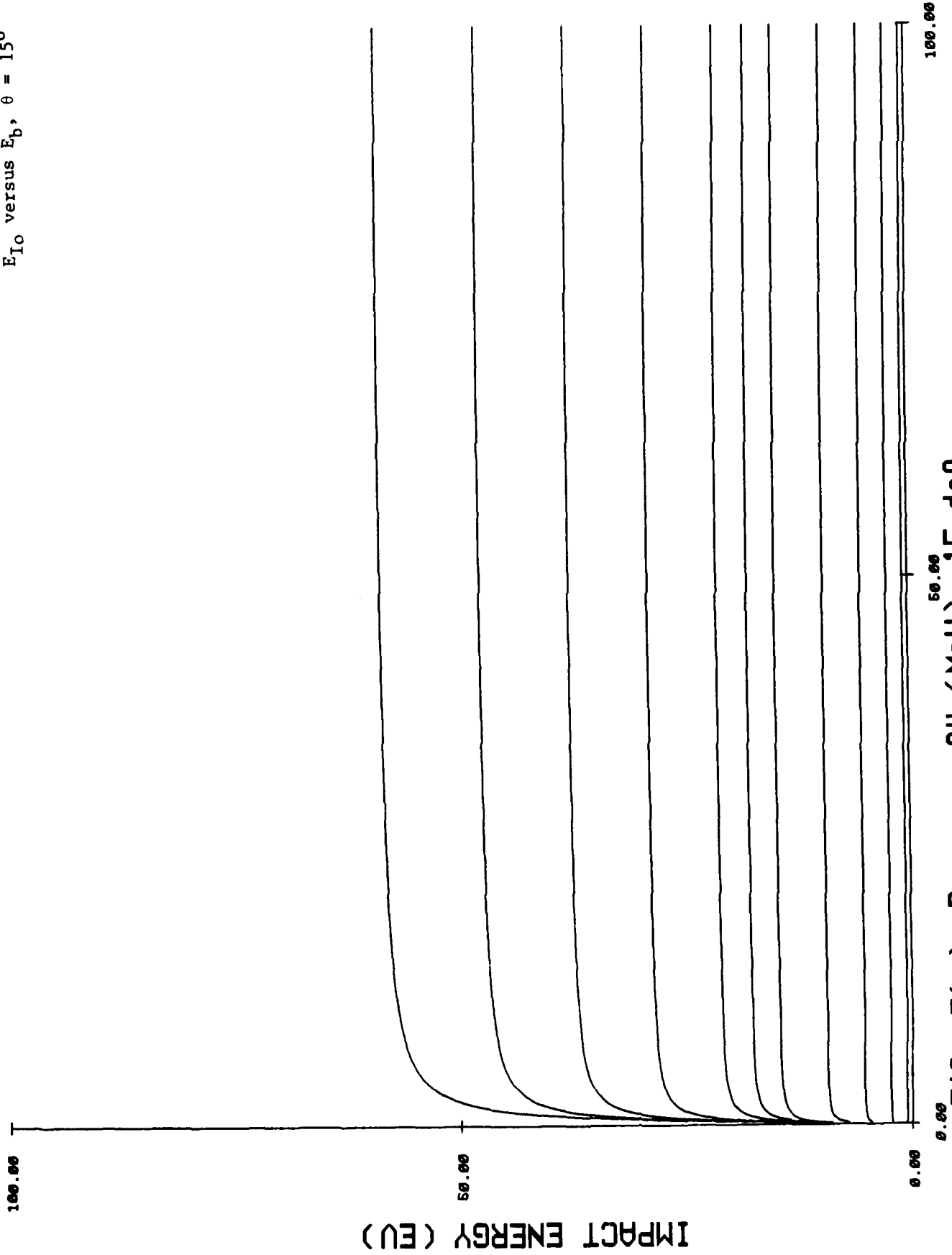


Fig. 7(a): Beam energy (MeU), 15 de9.

Fig. 7(b)

E_{I0} versus E_b , $\theta = 20^\circ$

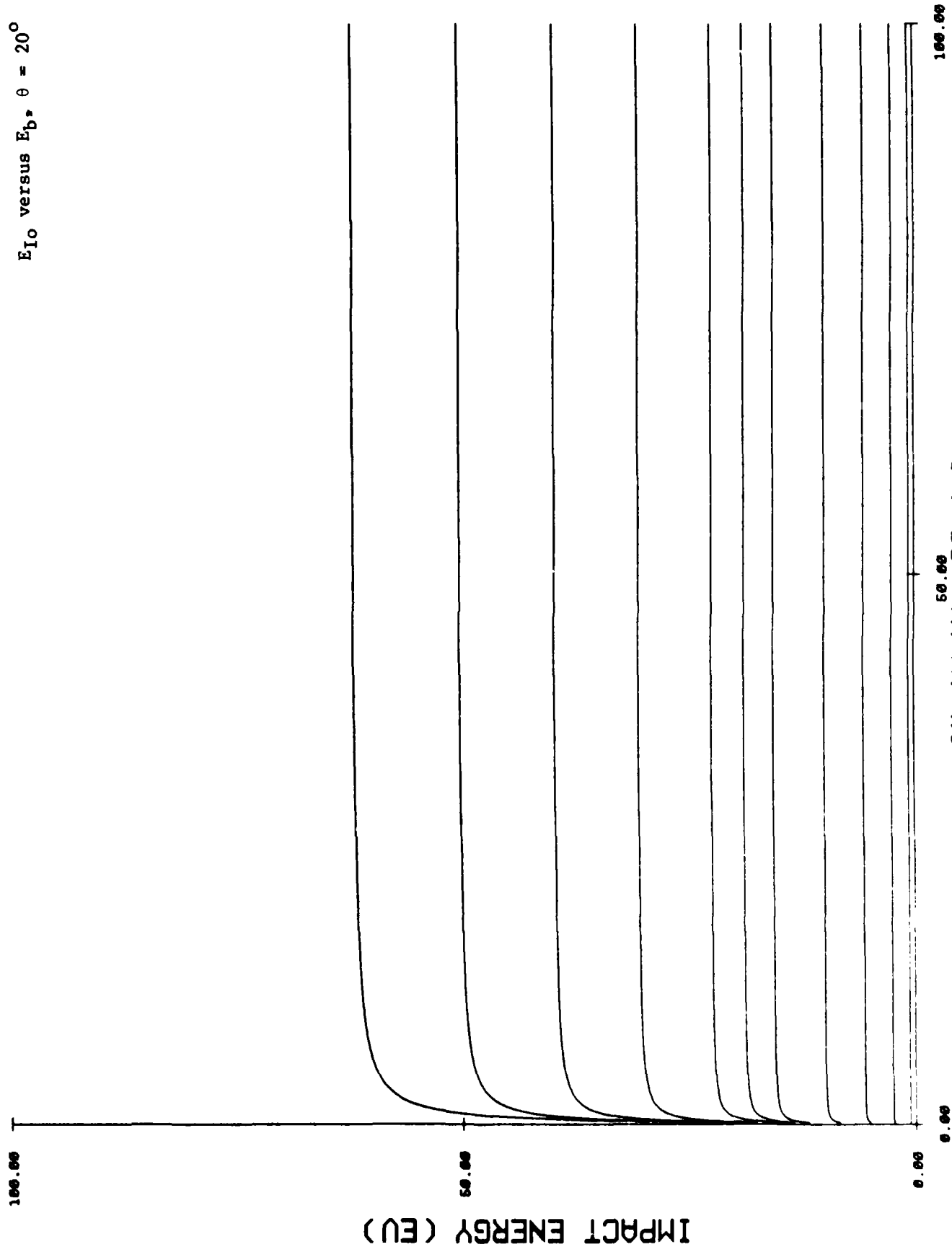


Fig. 7(b): Beam energy (MeV), 20 deg.

Fig. 7(c)

E_{I0} versus E_b , $\theta = 25^\circ$

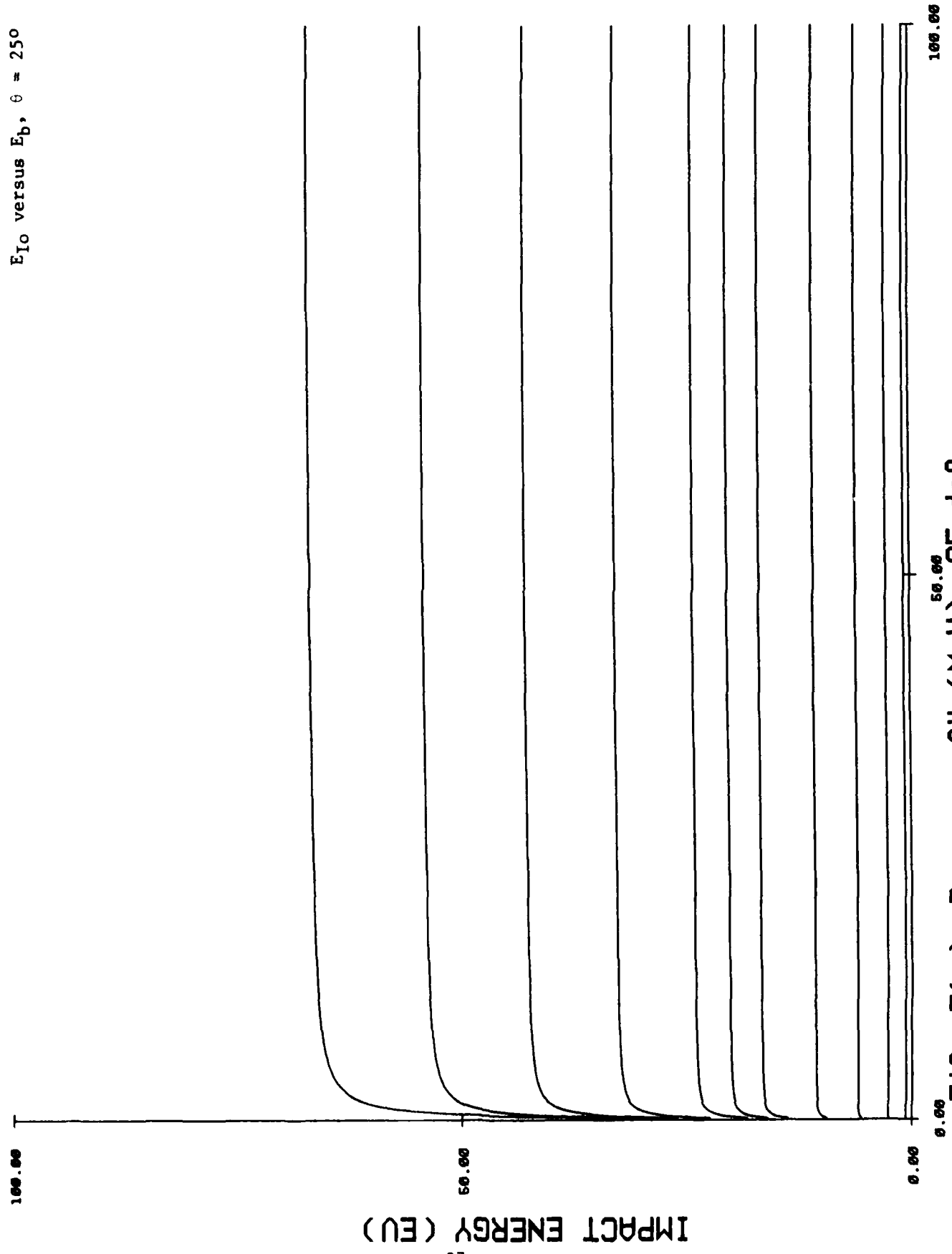


Fig. 7(c): Beam energy (MeV), 25 de9.

Fig. 7(d)

E_{I0} versus E_b , $\theta = 30^\circ$

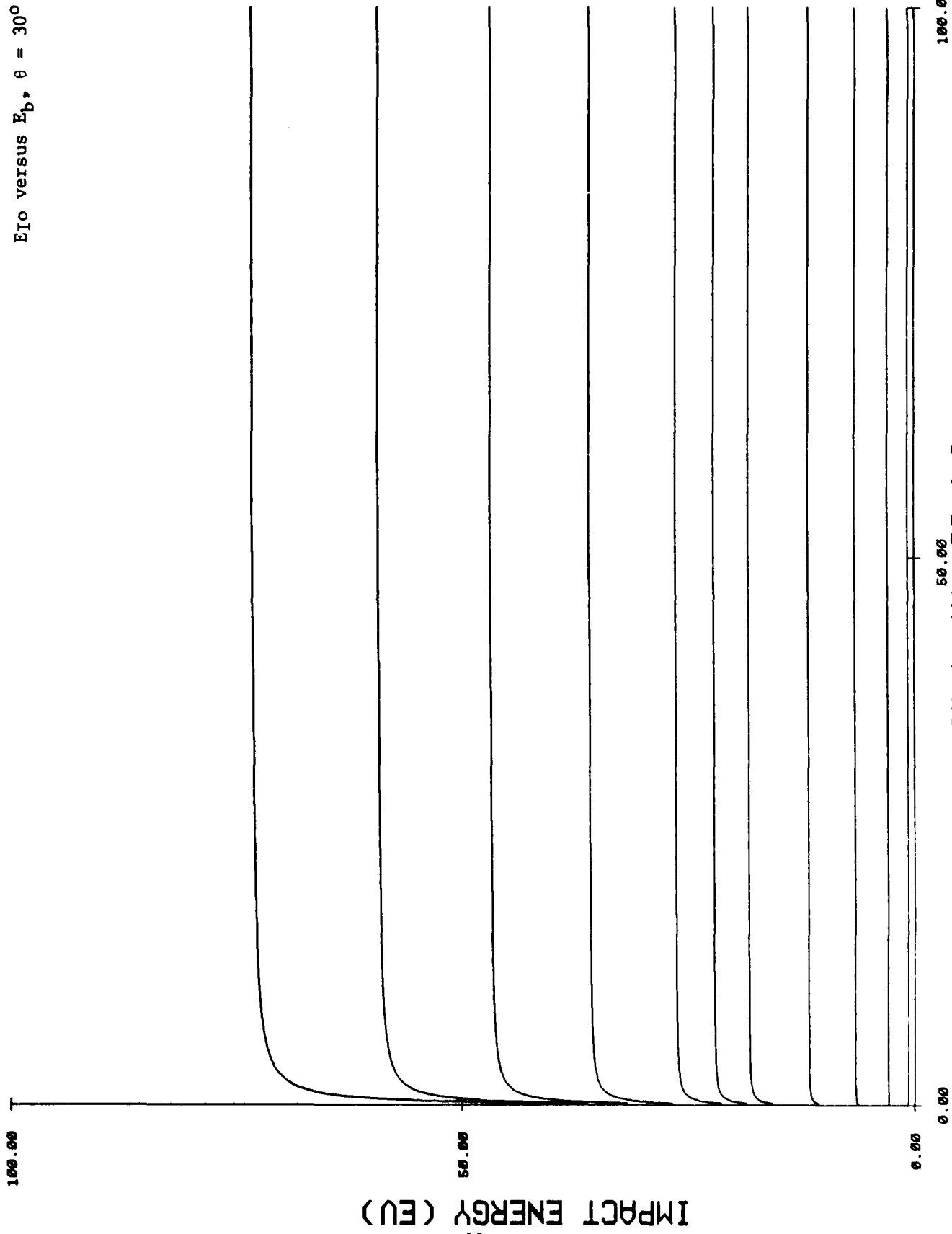


Fig. 7(d): Beam energy (MeU), 30 de9.

Fig. 7(e)

E_{I0} versus E_b , $\theta = 35^\circ$

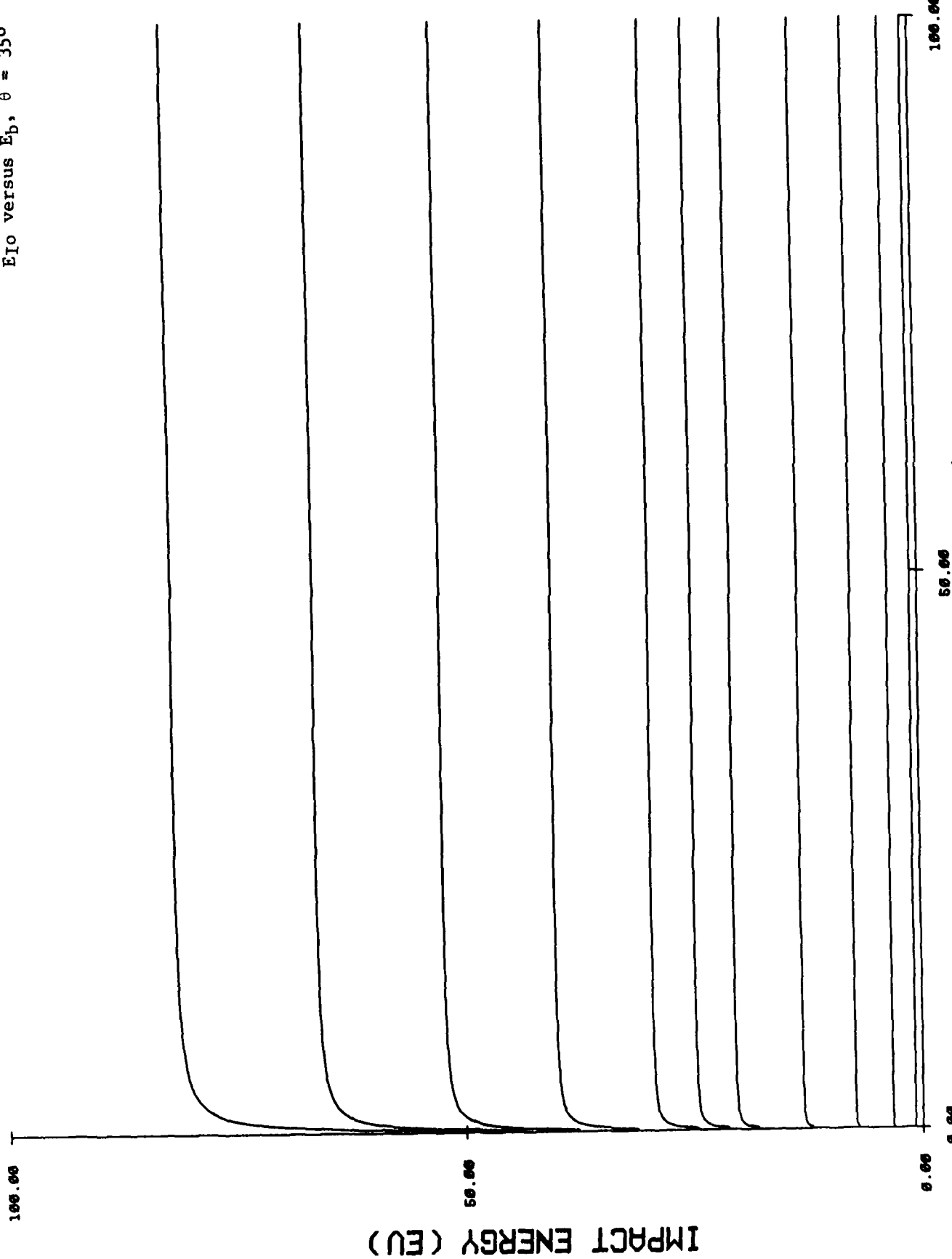


Fig. 7(E): Beam energy (MeU), 35 deg.

Fig. 7(f)

E_{I0} versus E_b , $\theta = 40^\circ$

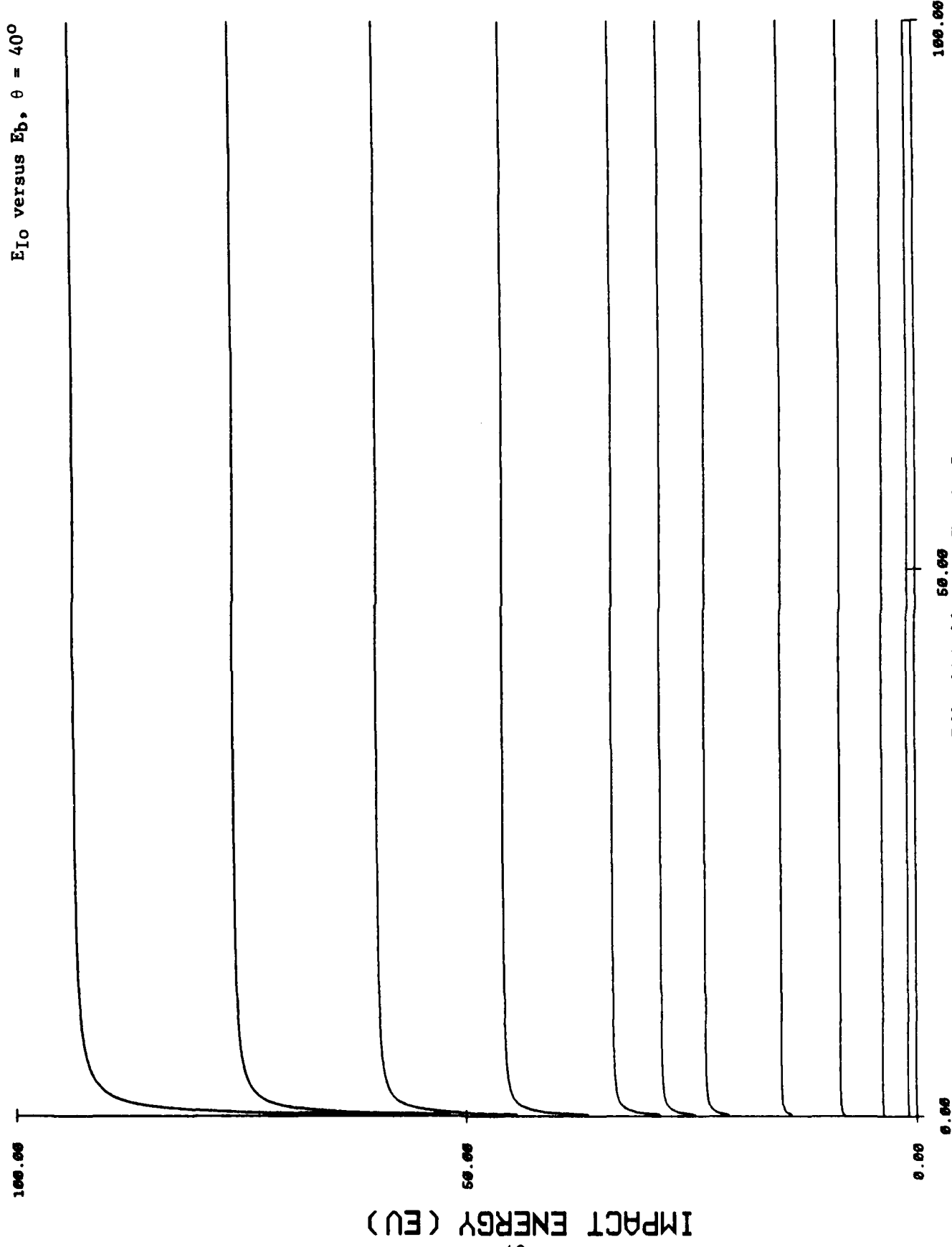


Fig. 7(f): Beam energy (MeV), 40 de9.

Fig. 7(b)

E_{i0} versus E_b , $\theta = 45^\circ$

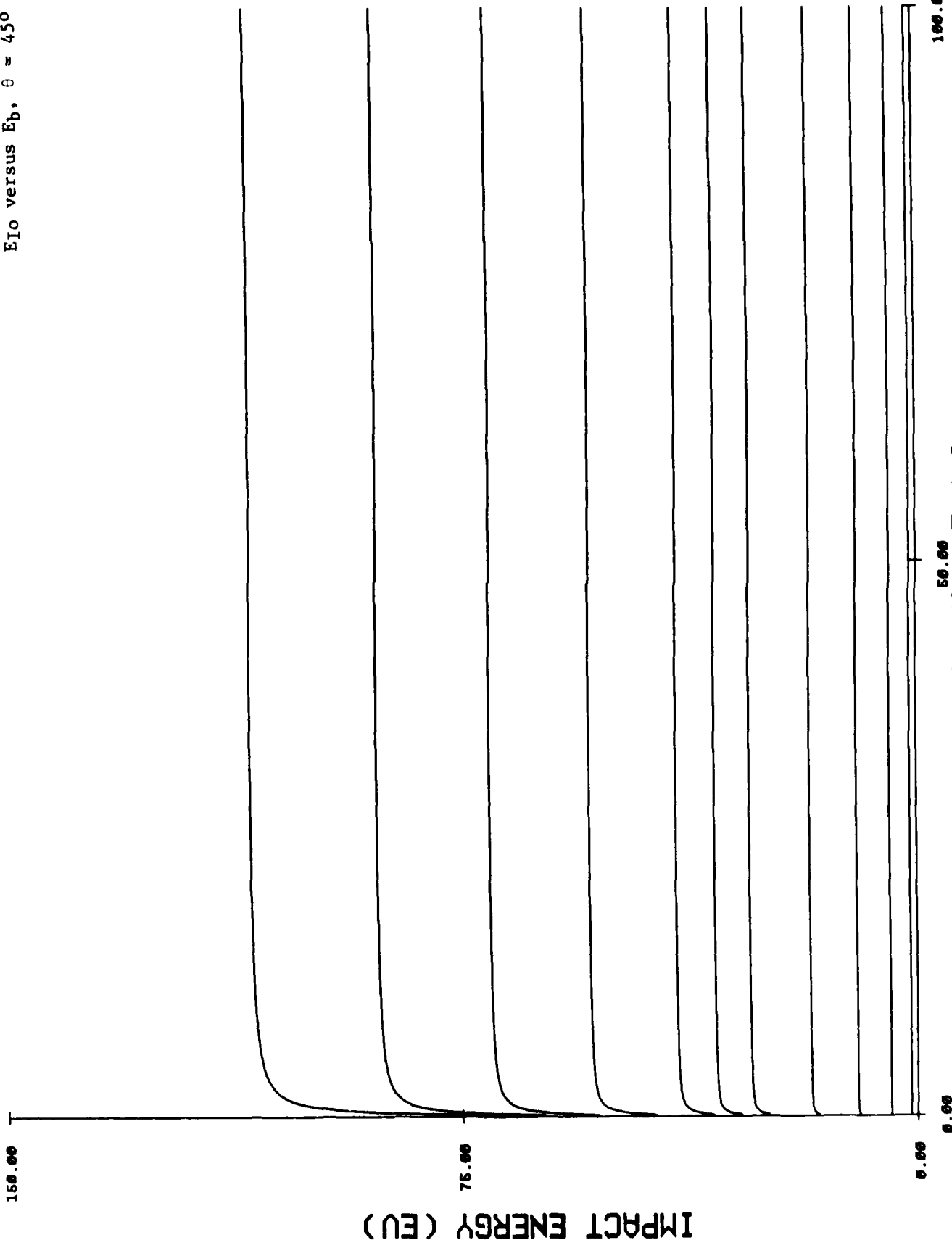


Fig. 7(9): Beam energy (MeV), 45 de9.

Fig. 7(h)

E_{I0} versus E_b , $\theta = 50^\circ$

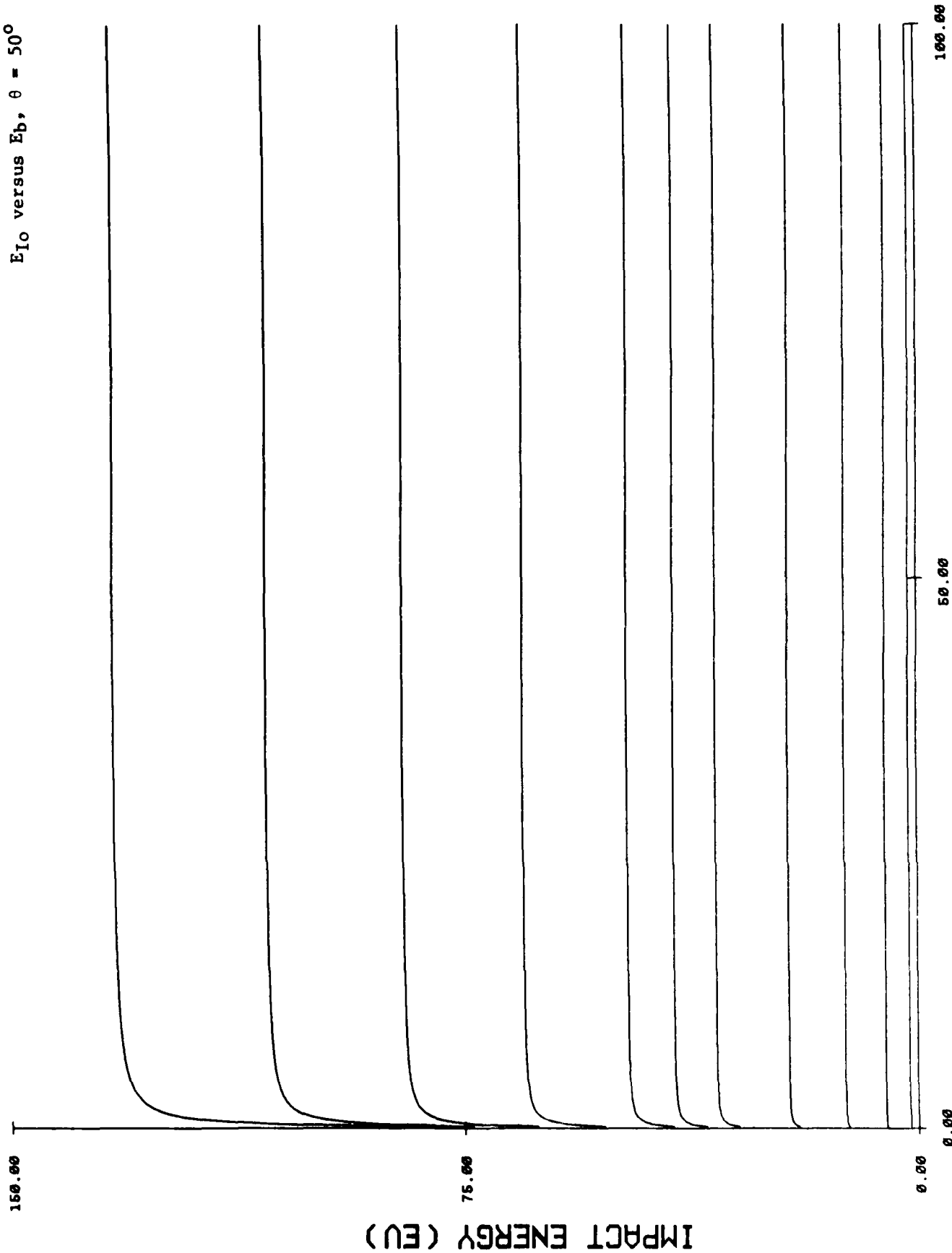


Fig. 7(h): Beam energy (MeV), 50 de9.

Fig. 7(1)

E_{I_0} versus E_b , $\theta = 55^\circ$

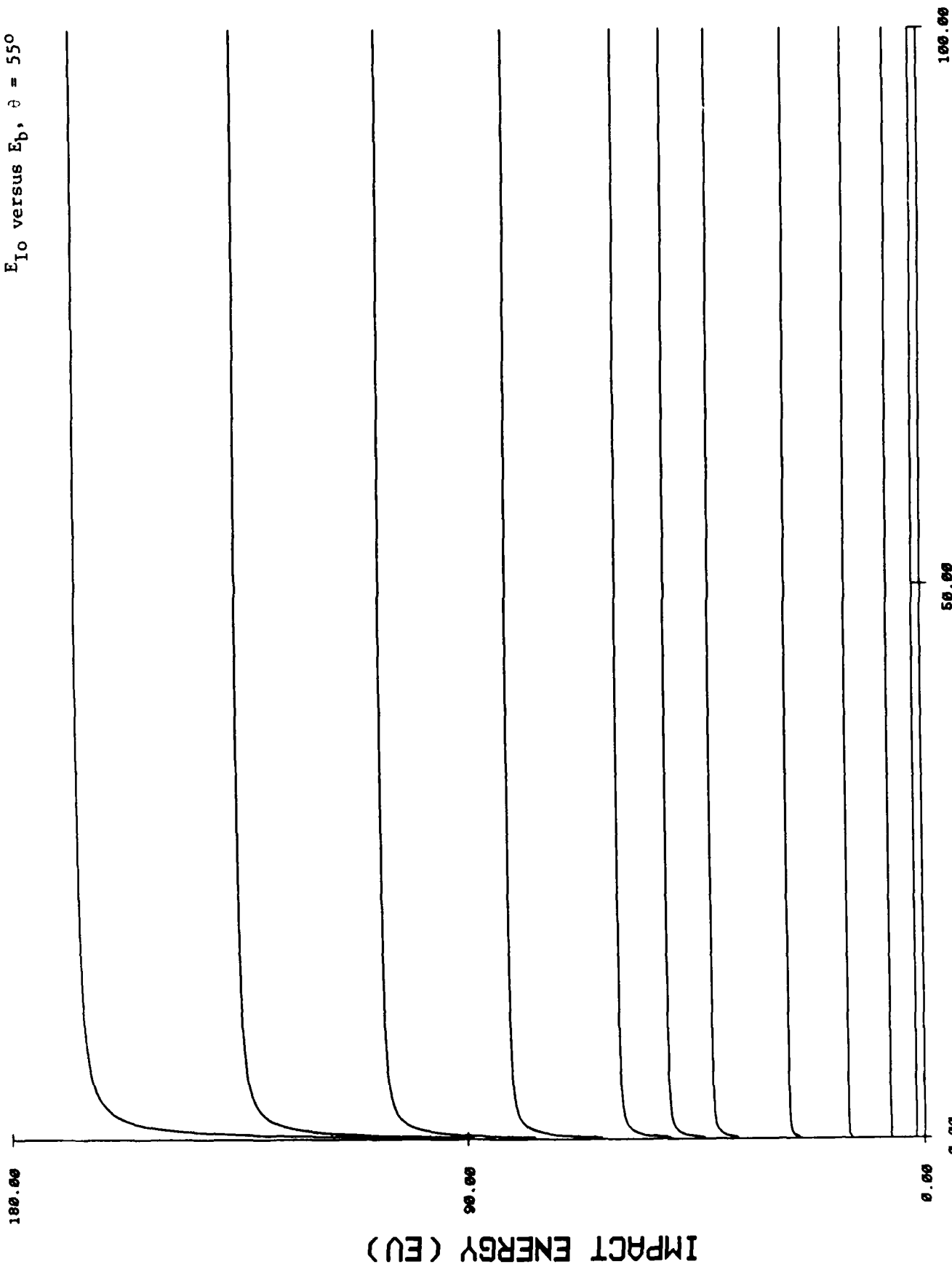


Fig. 7(i): Beam energy (MeU), 55°

Fig. 7(j)

E_{i0} versus E_b , $\theta = 60^\circ$

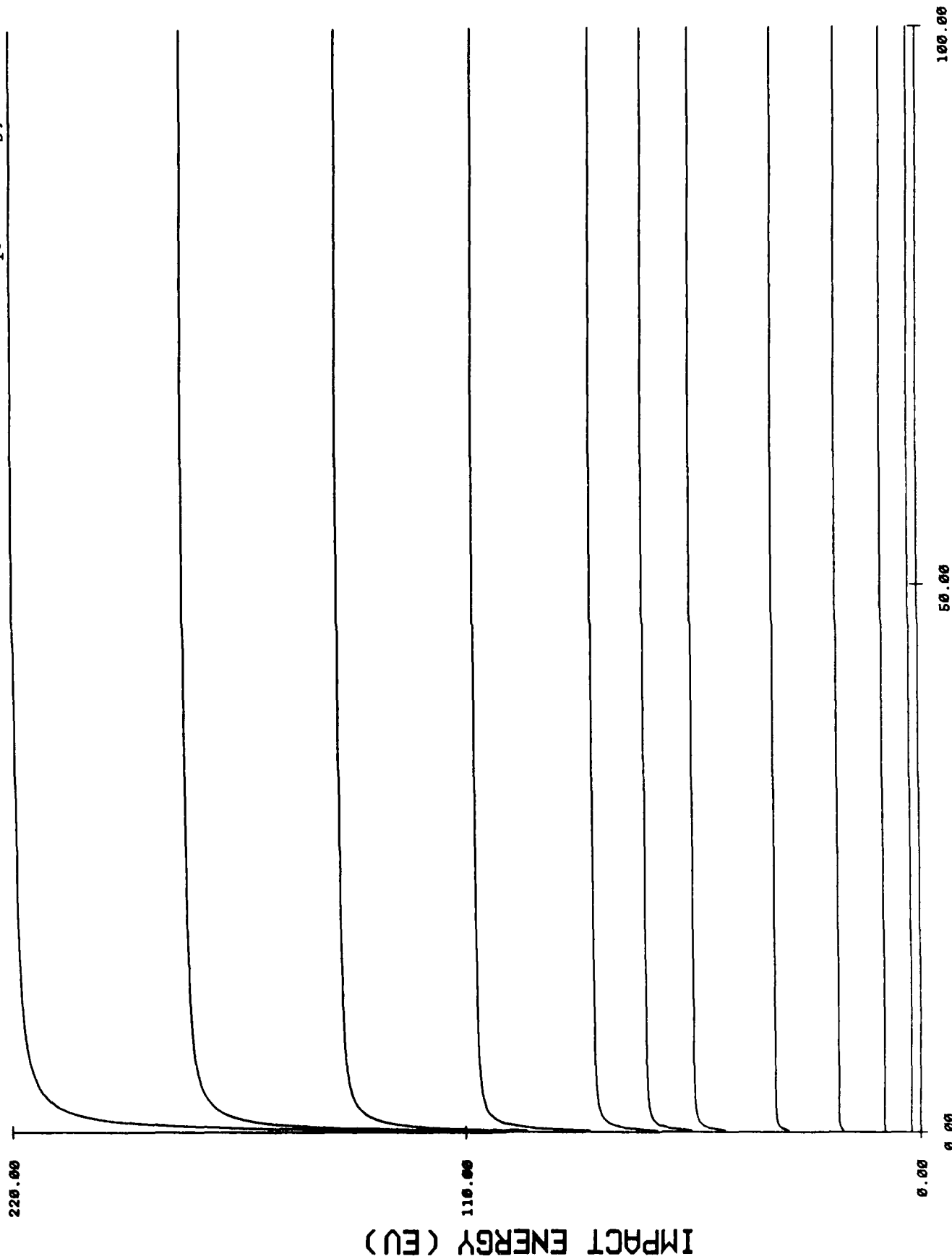


Fig. 7(j): Beam energy (MeU), 60° .

Fig. 7(k)

E_{Io} versus E_b , $\theta = 65^\circ$

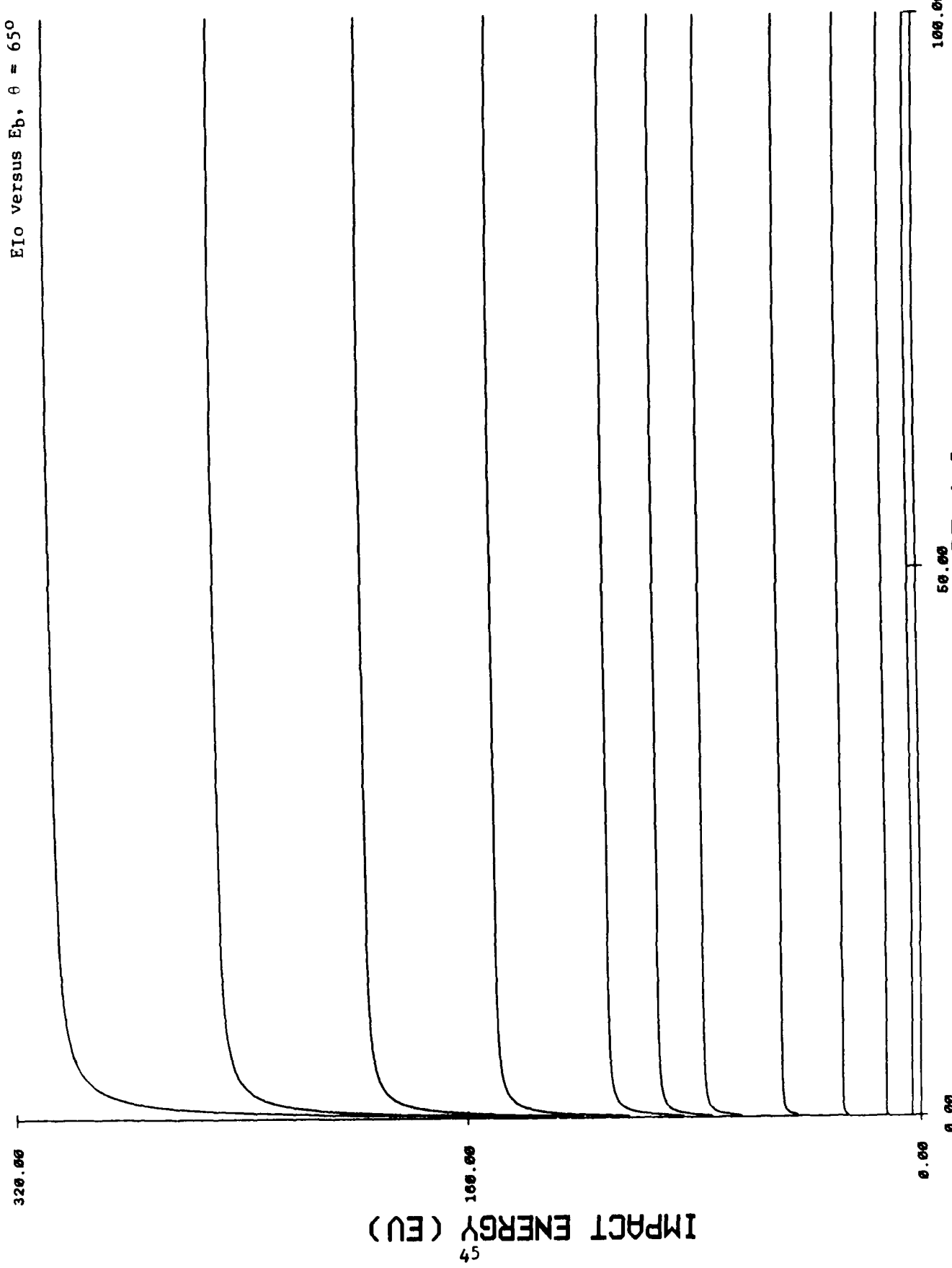


FIG. 7(k): Beam energy (MeU), 65° .

Fig. 7(1)

E_{Io} versus E_b , $\theta = 70^\circ$

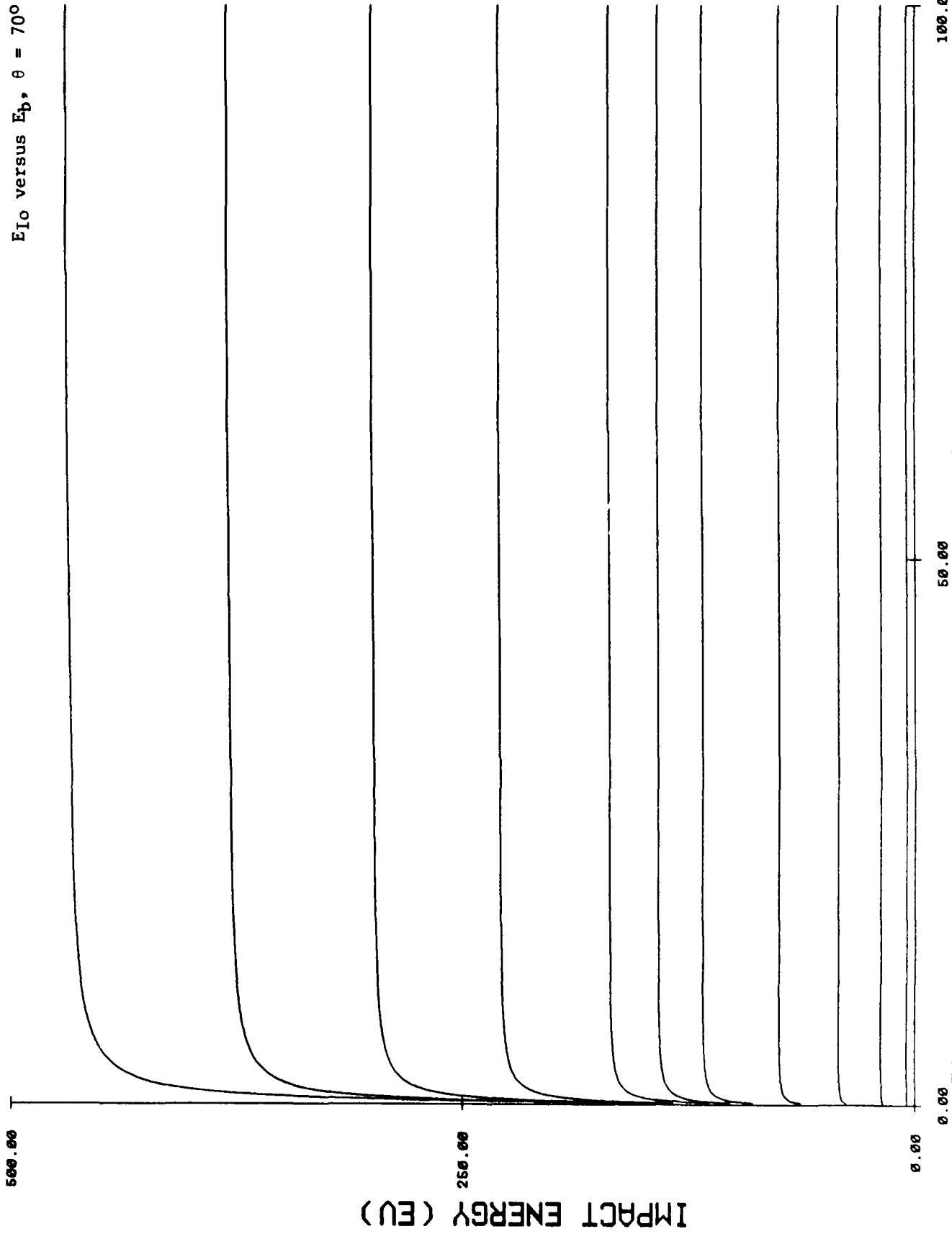


Fig. 7(1): Beam energy (MeV), 70° de θ .

Fig. 7(m)

E_{I0} versus E_b , $\theta = 75^\circ$

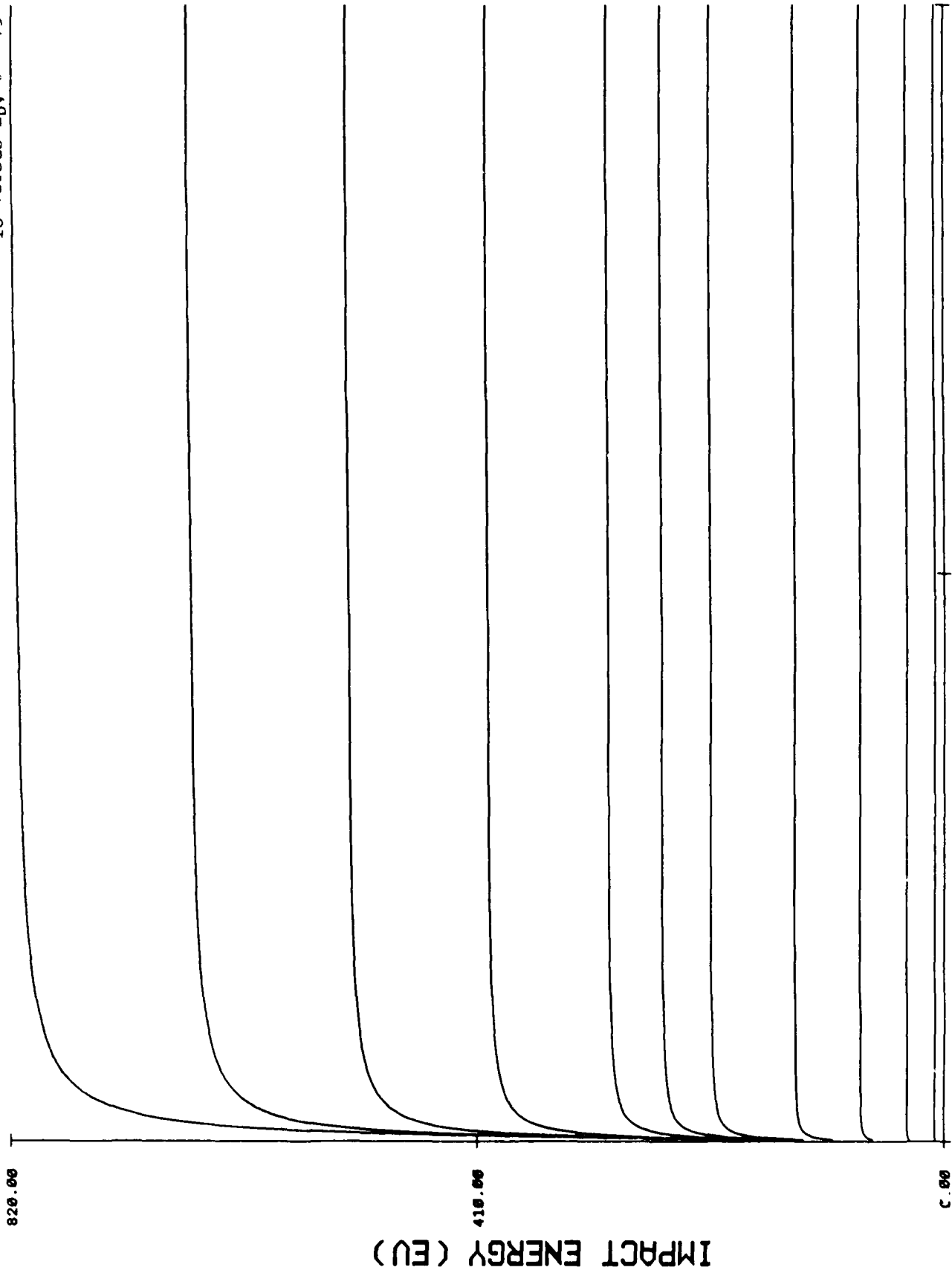


Fig. 7(m): Beam energy (MeV), 75° de θ .

Fig. 7(n)

E_{Io} versus E_b , $\theta = 80^\circ$

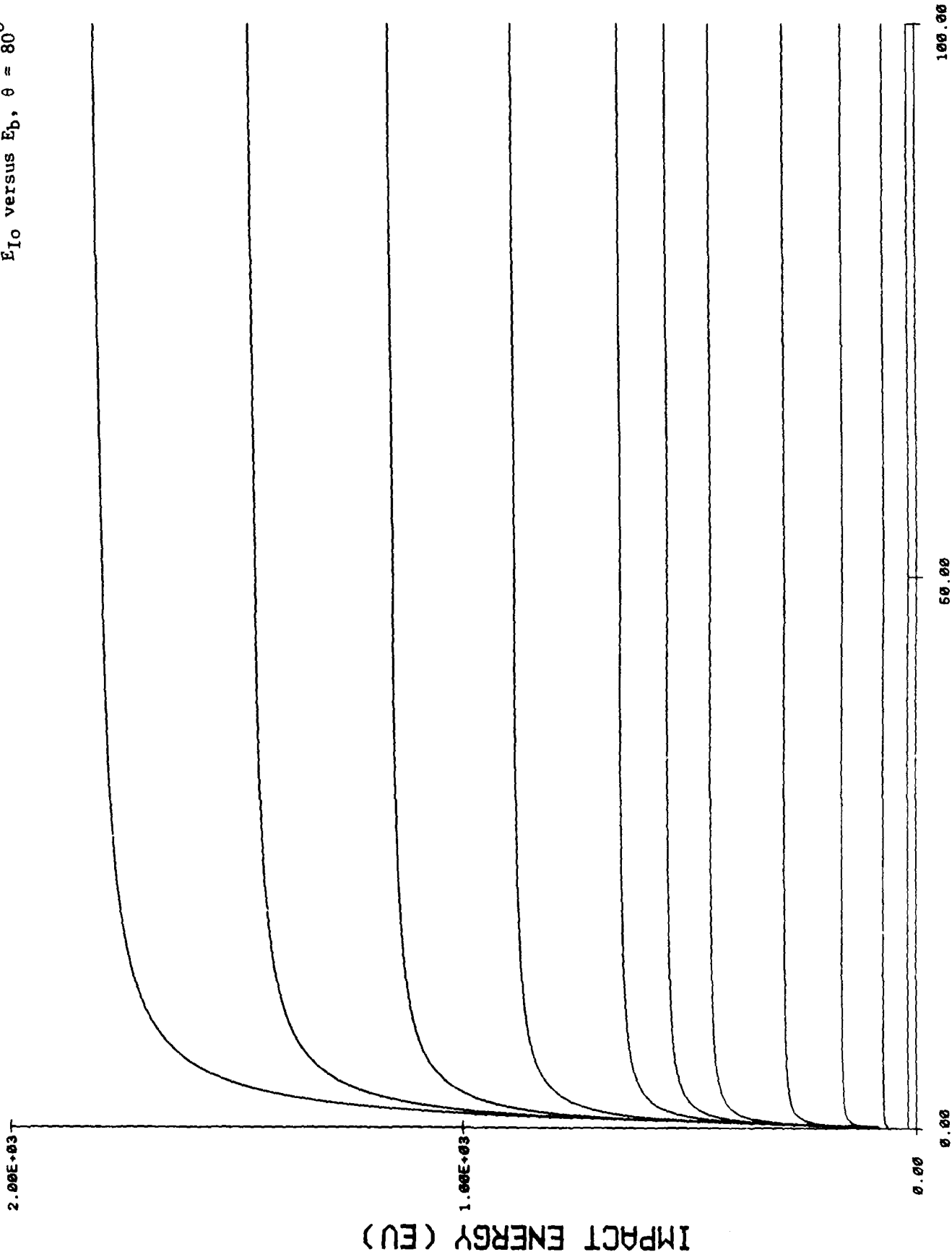


Fig. 7(n): Beam energy (MeU), 80 deg.

Fig. 7(o)
E₁₀ versus E_b, θ = 85°

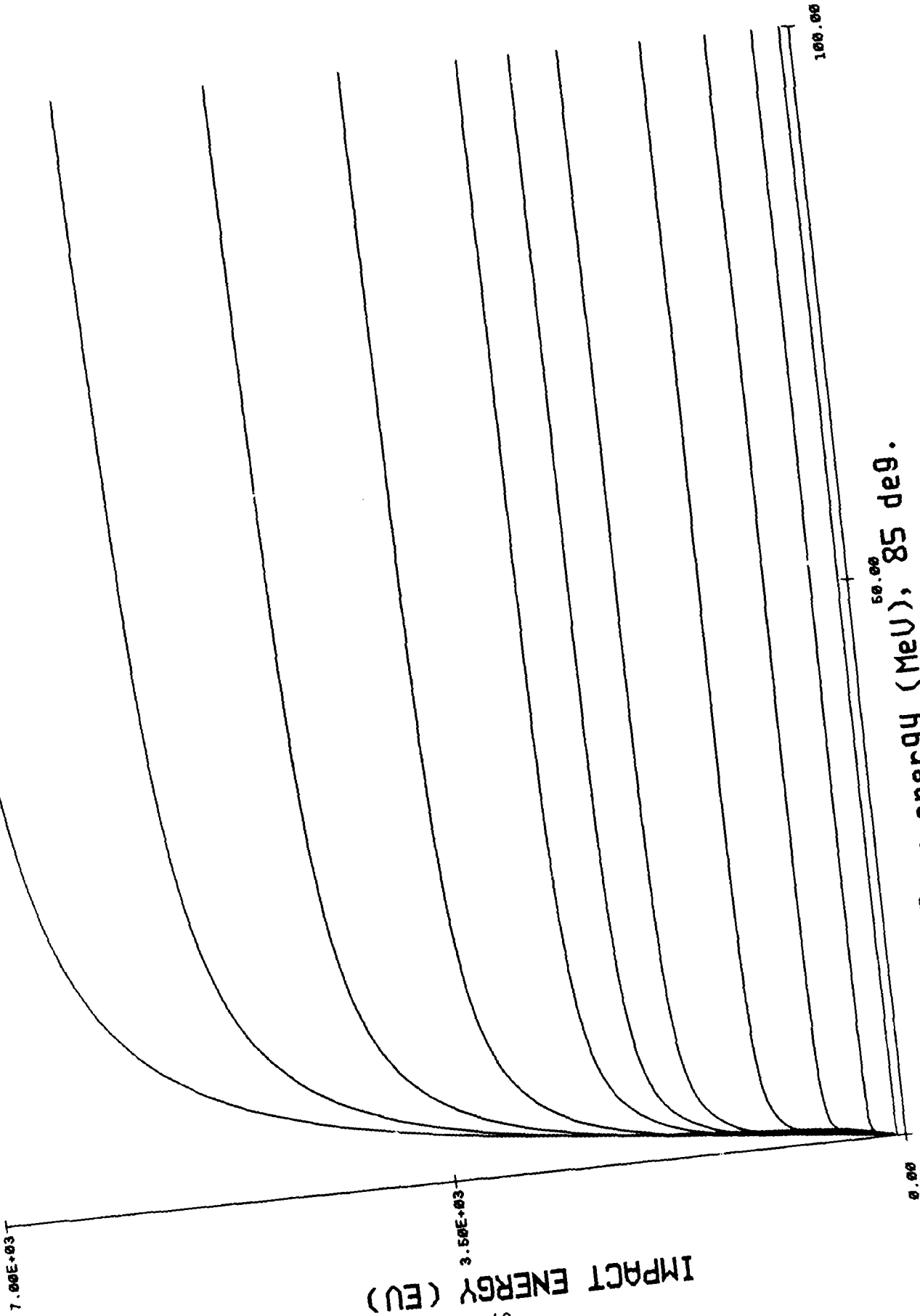


Fig. 7(o): Beam energy (MeV), 85 deg.

IMPACT ENERGY (EU)

Fig. 8

Cross-section for ionization of atomic hydrogen taken from Kieffer and Dunn,
Rev. Mod. Phys. 38, 1 (1966)

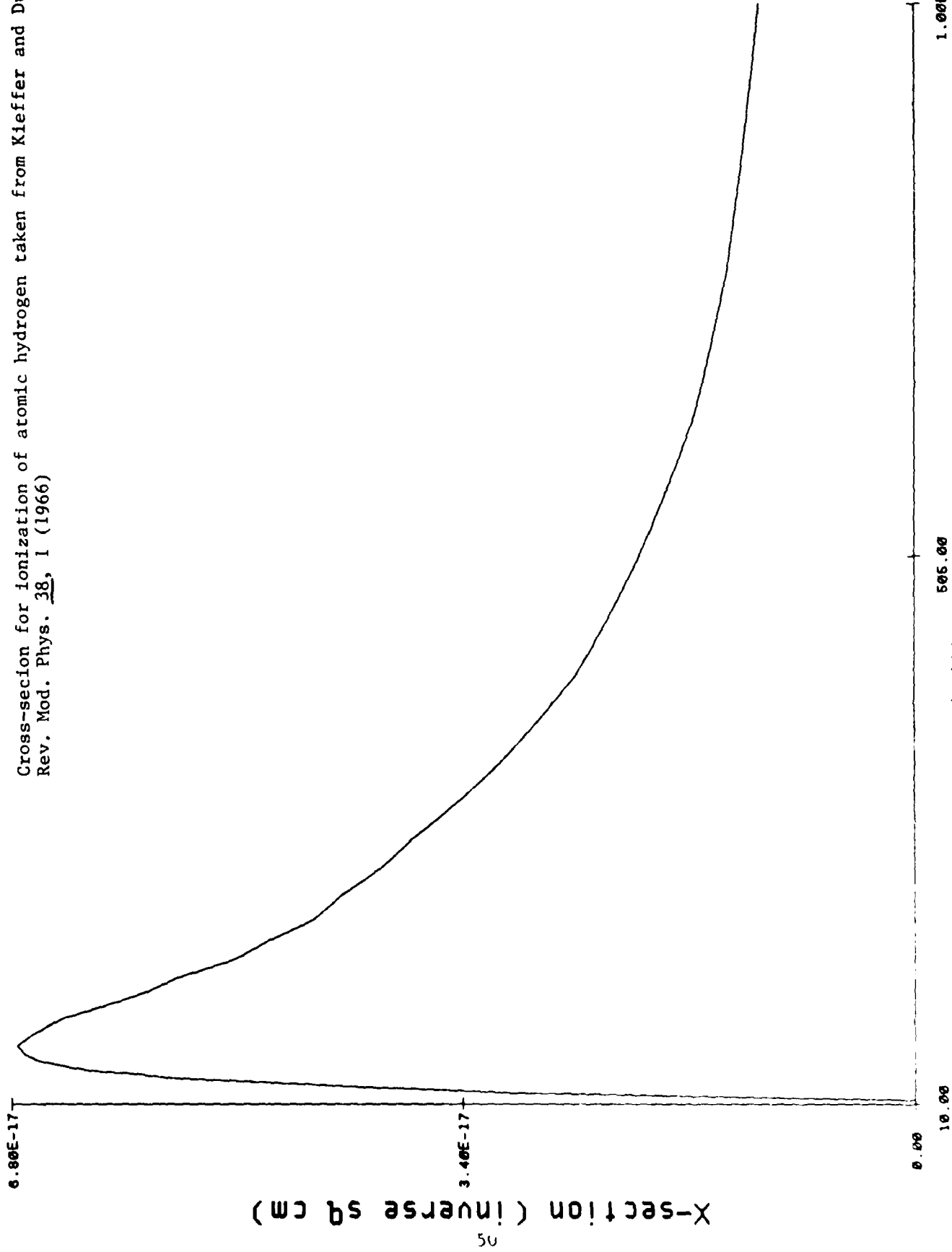
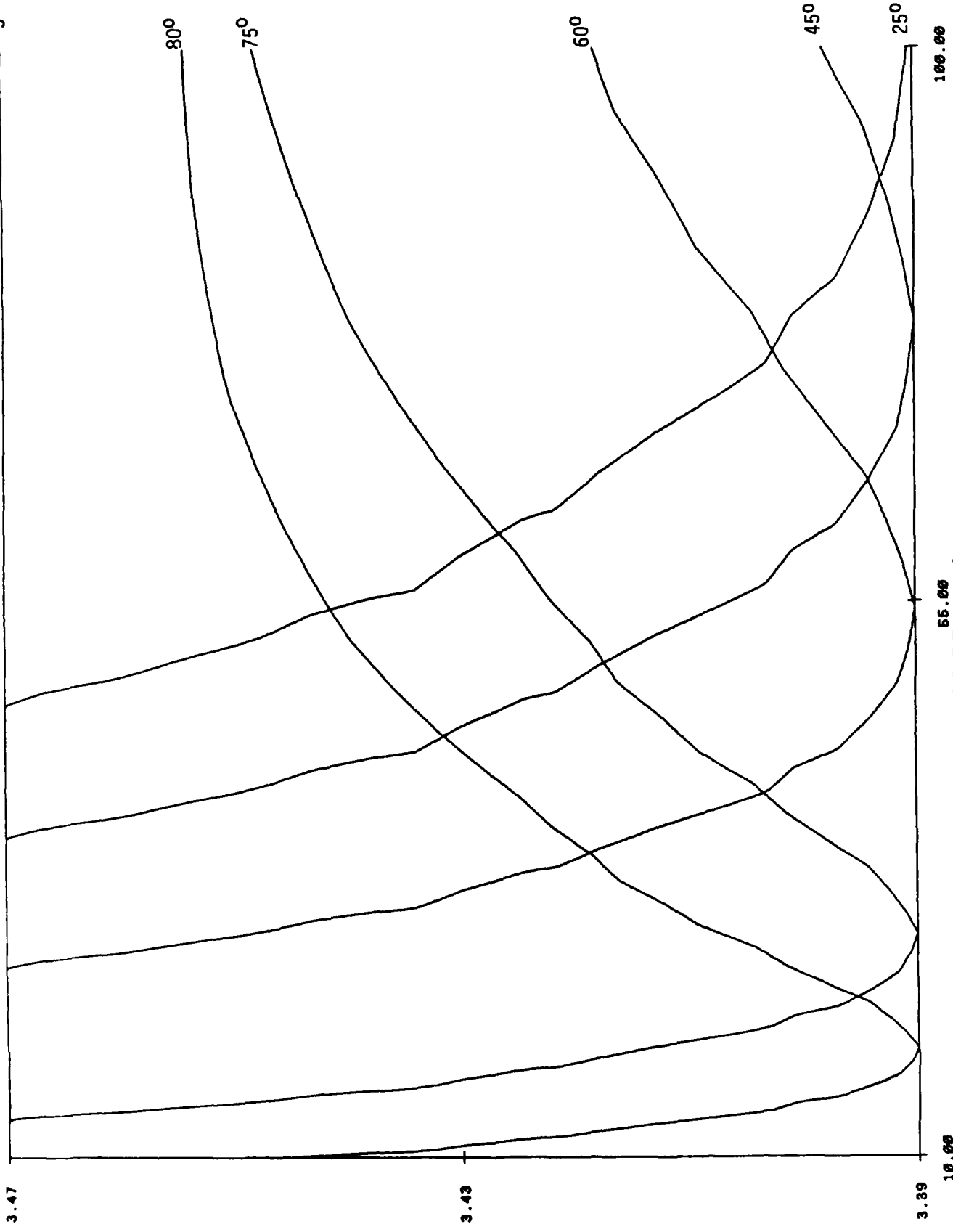


Fig. 8: Impact energy (eV)

Fig. 9a

1 MeV; 1,000 mA/cm²
50



DISTANCE TO 0.5 ATTENUATION
51

Fig (9a): R (NSC, 1 MeV, 1000 ma)

Fig. 9b

1 MeV; 10,000 mA/cm²

50

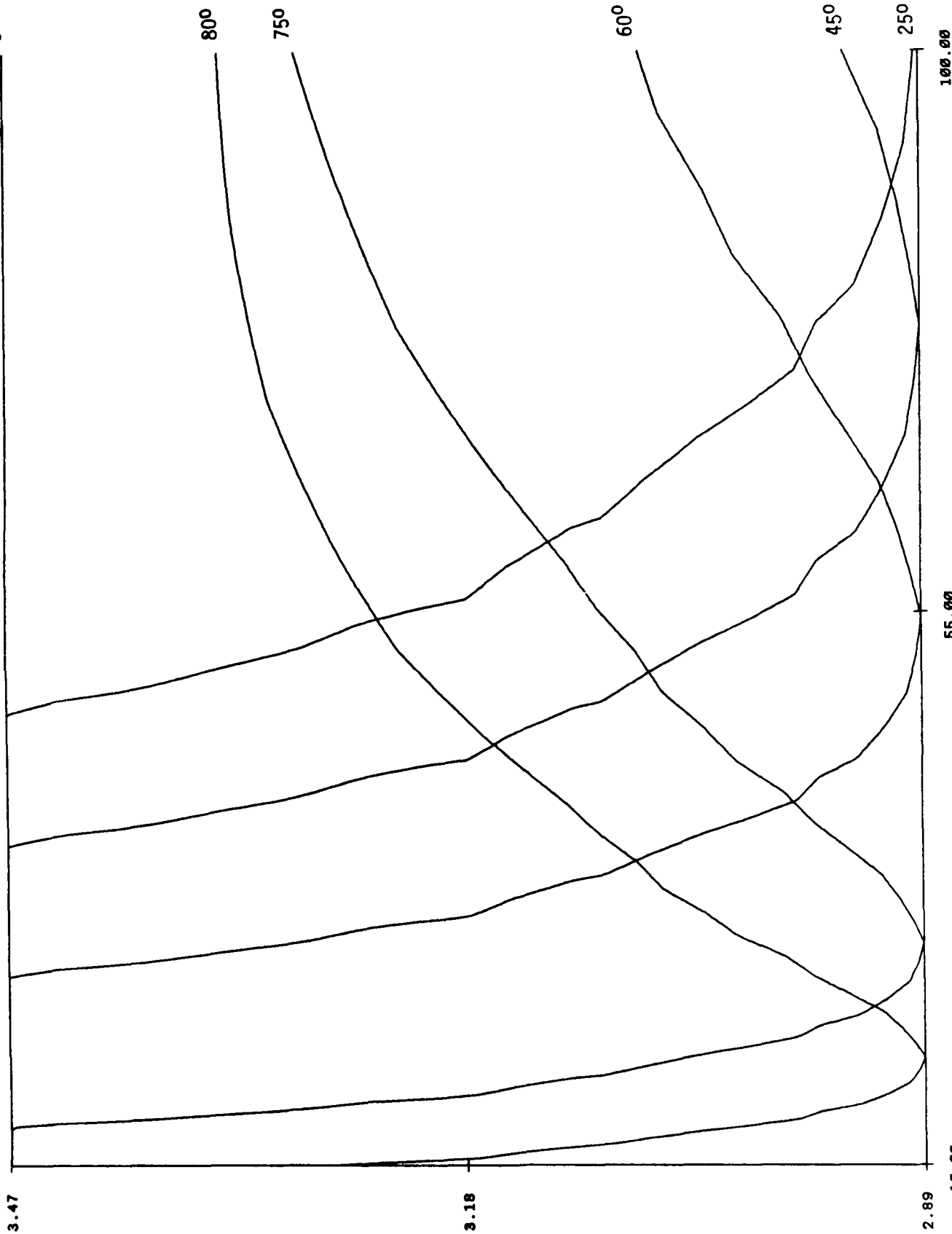


FIG (9b): R (NSC, 1 MeV, 10,000 ma)

DISTANCE TO 0.5 ATTENUATION

Fig. 9c

10MeV; 1,000 mA/cm²

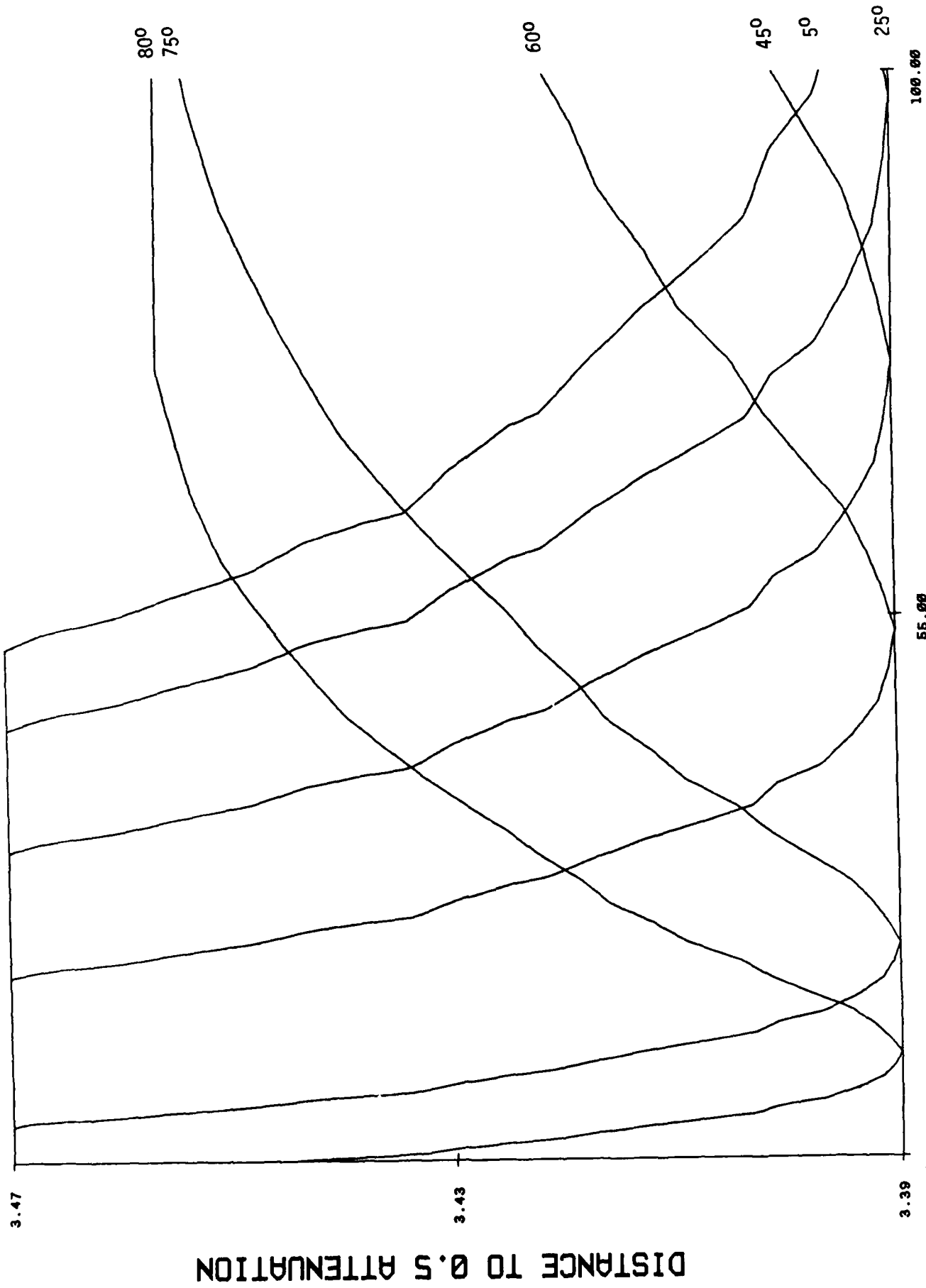


Fig (9c): R (NSC, 10 MeU, 1000 ma)

DISTANCE TO 0.5 ATTENUATION

Fig. 9d

10 MeV; 10,000 mA/cm²

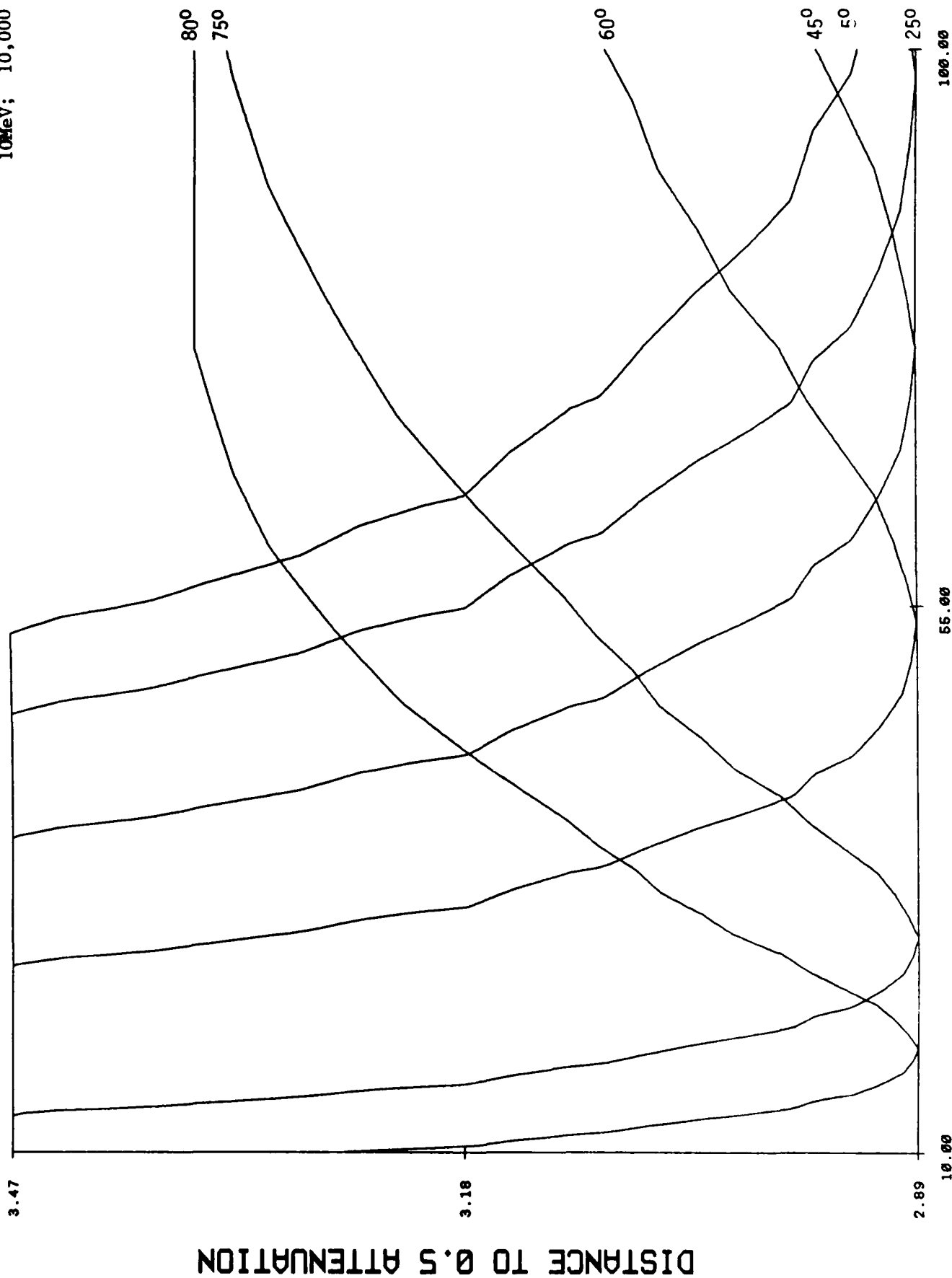


FIG (9d): R (NSC, 10 MeV, 10,000 ma)

Fig. 9e

100MeV; 1,000 mA/cm²

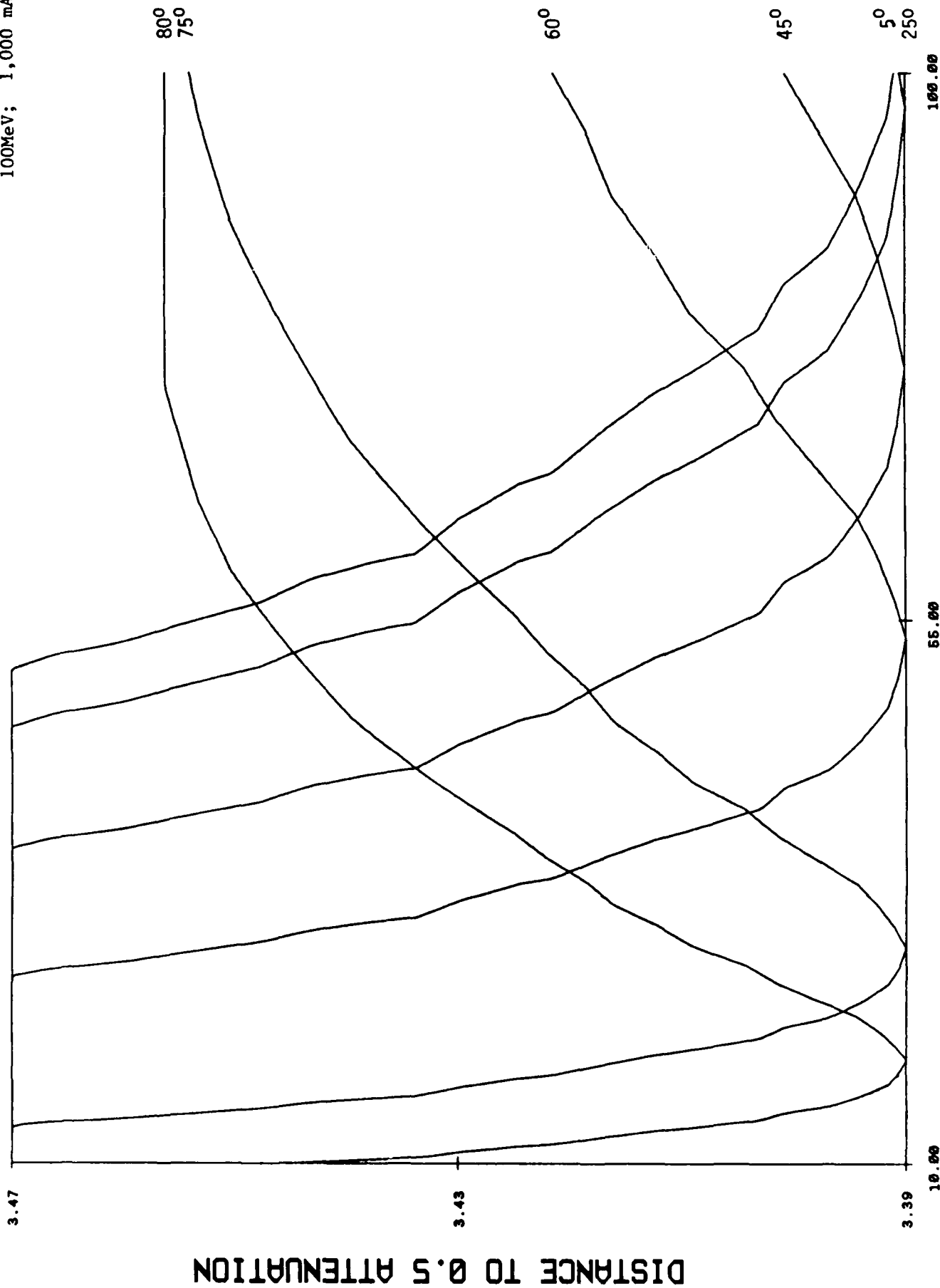


FIG (9e): R (NSC, 100 MeV, 1000 ma)

Fig. 9f

100MeV; 10,000 mA/cm²

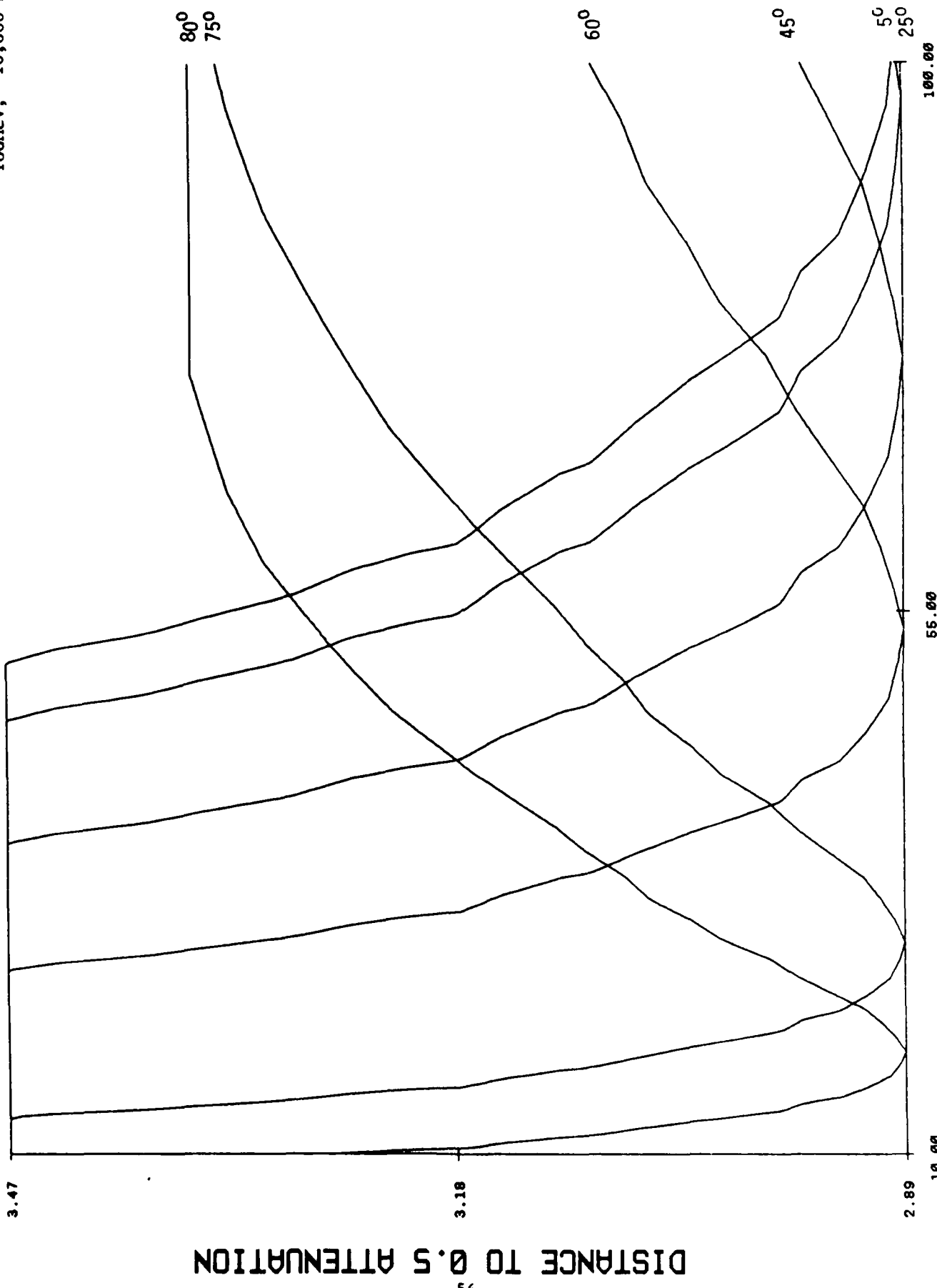


FIG (9f): R (NSC, 100 MeV, 10,000 ma)

DISTANCE TO 0.5 ATTENUATION

Fig. 10a
1 MeV; 1,000 mA/cm²
50

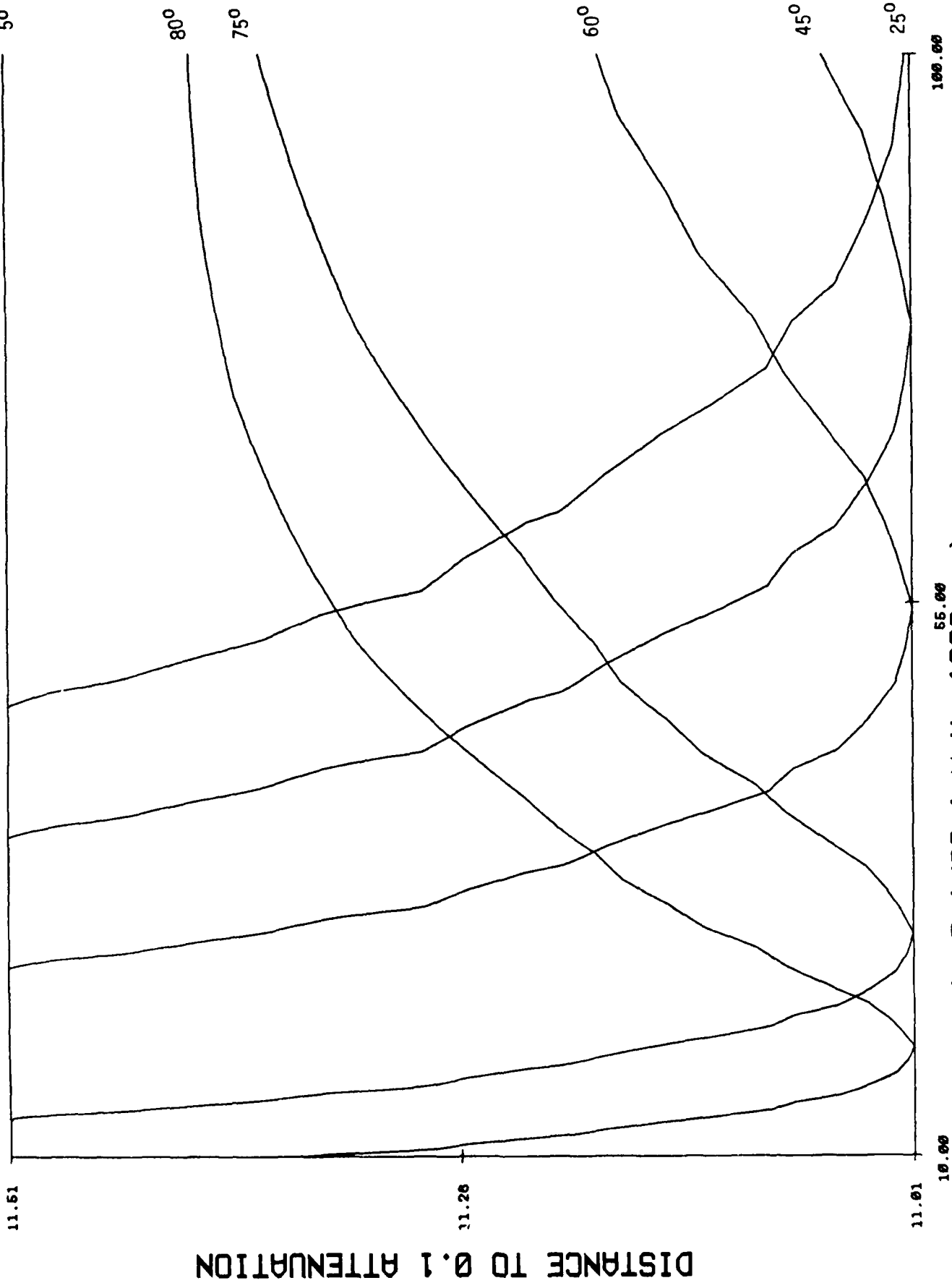


Fig (10a): R (NSC, 1 MeV, 1000 ma)

DISTANCE TO 0.1 ATTENUATION

Fig. 10b

1 MeV; 10,000 mA/cm²

50

11.61

9.78

8.04

10.00

55.00

100.00

DISTANCE TO 0.1 ATTENUATION

58

FIG (10b): R (NSC, 1 MeV, 10,000 ma)

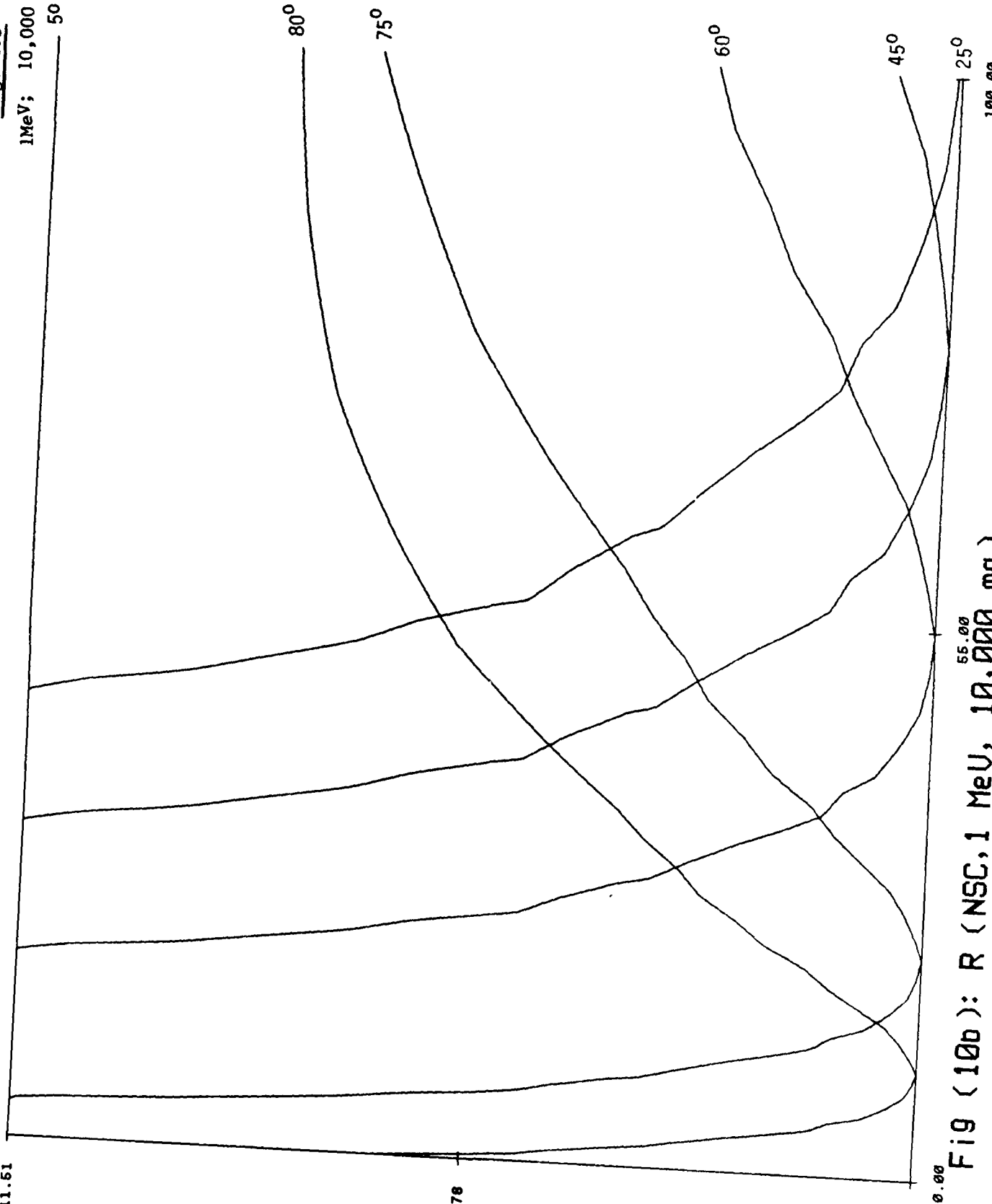


Fig. 10c

10MeV; 1,000 mA/cm²

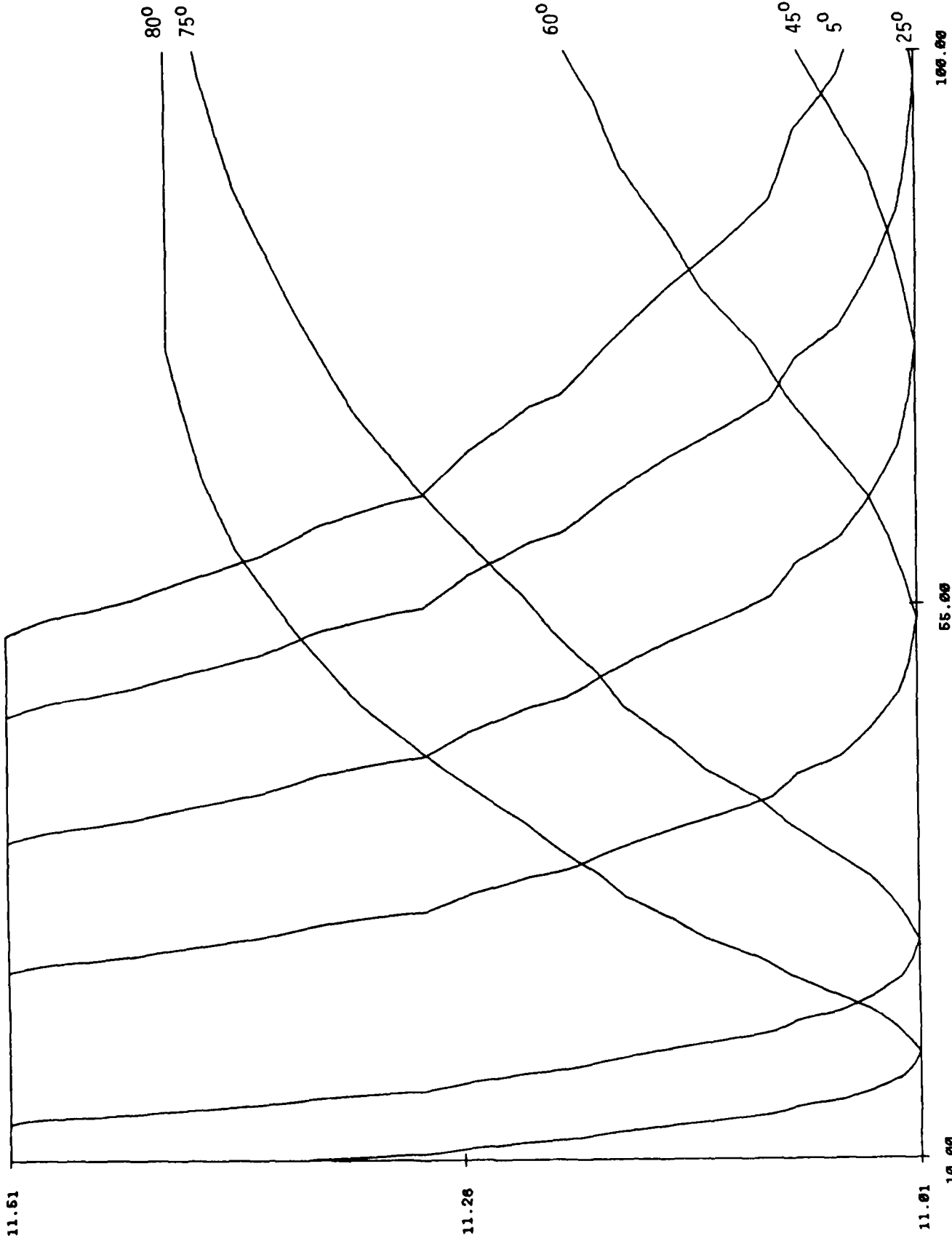


Fig (10c): R (NSC, 10 MeV, 1000 ma)

DISTANCE TO 0.1 ATTENUATION

Fig. 10d

10MeV; 10,000 mA/cm²

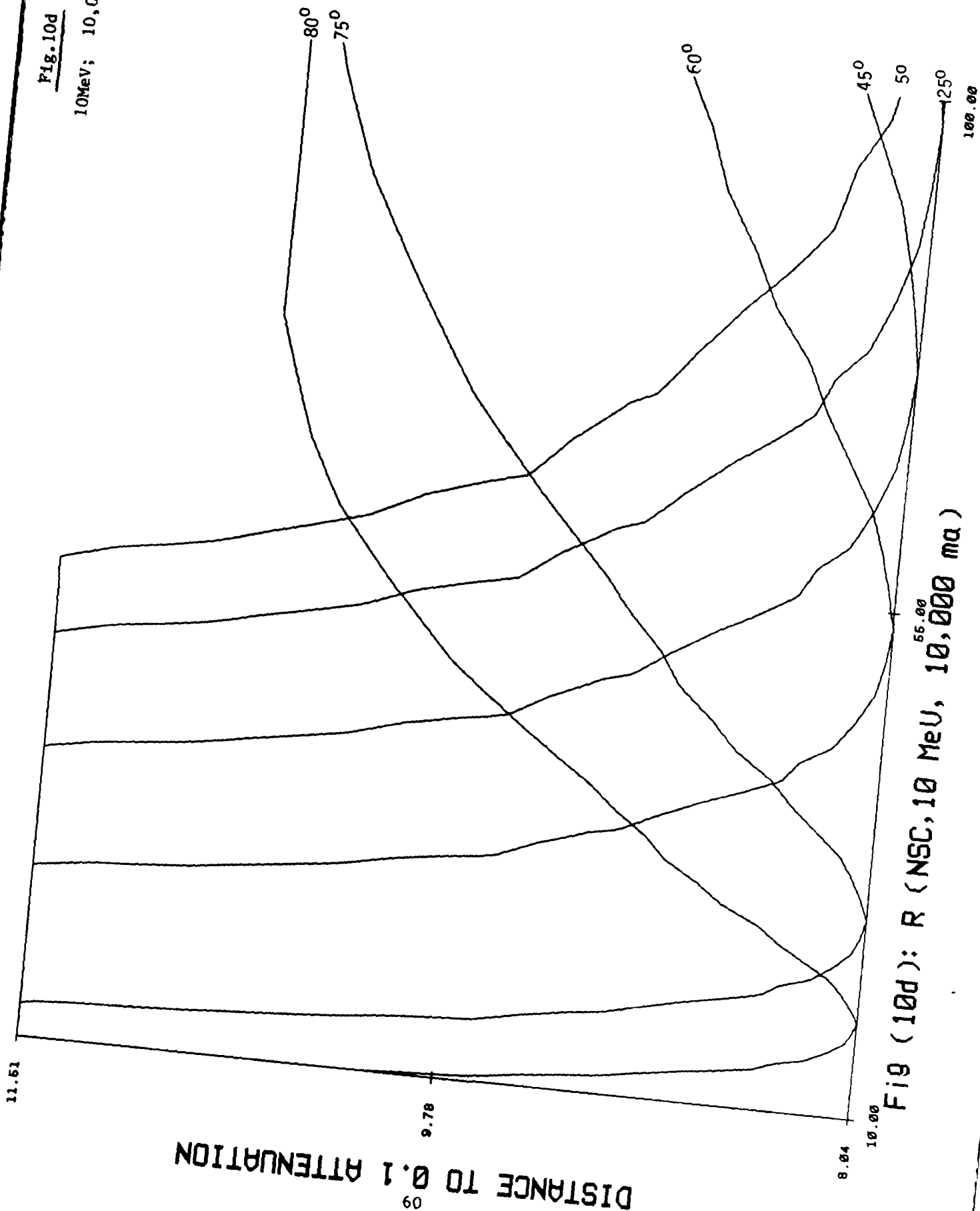
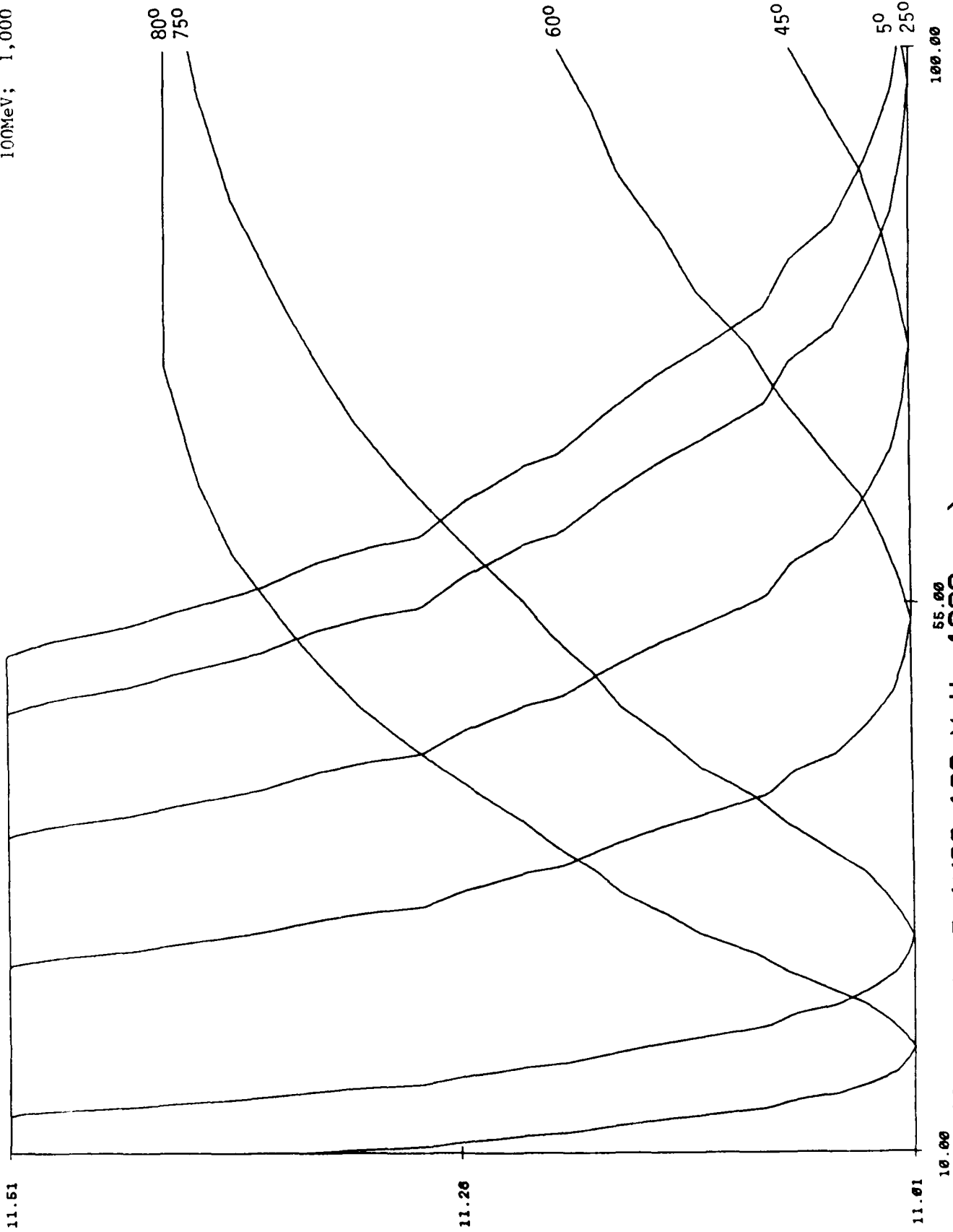


Fig (10d): R (NSC, 10 MeU, 10,000 ma)

Fig. 10e

100MeV; 1,000 mA/cm²



DISTANCE TO 0.1 ATTENUATION

Fig (10e): R (NSC, 100 MeV, 1000 ma)

Fig. 10f

100MeV; 10,000 mA/cm²

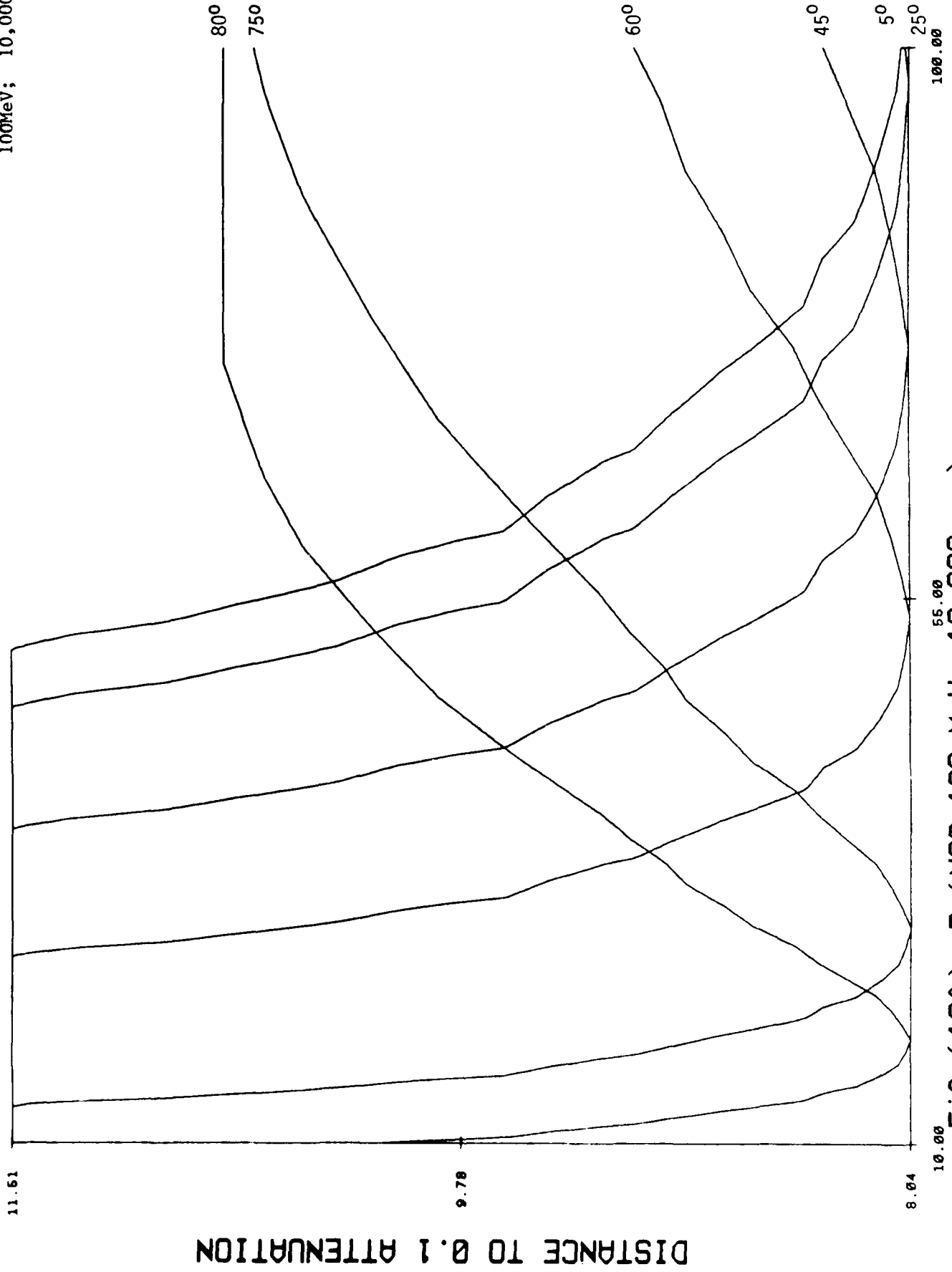
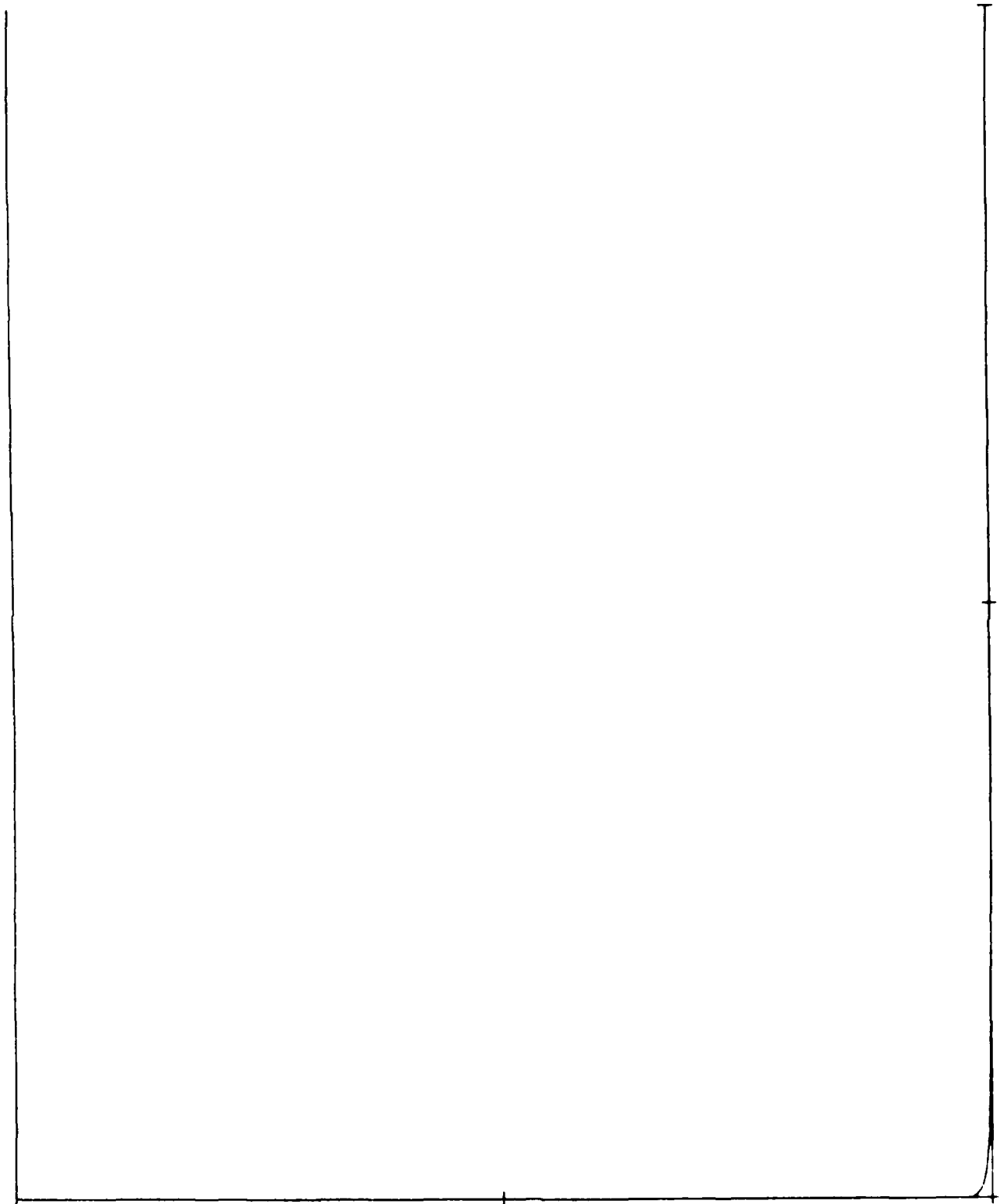


Fig (10f): R (NSC, 100 MeV, 10,000 ma)

Fig. 11a

10 cm; 1,000 mA/cm²
50



DISTANCE TO 0.5 ATTENUATION

Fig 11(a): E (NSC, 10 cm, 1000 ma)

Fig. 11b

10 cm; 10,000 mA/cm²
50

3.47

DISTANCE TO 0.5 ATTENUATION

64

1.8

1.36

Fig 11(b): E (NSC, 10 cm, 10,000 ma)

100.00

Fig. 11c

55 cm, 1,000 mA/cm²

DISTANCE TO 0.5 ATTENUATION

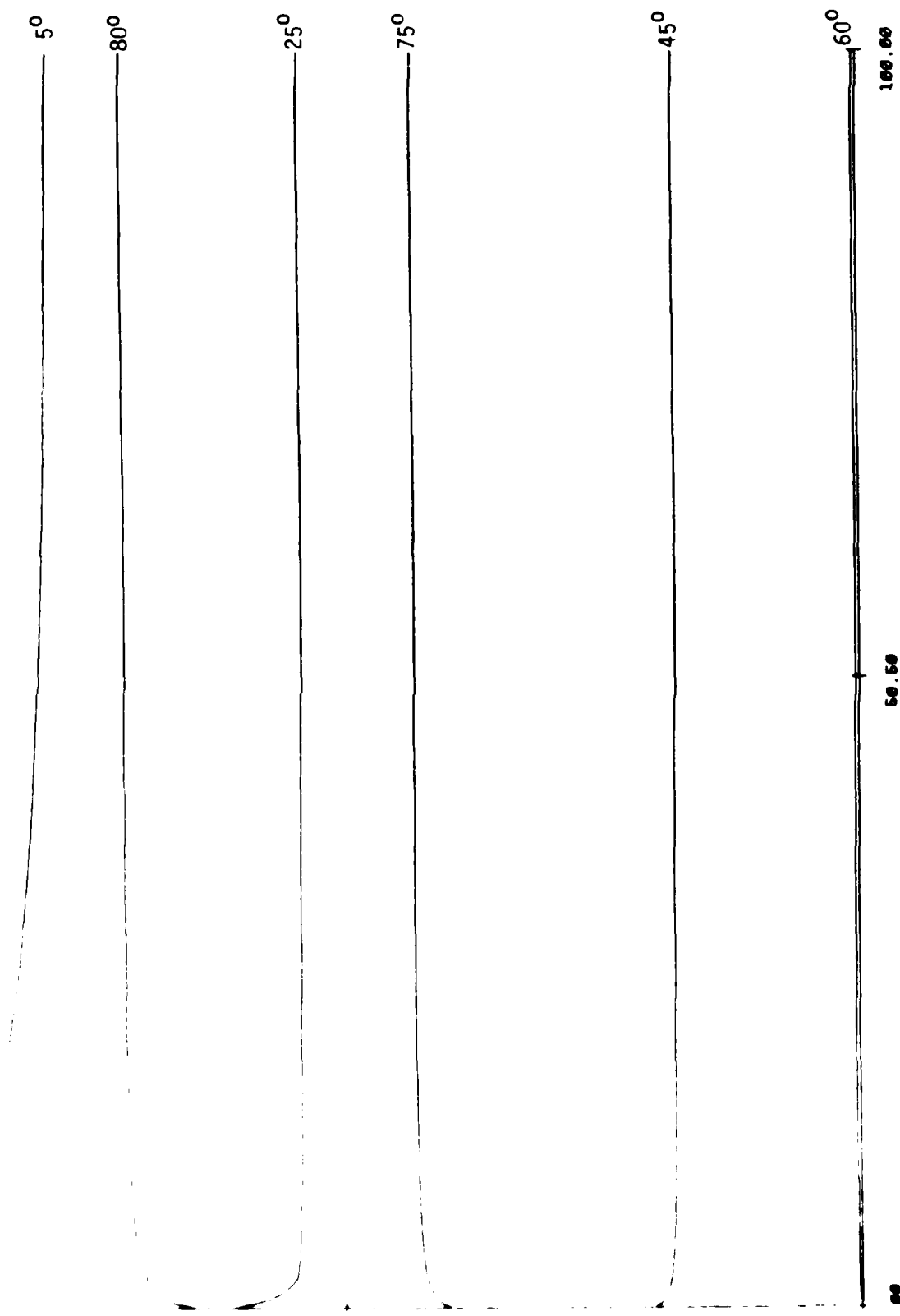


FIG 11(c): E (NSC, 55 cm, 1000 ma)

Fig. 11d

55 cm; 10,000 mA/cm²

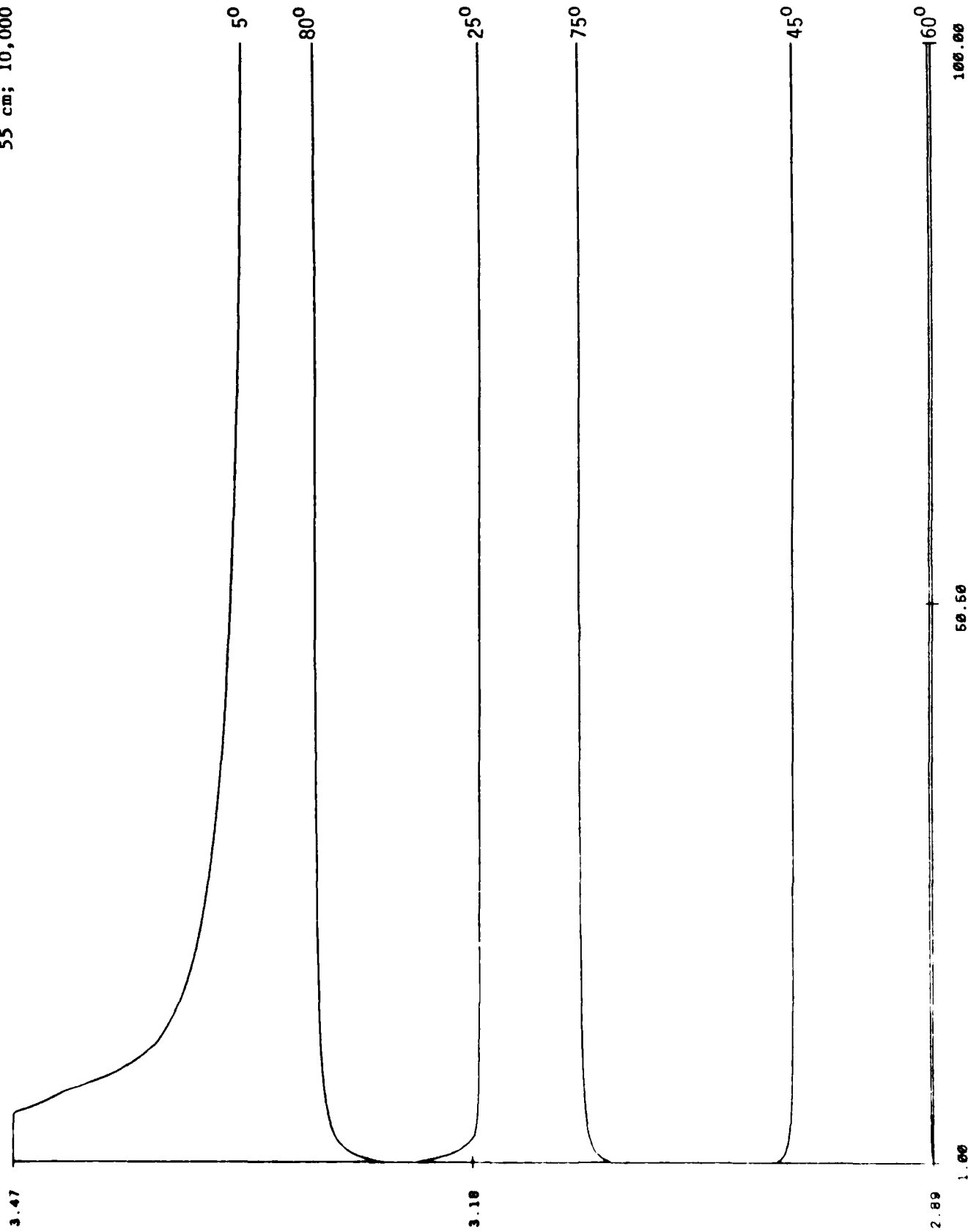


Fig 11(d): E (NSC, 55 cm, 10,000 ma)

Fig. 11e

100 cm; 1,000 mA/cm²

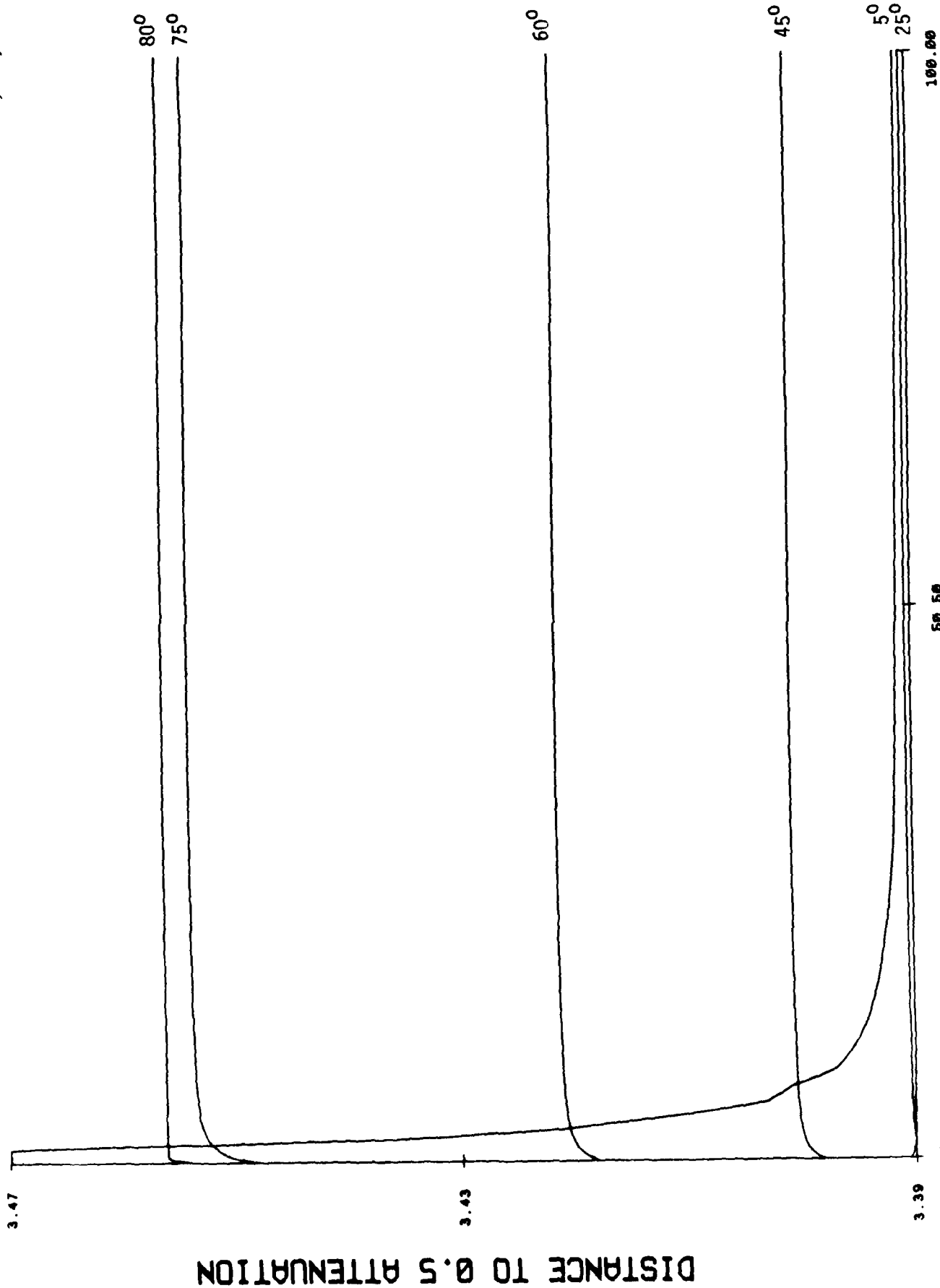


Fig 11(e): E (NSC, 100 cm, 1000 ma)

DISTANCE TO 0.5 ATTENUATION

Fig. 11f

100 cm; 10,000 mA/cm²

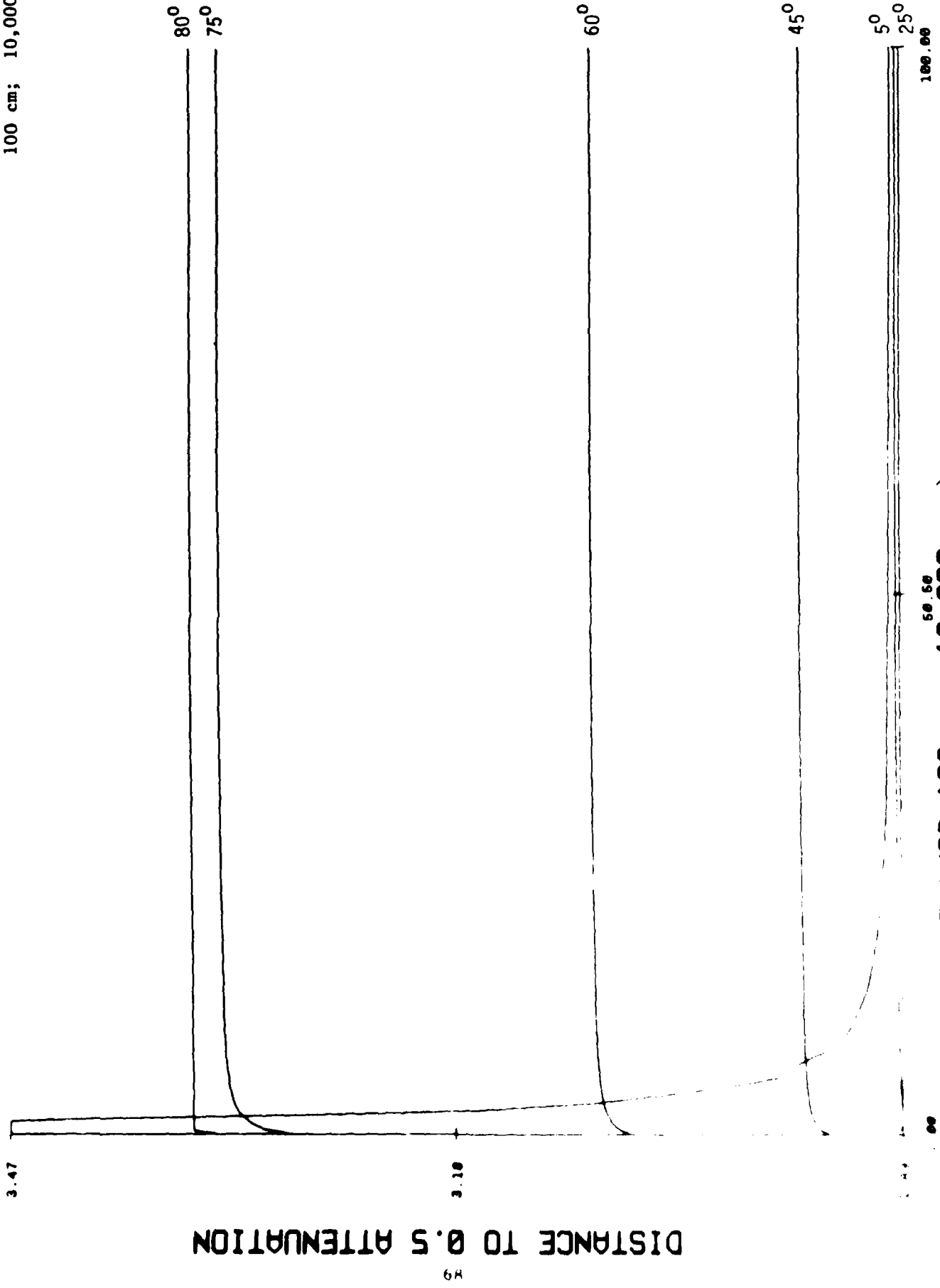


FIG 11(f): E (NSC, 100 cm, 10,000 ma)

Fig. 12a
10 cm; 1,000 mA/cm²
50

DISTANCE TO 0.1 ATTENUATION

Fig 12(a) E (NSC, 10 cm, 1000 ma)

100.00

Fig. 12b

10 cm; 10,000 mA/cm²
50

11.61

DISTANCE TO 0.1 ATTENUATION

10.00

12.89

50.50

100.00

Fig 12(b): E (NSC, 10 cm, 10,000 ma)

Fig. 12c

55 cm; 1,000 mA/cm²

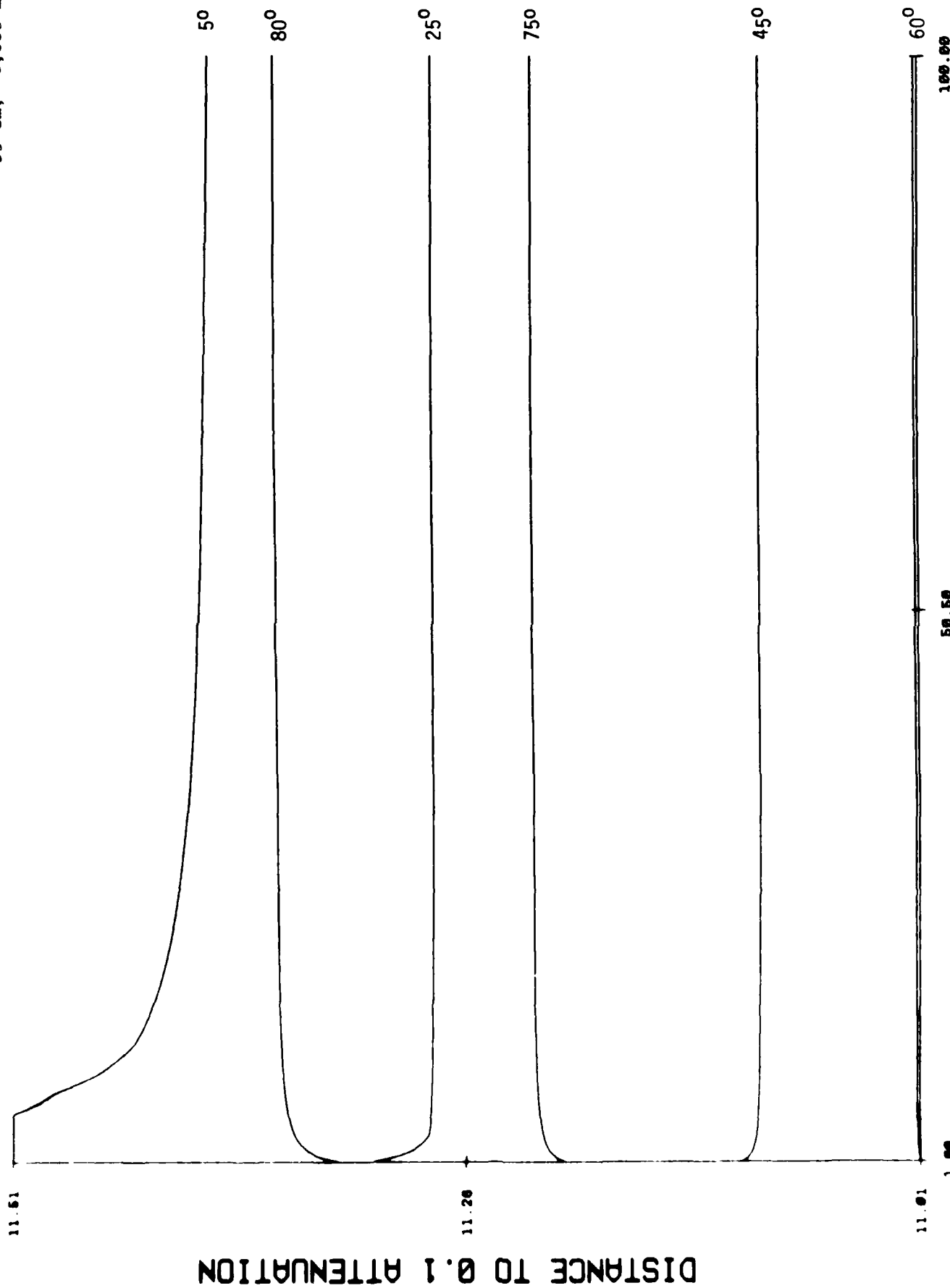


FIG 12(c): E (NSC, 55 cm, 1000 ma)

Fig. 12d

55 cm; 10,000 mA/cm²

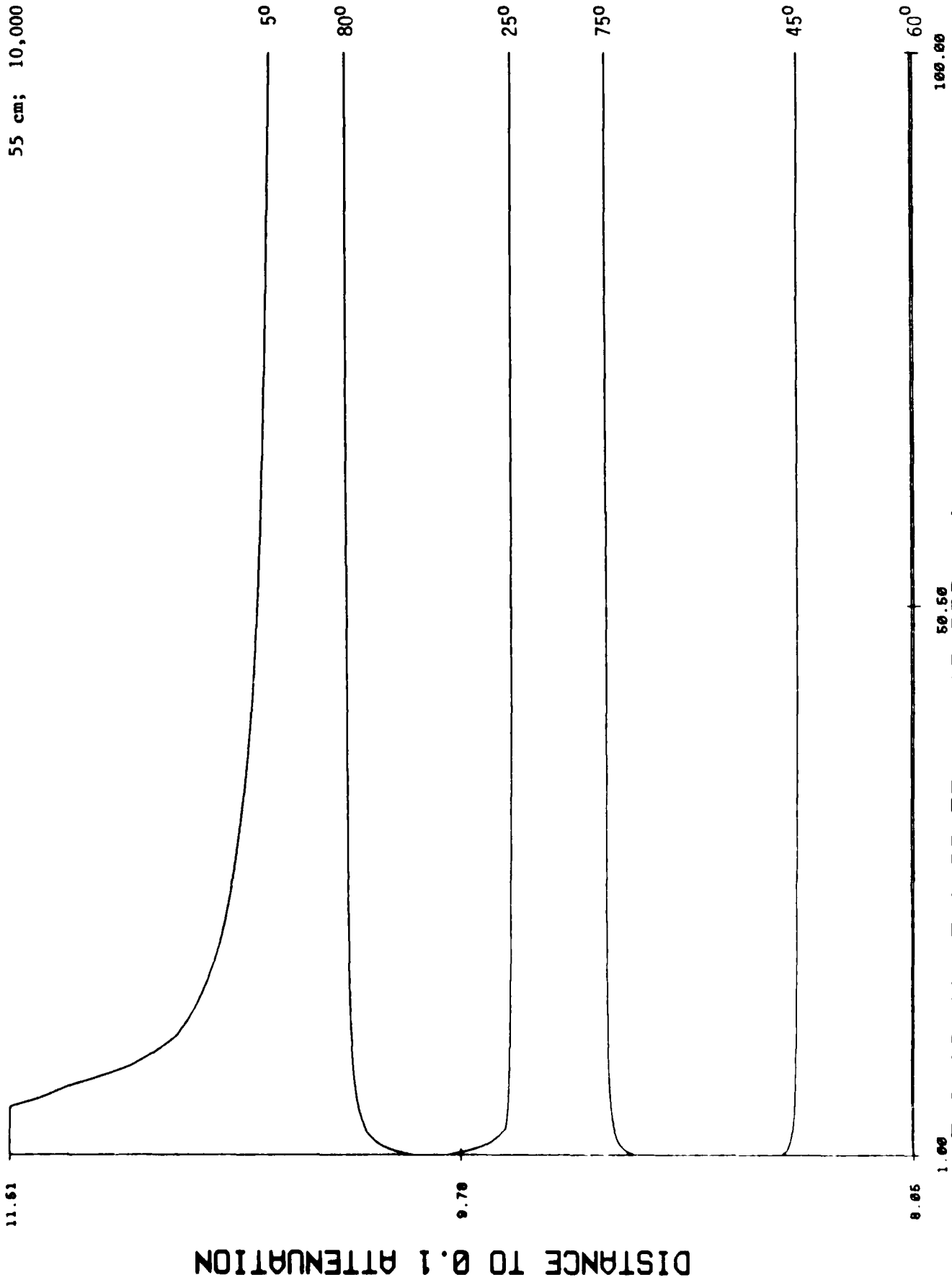


Fig 12(d): E (NSC, 55 cm, 10,000 ma)

Fig. 12e

100 cm; 1,000 mA/cm²

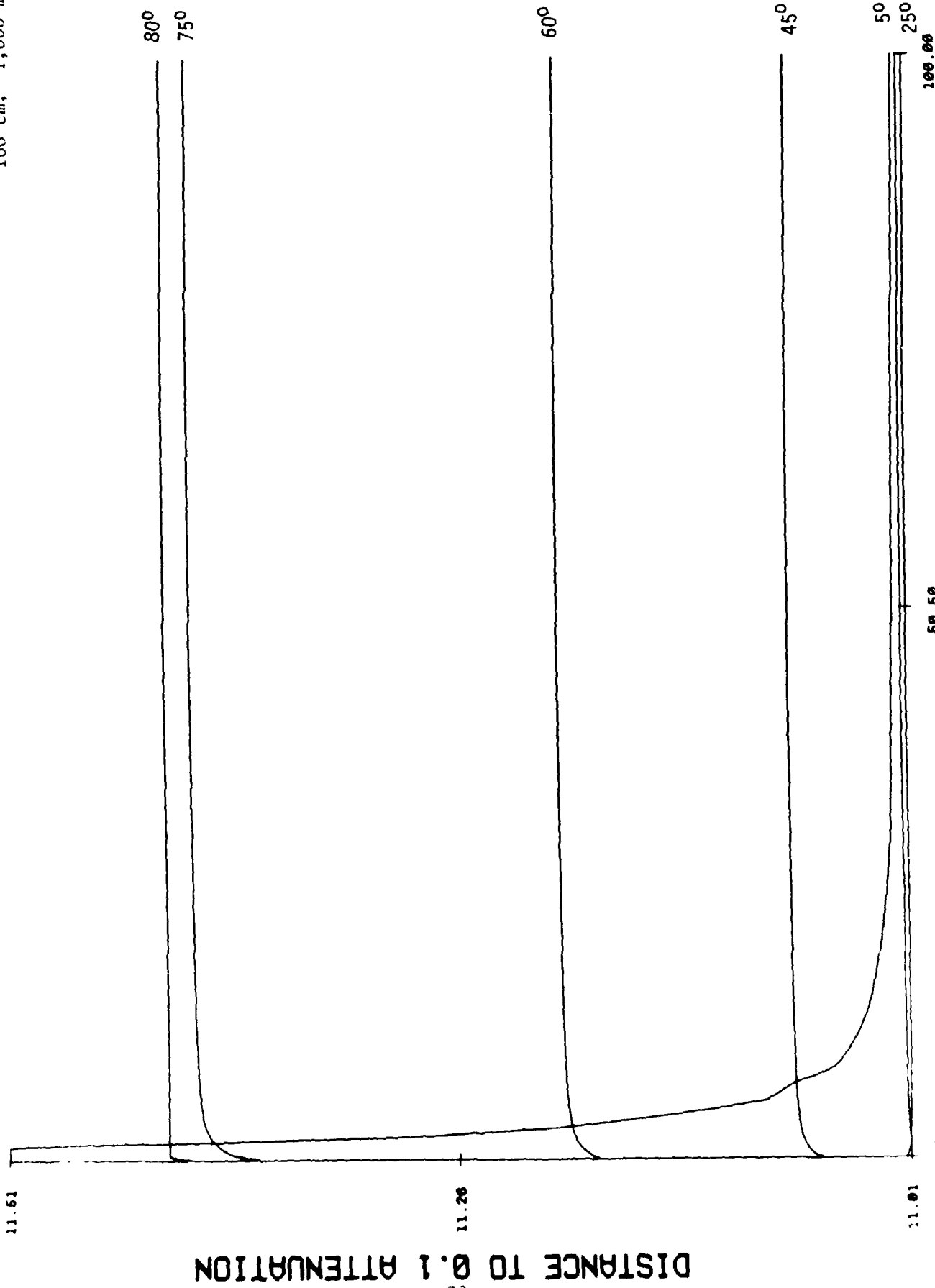


Fig 12(e): E (NSC, 100 cm, 1000 ma)

DISTANCE TO 0.1 ATTENUATION

Fig. 12f

100 cm; 10,000 mA/cm²

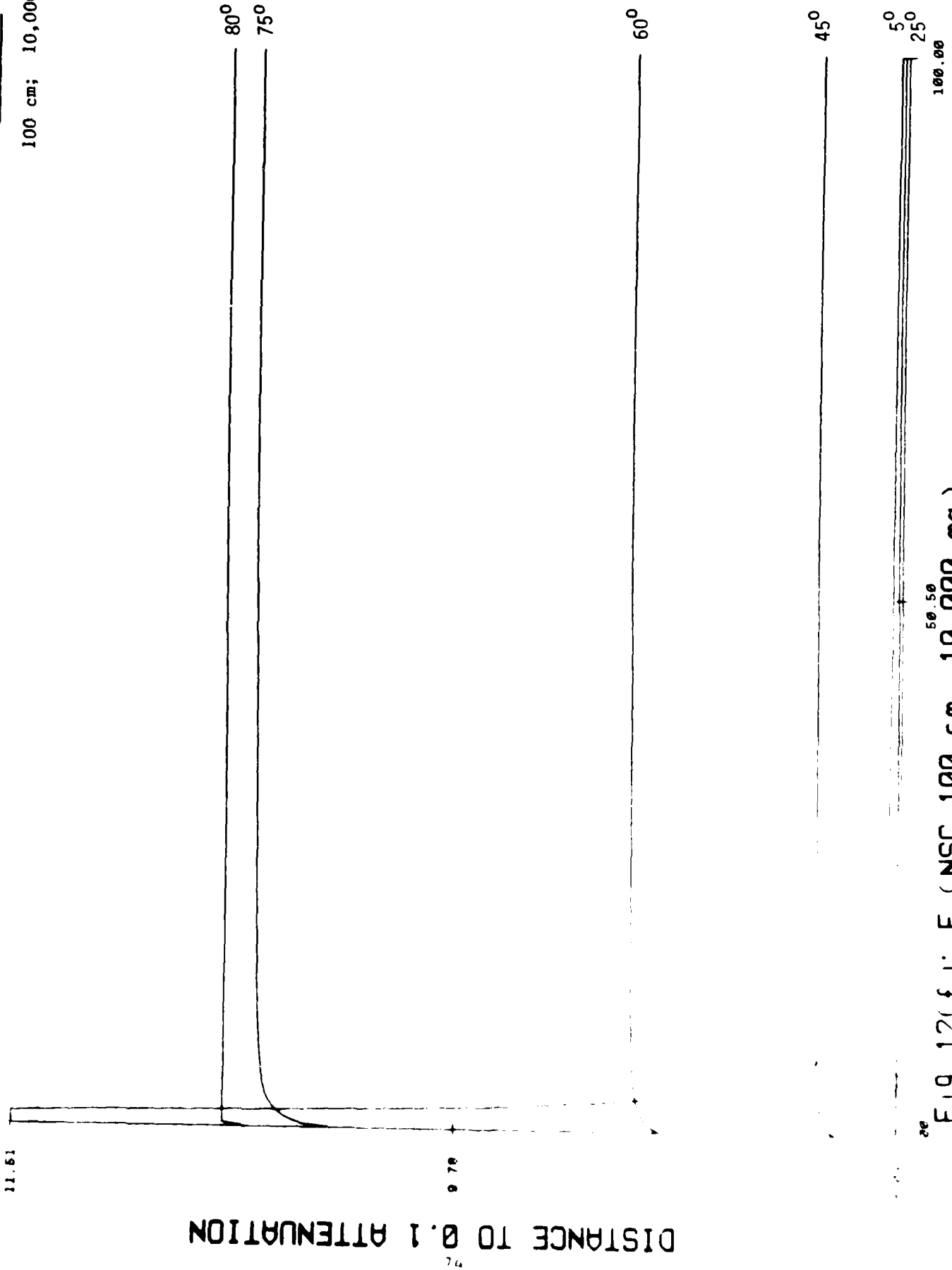


Fig 12(f) : E (NSC, 100 cm, 10,000 ma)

Fig. 13a
1 MeV; 1,000 mA/cm²



DISTANCE TO 0.5 ATTENUATION

Fig 13a P = SC.1 MeV. 1000 ma

Fig. 13b
1 MeV: 10,000 mA/cm²

DISTANCE TO 0.5 ATTENUATION

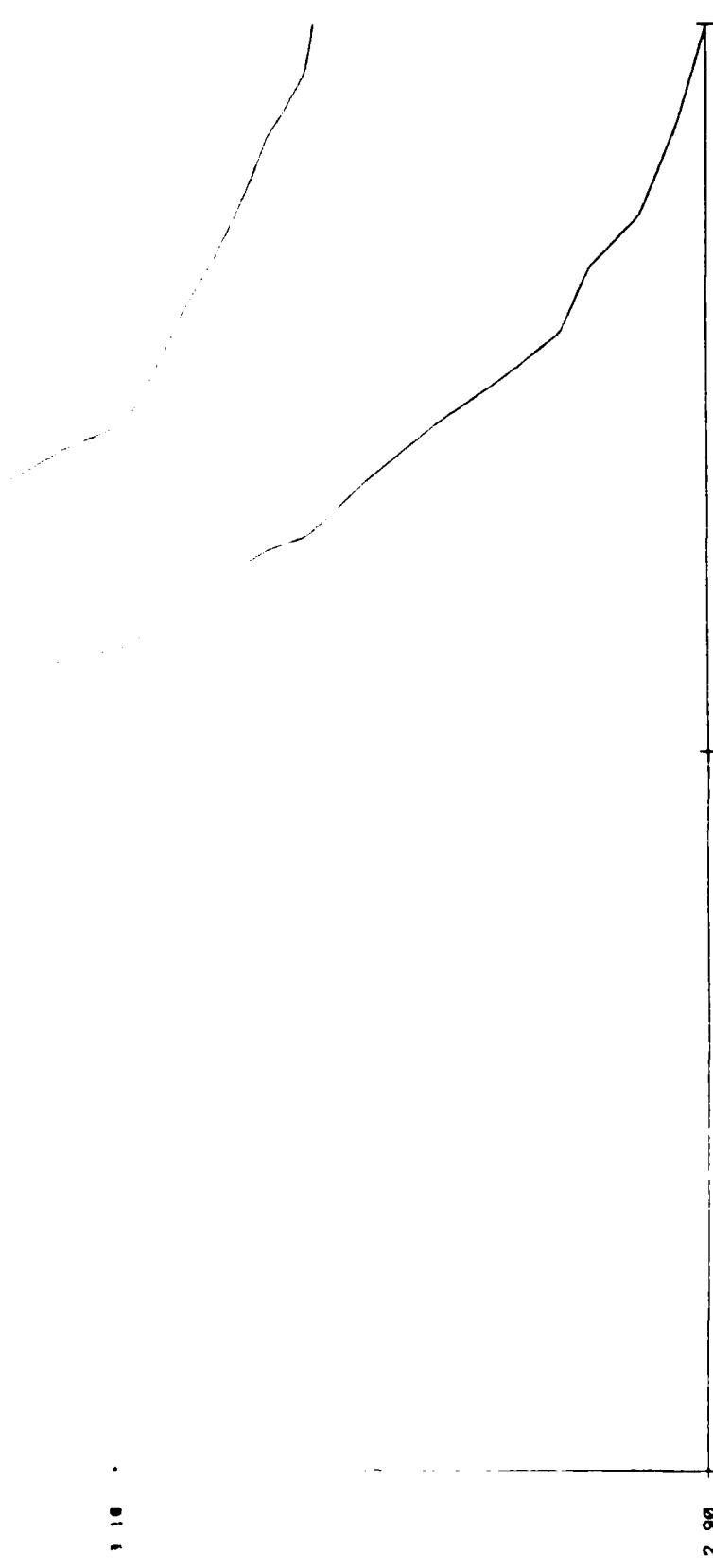


FIG (13b): R (SC, 1 MeV, 10,000 ma)

Fig. 13c

10MeV; 1,000 mA/cm²

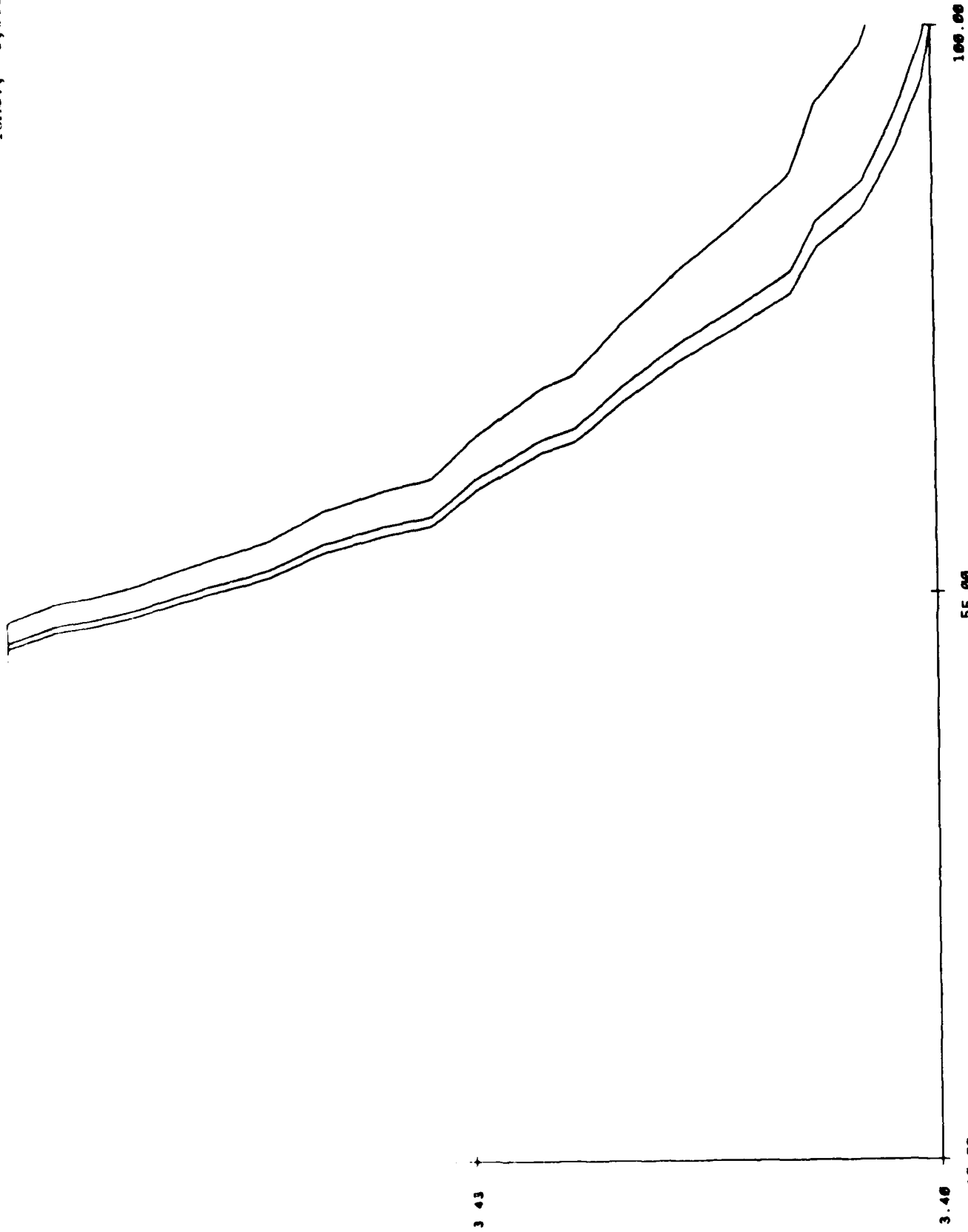


Fig (13c): R (SC, 10 MeV, 1000 ma)

Fig. 13d

10 MeV; 10,000 mA/cm²

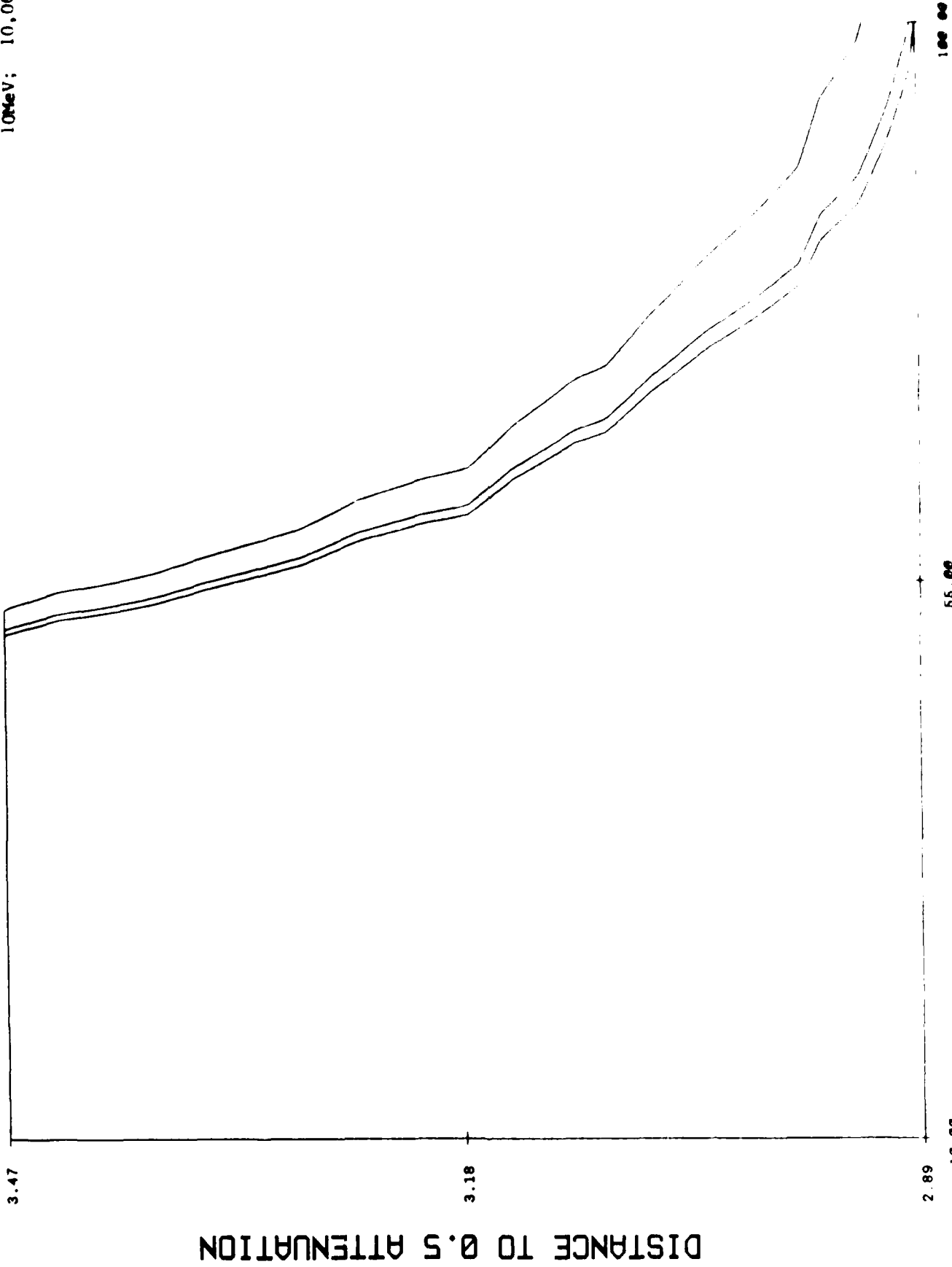


Fig (13d): R (SC, 10 MeV, 10,000 ma)

Fig. 13e

100MeV; 1,000 mA/cm²

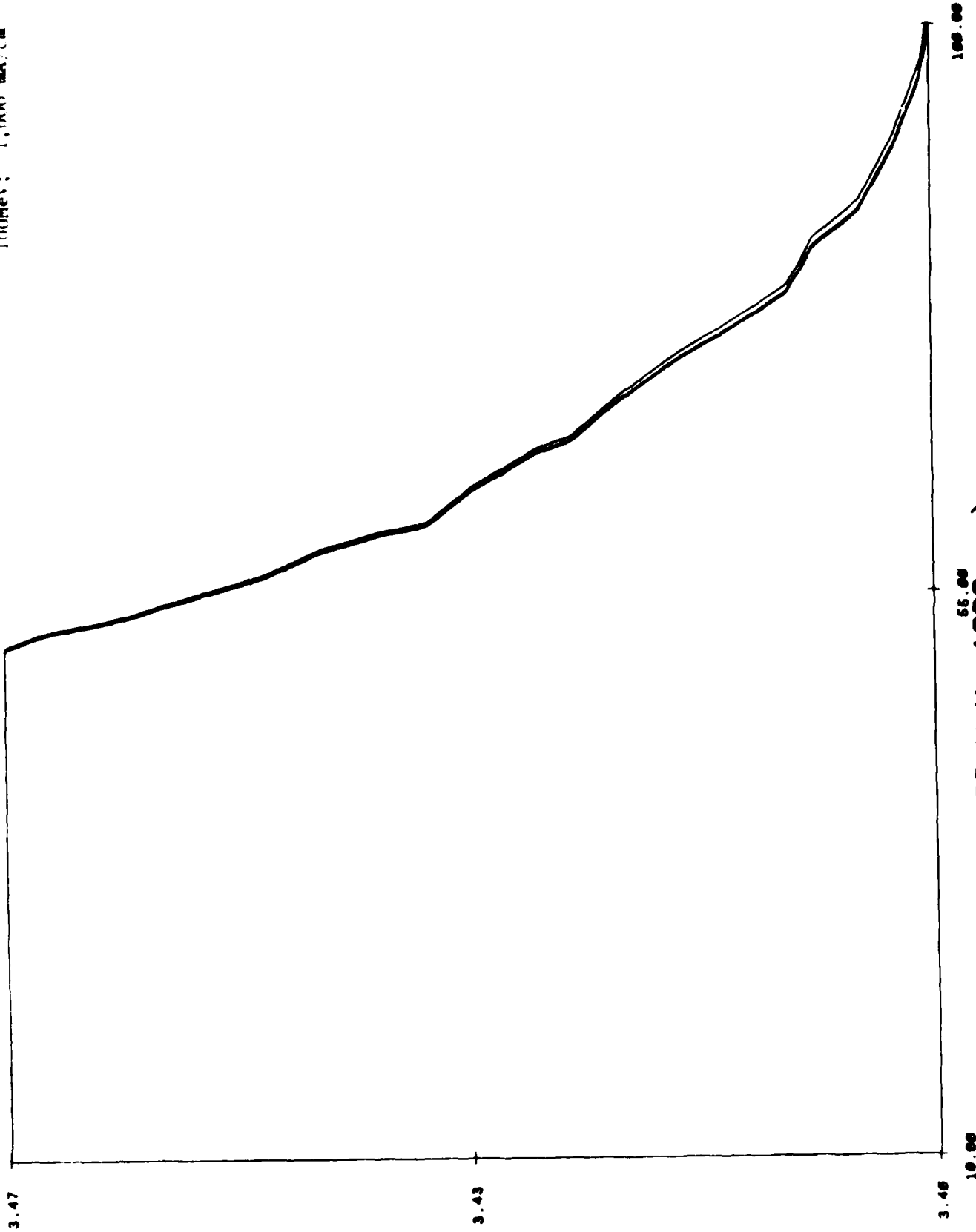
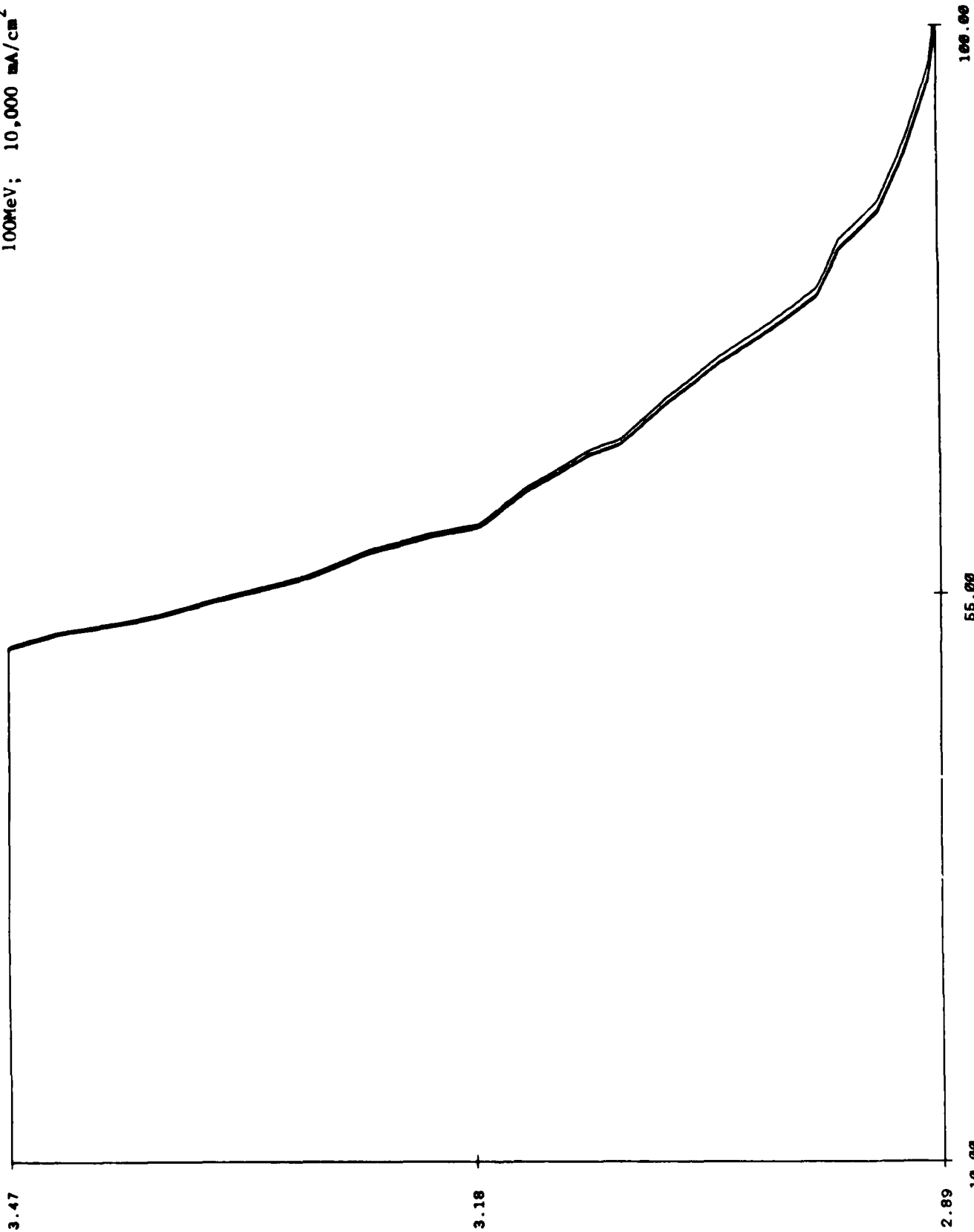


Fig (13e): R (SC, 100 MeV, 1000 ma)

DISTANCE TO 0.5 ATTENUATION

Fig. 13f

100MeV; 10,000 mA/cm²



DISTANCE TO 0.5 ATTENUATION

80

Fig 13(f): R (SC, 100 MeV, 10,000 ma)

Fig. 14a
1 MeV; 1,000 mA/cm²

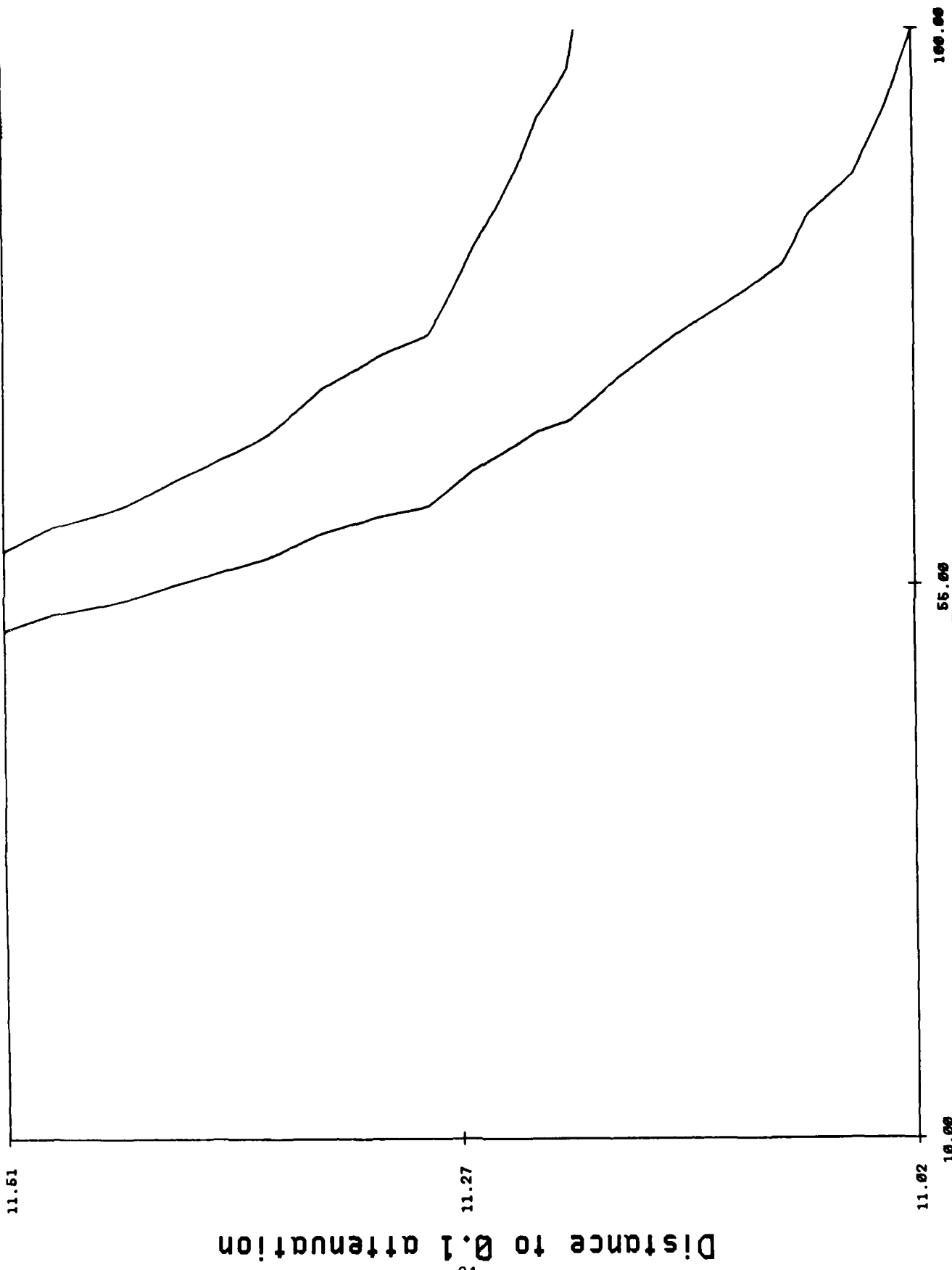


Fig 14(a): R (SC, 1 MeU, 1000 ma

Distance to 0.1 attenuation

Fig. 14b
1 MeV; 10,000 mA/cm²

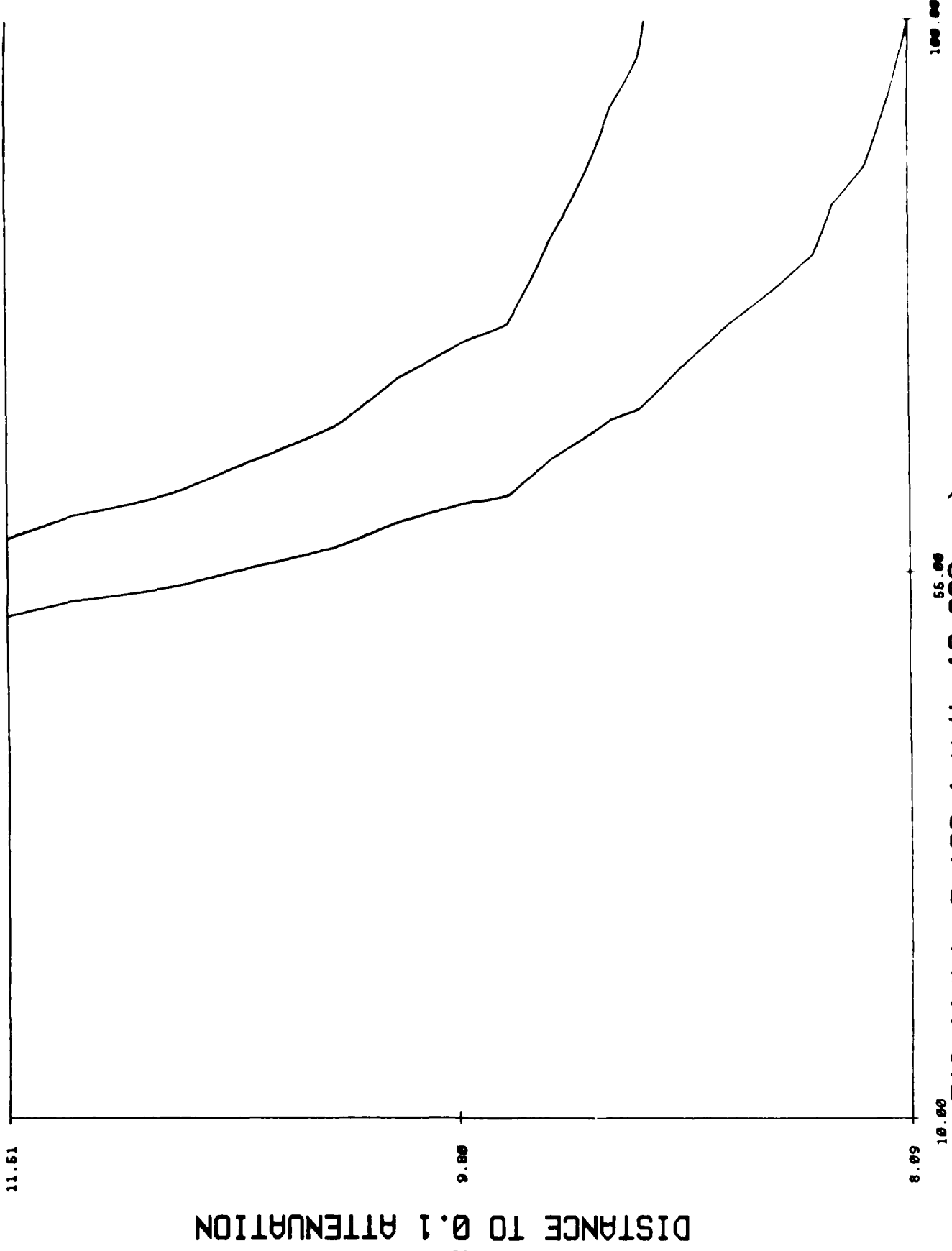


Fig (14b): R (SC, 1 MeV, 10,000 ma)

Fig. 14c

10 MeV: 1,000 mA/cm²

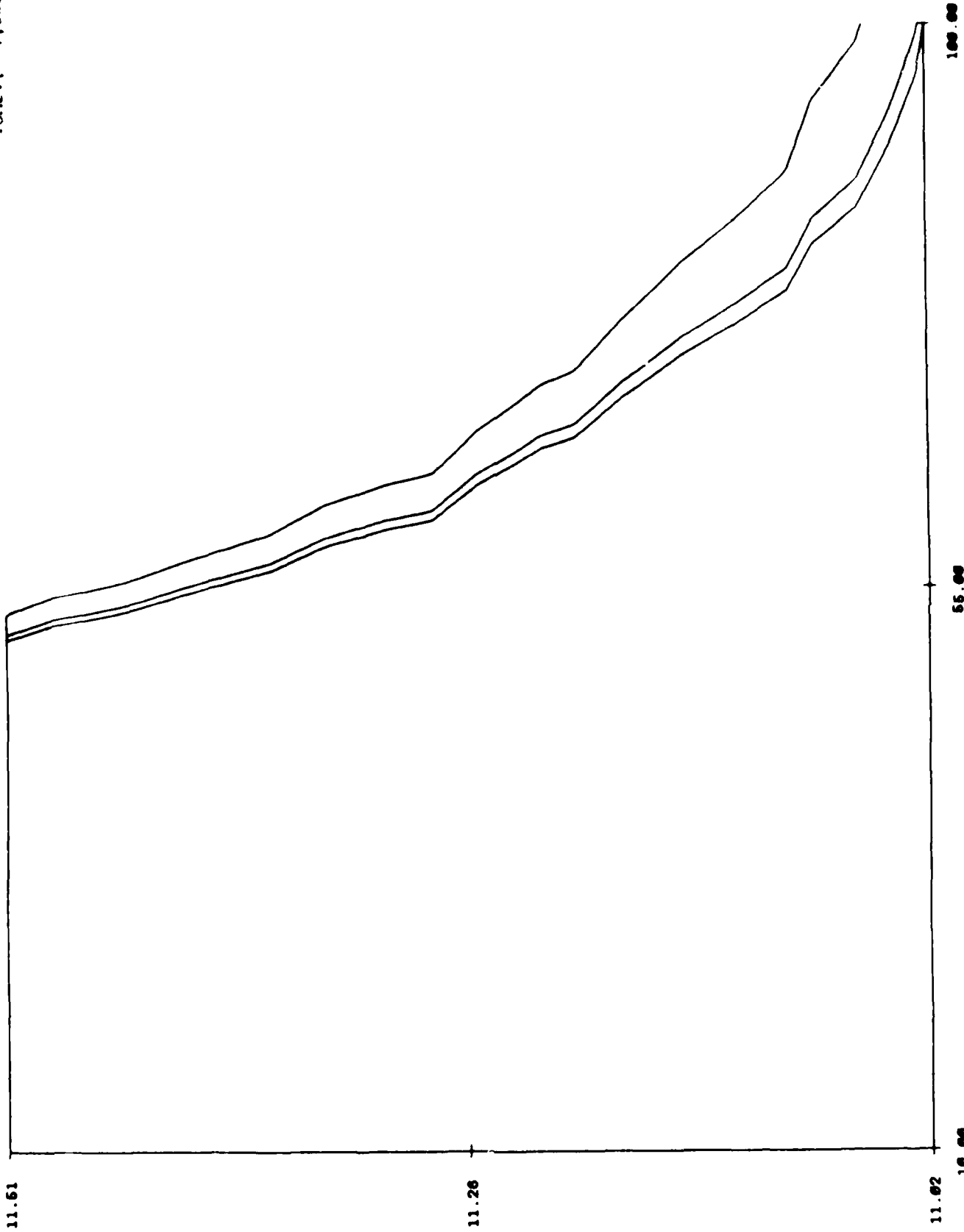
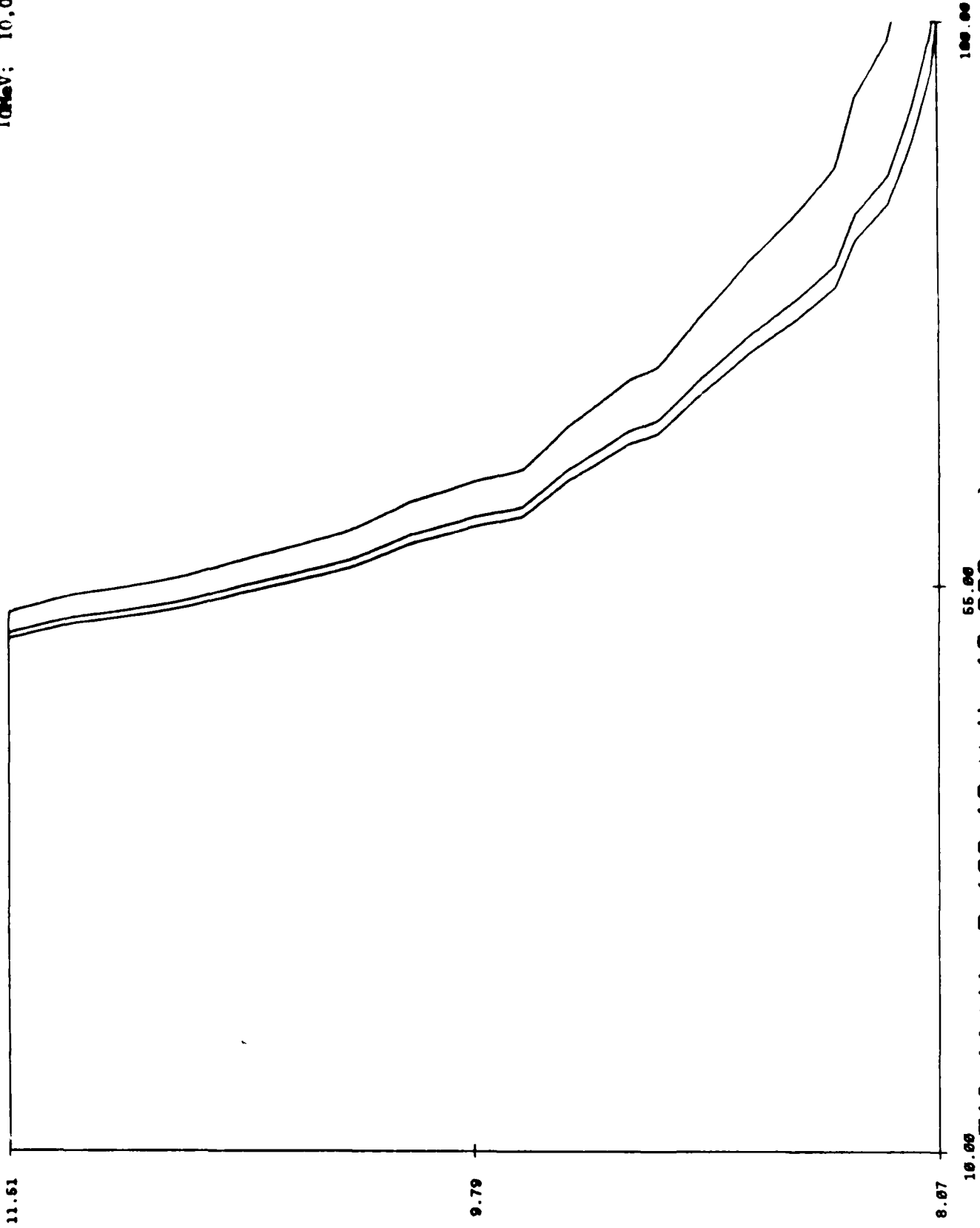


Fig (14c): R (SC, 10 MeU, 1000 ma)

DISTANCE TO 0.1 ATTENUATION

Fig. 14d

10 MeV; 10,000 mA/cm²



DISTANCE TO 0.1 ATTENUATION

78

Fig (14d): R (SC, 10 MeV, 10,000 ma)

Fig. 14e

100 MeV; 1,000 mA/cm²

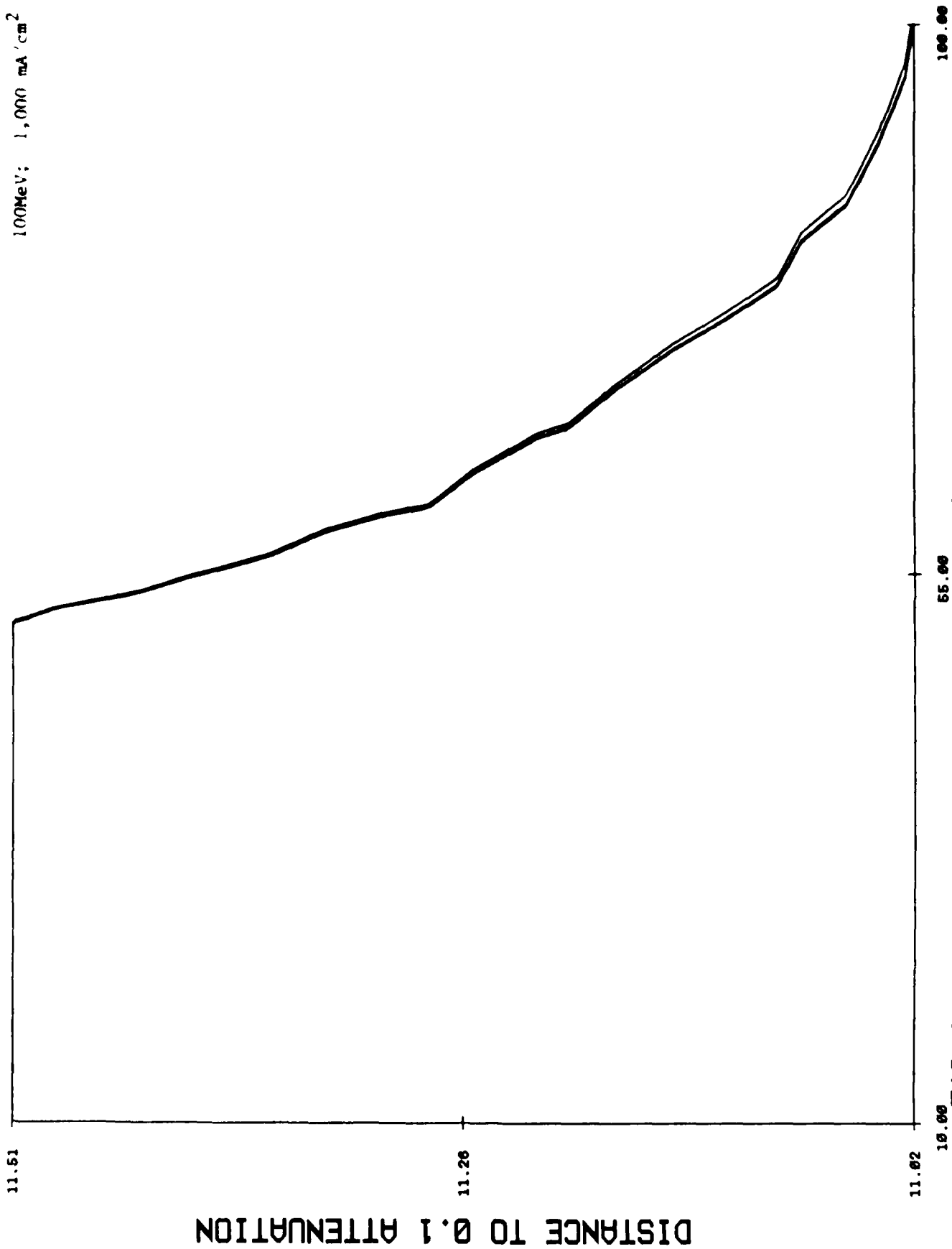


FIG (14e): R (SC, 100 MeU, 1000 ma)

DISTANCE TO 0.1 ATTENUATION

Fig. 14f

100NeV; 10,000 mA/cs

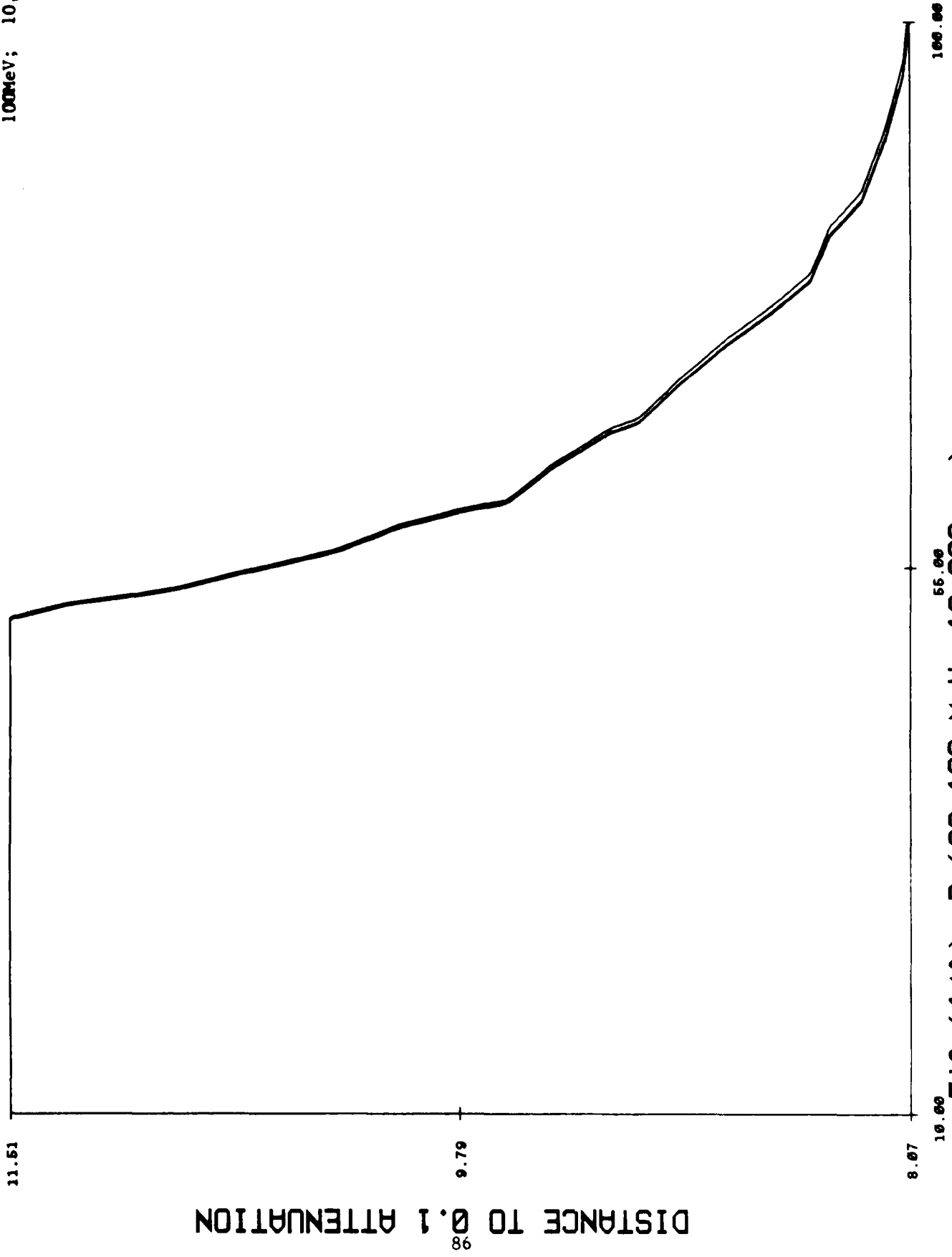


Fig (14f): R (SC, 100 MeU, 10,000 ma)

DISTANCE TO 0.1 ATTENUATION

• Fig. 15a

55cm; 1,000 mA/cm²

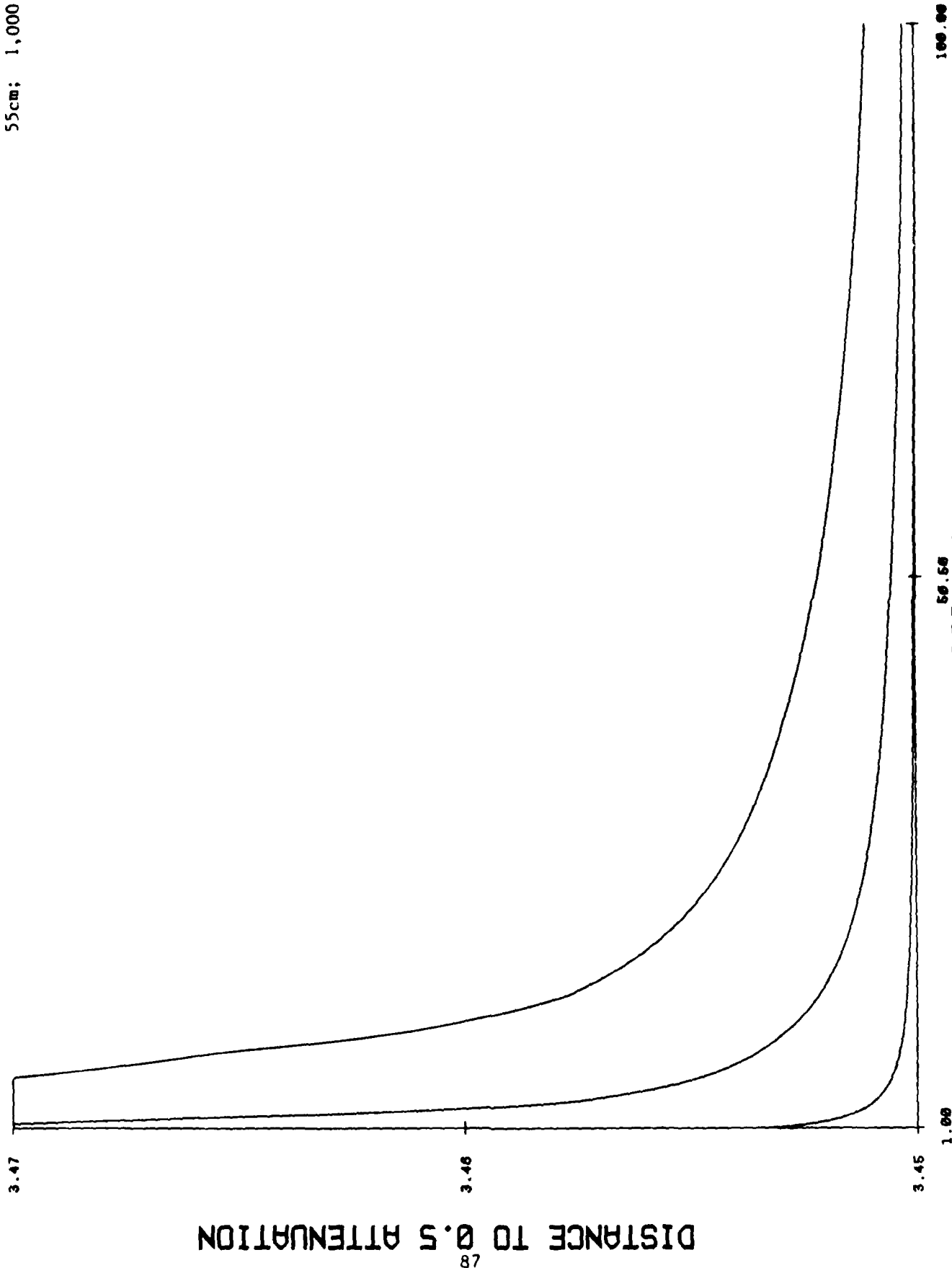


Fig 15(a): E (SC, 55 cm, 1000 ma)

Fig. 15b

55 cm; 10,000 mA/cm²

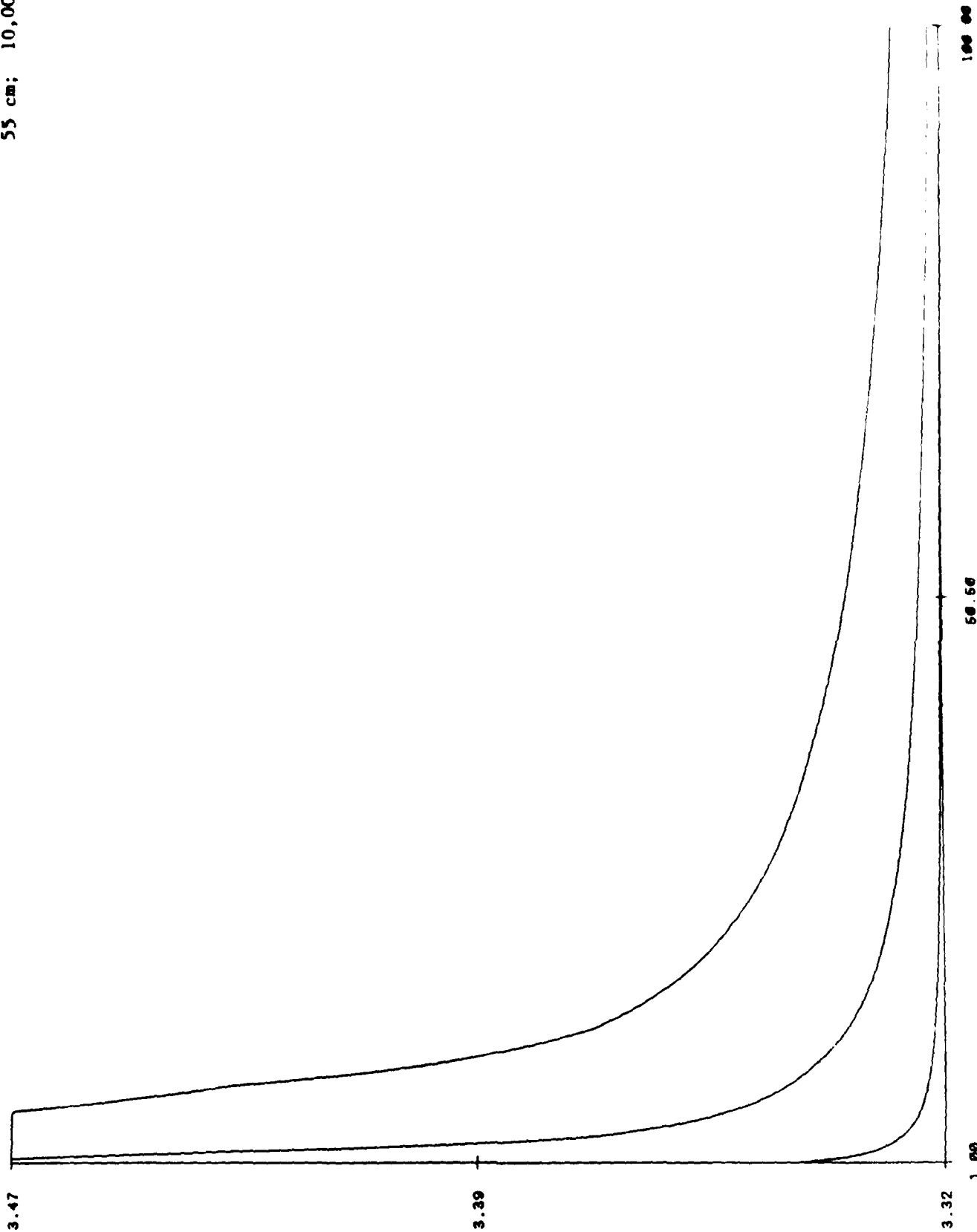


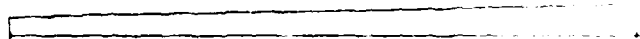
Fig 15(b): E (50.50 keV, 10,000 ma)

DISTANCE TO 0.5 ATTENUATION

Fig. 154

100 cm, 10,000 mA

3.47



3.48

ATTEN TO 0.5

100.00

50.50
E : SC, 100 cm, 10,000 ma)

NO-A102 601

NEUTRAL BEAM PROPAGATION EFFECTS IN THE UPPER
ATMOSPHERE 2(U) BOSTON COLL CHESTNUT HILL MA DEPT OF
PHYSICS T LI ET AL. 01 MAR 86 SCIENTIFIC-2 F/G 2077
AFGL-TR-86-0192 F19628-04-K-0039

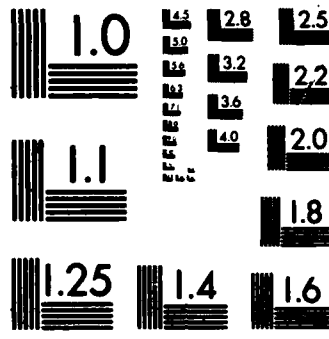
2/2

NL

UNCLASSIFIED



END
8 87
DTIC



MICROCOPY RESOLUTION TEST CHART
NATIONAL BUREAU OF STANDARDS-1963-A

Fig. 16a

55cm; 1,000 mA/cm²

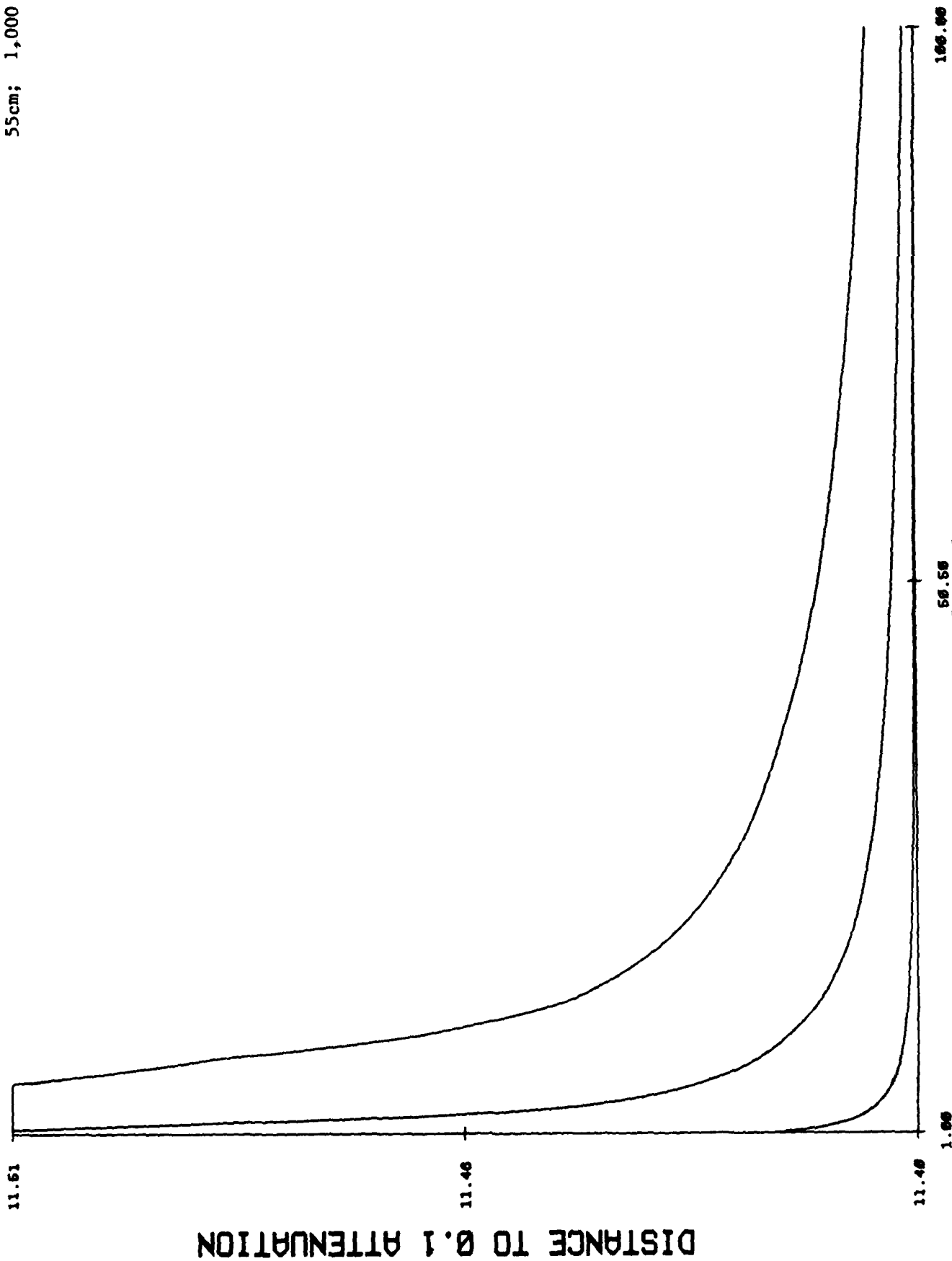


FIG 16(a): E (SC, 55 cm, 1000 ma)

DISTANCE TO 0.1 ATTENUATION

Fig. 16b

55 cm; 10,000 mA/cm²

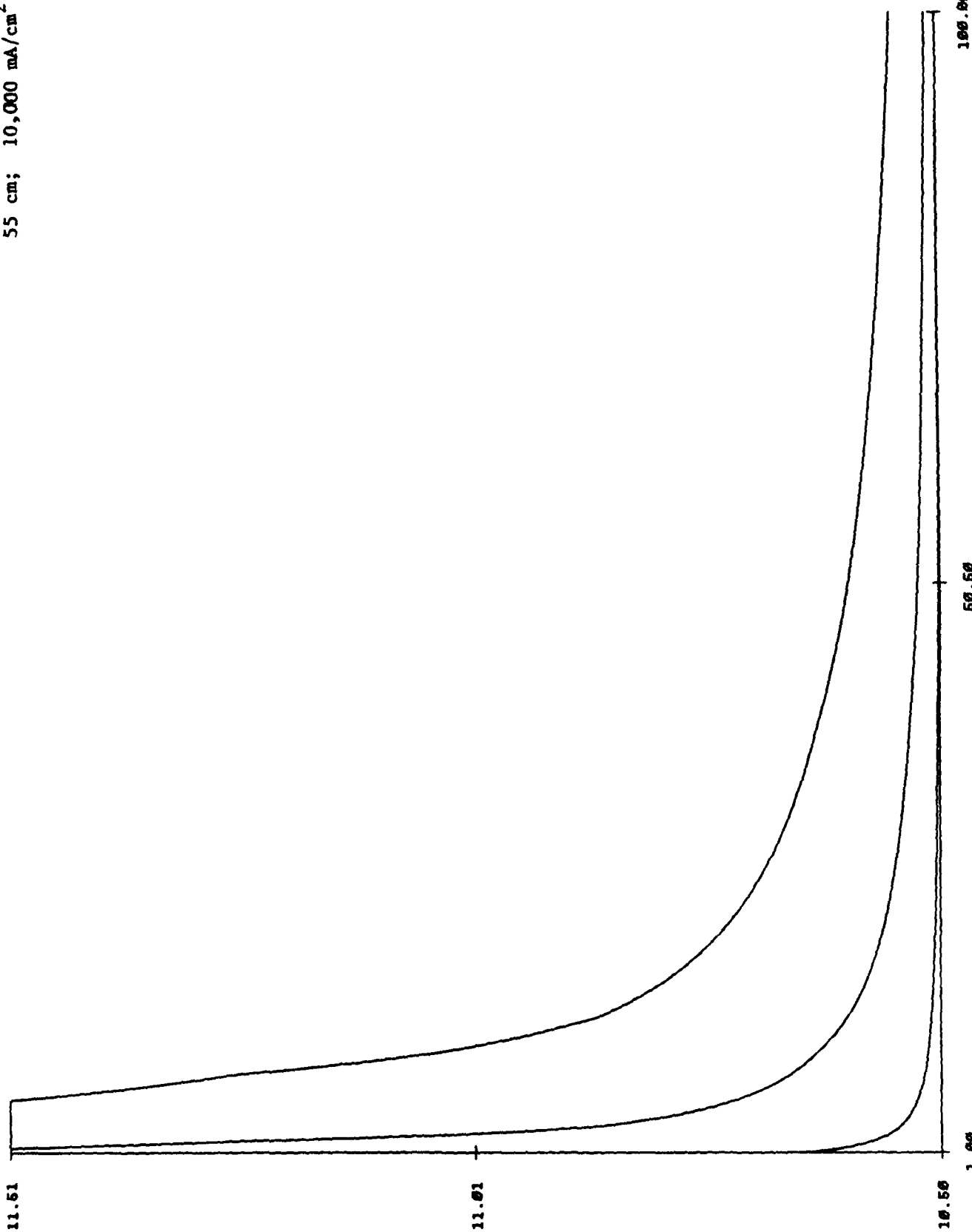


Fig 16(b): E (SC, 55 cm, 10,000 ma)

DISTANCE TO 0.1 ATTENUATION

Fig. 16c

100 cm; 1,000 mA/cm²



Fig 16(c): E (SC, 100 cm, 1000 ma)

100.00

DISTANCE TO 0.1 ATTENUATION

Fig. 16d

100 cm; 10,000 mA/cm²

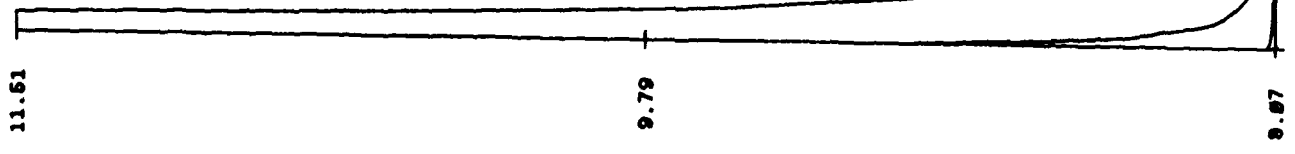


Fig 16(d): E (SC, 100 cm, 10,000 ma)

DISTANCE TO 0.1 ATTENUATION

END

8-87

DTIC